2000

An experimental investigation of potassium permanganate treatment of pooled DNAPL.

Melanie Rae. Marshall
University of Windsor

INFORMATION TO USERS

AN EXPERIMENTAL INVESTIGATION OF POTASSIUM PERMANGANATE TREATMENT OF POOLED DNAPL

By

Melanie Rae Marshall

A thesis submitted to the
College of Graduate Studies and Research through
Civil and Environmental Engineering
in partial fulfillment of the requirements for the
Degree of Master of Applied Science
at the University of Windsor

Windsor, Ontario, Canada
February, 2000

The author has granted a non-exclusive licence allowing the National Library of Canada to reproduce, loan, distribute or sell copies of this thesis in microform, paper or electronic formats.

The author retains ownership of the copyright in this thesis. Neither the thesis nor substantial extracts from it may be printed or otherwise reproduced without the author's permission.

L'auteur a accordé une licence non exclusive permettant à la Bibliothèque nationale du Canada de reproduire, prêter, distribuer ou vendre des copies de cette thèse sous la forme de microfiche/film, de reproduction sur papier ou sur format électronique.

L'auteur conserve la propriété du droit d'auteur qui protège cette thèse. Ni la thèse ni des extraits substantiels de celle-ci ne doivent être imprimés ou autrement reproduits sans son autorisation.

0-612-52604-6

Canada

ABSTRACT

In situ chemical oxidation using potassium permanganate ($KMnO_4$) is an innovative technology applied in the remediation of dense non-aqueous phase liquids (DNAPL) from contaminated groundwater and soil. Experiments were designed to examine important processes that occur during oxidation of pooled DNAPL treated by $KMnO_4$. All experiments were conducted in a two-dimensional tank that contained a single DNAPL pool of either perchloroethylene (PCE) or trichloroethylene (TCE) in a homogeneous porous media. Visual observations and chemical analysis of reactants and products were completed to establish and quantify important oxidation processes.

Experimental results showed the effectiveness of $KMnO_4$ treatment and removal of pooled DNAPL to be dependent upon several factors. Extensive manganese dioxide (MnO_2) precipitation occurred around the DNAPL pool that potentially reduced the effectiveness of treatment. Significant production of carbon dioxide (CO_2) caused de-saturation of the porous media containing the DNAPL. Subsequent reduction of $KMnO_4$ flow into this area resulted in a reduction in treatment efficiency. Mobilization of DNAPL pools due to CO_2 de-gassing was also observed in all experiments. Movement of CO_2 gas carrying DNAPL vapour was identified as an important mass transport mechanism.

ACKNOWLEDGEMENTS

TABLE OF CONTENTS

LIST OF TABLES

LIST OF FIGURES

1   INTRODUCTION

1.1   Groundwater Contamination

Non-aqueous phase liquids (NAPL) are sources of soil and groundwater contamination at numerous commercial and government sites in Canada and the United States. Pools or entrapped blobs of dense non-aqueous phase liquids (DNAPL) in the subsurface act as sources of long term contamination. Cleanup of sites contaminated with DNAPL pose an exceptional challenge to groundwater remediation technologies.

The special nature of DNAPLs in the subsurface received recognition in the early 1980's and have since been classified as priority environmental pollutants (Pankow et al., 1996). Chlorinated solvents are common DNAPL components and are among the most common groundwater pollutants (Fountain, 1998). Industrial use of trichloroethylene (TCE) and perchloroethylene (PCE) as cleaners/degreasers for metals and dry cleaning solvents has resulted in widespread groundwater contamination due to improper storage and disposal practices as well as accidental spills. Production quantities range from millions to billions of kilograms annually as modern society continues to utilize and dispose of these chemicals (Pankow et al., 1996).

Aquifers contaminated with DNAPL, such as PCE and TCE are regarded as serious threats to groundwater systems. Concern has arisen over the health effects of PCE which has been classified as a suspected human carcinogen

(ACGIH, 1995). While TCE has been classified as an animal carcinogen, available epidemiological studies do not confirm an increased risk of cancer in exposed humans except under uncommon or unlikely routes or levels of exposure (ACGIH, 1995). The Maximum Concentration Limit (MCL) for drinking water set by the US Environmental Protection Agency (EPA) for both PCE and TCE is 5 parts per billion or 0.005 mg/L (Pankow et al., 1996). In addition to health issues related to contaminated aquifers used for drinking water, the degradation of ecosystems is another incentive for cleanup of contaminated sites.

Two characteristics of PCE and TCE are low aqueous solubility and high interfacial tension with water, which result in the persistence of a non-aqueous phase and irregular distribution in the subsurface. DNAPL spills in aquifers are generally very difficult to cleanup and natural degradation in groundwater environments occurs extremely slowly. The ability of PCE/TCE to persist in the subsurface for long periods of time requires innovative remediation approaches.

1.2   Development of a DNAPL Contaminated Zone

Complex processes affect the interaction between phases of DNAPL and water, which ultimately influence the development of contaminated DNAPL zones. Subsurface contamination may consist of residual zones, pools or dissolved plumes of DNAPL. A basic understanding of DNAPL behaviour is important to the characterization and remediation of DNAPL sites.

When a volume of NAPL is released into the environment near ground level due to a spill, leak, or other release, gravity acts by pulling the NAPL downward into the vadose or unsaturated zone. In the unsaturated zone, NAPL compounds can exist as a separate organic phase, dissolved in the aqueous phase, vapour in the gas phase and/or absorbed onto the solid phase. NAPL is often described as being "immiscible" with soil and groundwater due to the fact that the solvent remains as a distinct separate phase. NAPL usually flows downward through the unsaturated zone with relatively little spreading. The migration of NAPL is dependent upon its density, viscosity, and volume of release and hydraulic conductivity variations in the porous media. Light non-aqueous phase liquids (LNAPL) have densities less than water and will tend to reside near the top of the capillary fringe and water table. However, DNAPL, which has a density greater than water, will normally penetrate the water table and continue to migrate downwards through the saturated zone. Eventually, the DNAPL may reach the confining layer at the bottom of an aquifer and accumulate as a pool. Plumes of dissolved DNAPL develop as groundwater flows around the contaminant zone. Figure 1.1 represents a typical DNAPL contamination scenario.

Interfacial forces that exist between two fluids and among fluids and solids are the result of energy at the contacting surface and are due to different attractive forces of the molecules. Resulting interfacial tension is determined by the properties of the fluids and the surfaces. When two fluids are in contact with
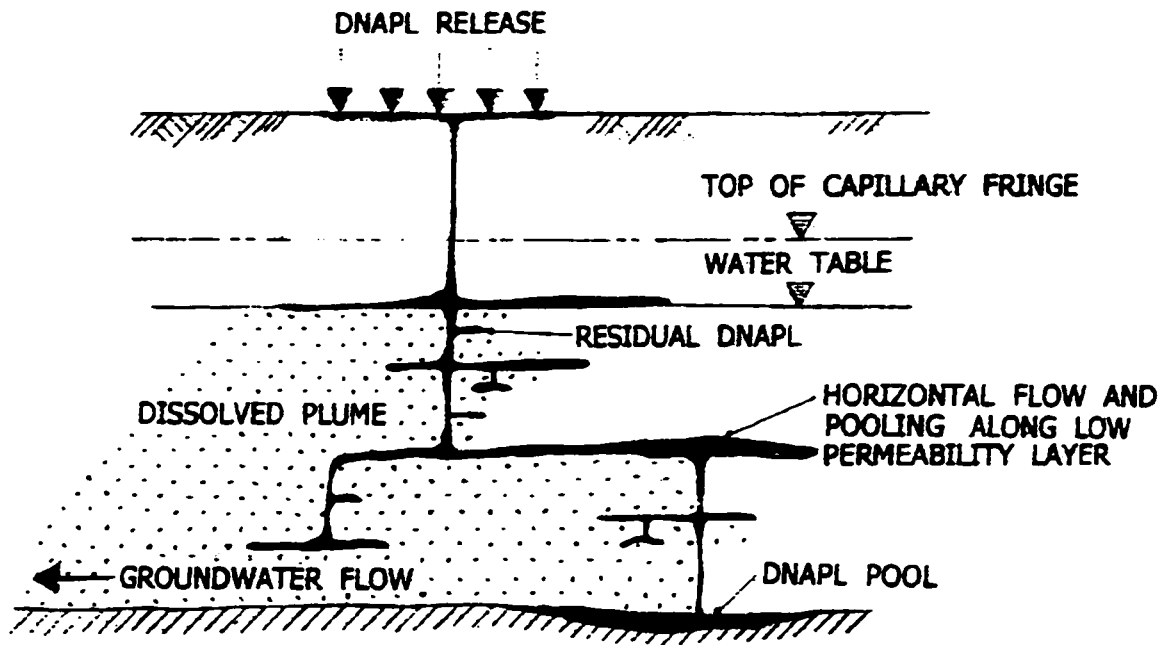
Figure 1.1: A typical DNAPL contamination site.
(modified after Kueper, 1989)

a solid, the fluid with greater affinity for the solid is called the wetting fluid and the other is the non-wetting fluid (McWhorter and Kueper, 1996). In the unsaturated zone, water is normally wetting with respect to the NAPL, and NAPL is wetting with respect to air on the soil solid. Below the water table in the saturated zone, water is normally the wetting phase with respect to DNAPL.

In order for DNAPL to enter the saturated zone, it must overcome interfacial forces. The capillary pressure, which is the difference in pressure between the non-wetting and wetting phases, required to overcome interfacial forces is known as the capillary threshold pressure or entry pressure (McWhorter and Kueper, 1996). Passage of DNAPL into a porous medium saturated with a

4

wetting fluid begins first with the largest pore spaces or throats. As the DNAPL capillary pressure increases, the wetting fluid is displaced by the non-wetting DNAPL which gradually invades smaller pore throats.

As the DNAPL passes through the porous media, small droplets of DNAPL may become trapped in pores of the soil after the spill source of DNAPL has ceased. When the interfacial forces are strong enough to overcome viscous and a gravity force, entrapment of DNAPL within the soil pores occurs. The fraction of the pore space that can be occupied by the trapped DNAPL is called residual DNAPL saturation. Residual that is completely cutoff from the flowing groundwater is trapped in dead-end pores.

In relatively homogeneous porous media, vertical movement of DNAPL in the saturated zone may be controlled by a process known as fingering whereby DNAPL infiltrates the media as fingers instead of as a uniform front. In heterogeneous porous media, movement of DNAPL is dominated by variations in the capillary properties of the porous medium. Downward flow of DNAPL may be interrupted each time it encounters a layer with a smaller grain size. Even subtle variations in grain size distribution may produce significant deflection and extensive spreading of DNAPL flow due to variations in entry pressure (Fountain, 1998). This can result in a series of horizontal lenses of DNAPL connected by narrow vertical pathways. When DNAPL encounters a fine-grained layer that has a high entry pressure, the DNAPL will tend to accumulate on top of the layer forming a pool. Therefore, DNAPL may be found as multiple horizontal lenses

interconnected by thin vertical pathways, with one or more pools above fine-grained layers (Fountain, 1998). DNAPL saturation in most of the horizontal lenses and vertical pathways will approach residual DNAPL saturation while pools will have a higher DNAPL saturation. The most important distinction between residual DNAPL saturation and pools is pools may be mobile under induced gradients. Another important difference lies in the reduced permeability of an area occupied by DNAPL; groundwater will tend to flow around a DNAPL pool whereas it will penetrate zones of residual DNAPL saturation. Compared to entrapped residual DNAPL saturation, DNAPL pools present very low contact areas to the moving groundwater (Oostrom et al., 1999). Therefore, DNAPL pools by their very nature are more difficult to treat than residual DNAPL contamination.

Consequently, contamination of an aquifer results from a large number of small, isolated DNAPL pools and residual zones rather than one large, uniform source. The ultimate distribution of DNAPL below the water table is a function of the volume and rate of release, physical properties of the DNAPL and characteristics of the porous media.

1.3   Remediation Technology

This section represents an overview of current DNAPL remediation approaches. Remedial technologies are selected based on site conditions and constraints, contaminant migration pathways, regulatory interests, suitability of

the technology, effectiveness of risk reduction and cost. Cleanup goals and objectives of site remediation include plume containment, aquifer restoration and source zone containment or removal. Current technologies may remove DNAPL by displacement, increasing dissolution, volatilization, destruction of the contaminant through biodegradation or chemical reactions or they may simply immobilize organic contaminants. Table 1.1 lists existing and new technologies for treating DNAPL. These methods may suffer from serious drawbacks such as incomplete removal, remobilization of DNAPL, limited applicability to certain soils, lengthy treatment periods and high cost.

Table 1.1: Existing and Innovative Treatment Technologies for Chlorinated Compounds

EXISTING TECHNOLOGY
Pump and Treat Physical Barriers Excavation Soil Vapour Extraction/ In Situ Air Stripping Steam Flooding Water Flooding In-Well Vapour Stripping
EMERGING TECHNOLOGY
Source Removal - Chemical Flooding - In Situ Chemical Oxidation - In Situ Thermal Desorption Dissolved Plume Control - Permeable Reaction Walls - Phytoremediation - Natural Attenuation/ Bioremediaition

In situ chemical oxidation involves the injection of a strong oxidizing agent into the subsurface to destroy a DNAPL source zone through chemical oxidation. Any excess oxidant can be extracted by a water flush through the treatment zone. This technology may be designed with extraction of groundwater and/or recycling of unused oxidant. Oxidants that have been applied include potassium permanganate ($KMnO_4$), Fenton's reagent (H_2O_2 and Fe^{+2} solution) and ozone. Advantages of in situ chemical oxidation include minimal surface treatment of groundwater, reduced limitations imposed by heterogeneity and cost-effectiveness for certain soil types.

Laboratory and controlled field studies have shown that $KMnO_4$ has considerable potential for effective destruction of PCE and TCE. Further discussion of these studies is provided in Chapter 2. In situ oxidation using $KMnO_4$ has become a promising technology.

1.4 Objectives of Research

The primary objectives of this thesis are to examine two-dimensional mass transfer and mass removal rates from pooled DNAPL in porous media treated with a $KMnO_4$ solution within an experimental tank and to observe important processes that occur during treatment. Experiments focussed on visual observation of processes, including oxidation, formation of MnO_2, generation of CO_2 gas and potential DNAPL mobilization. Objectives included sampling and

chemical analyses which were to provide mass transfer rate and removal efficiency data.

1.5 Scope

A two-dimensional experiment was designed to determine the important processes that occurred during the treatment of a DNAPL pool with $KMnO_4$. Experiments were conducted within a newly designed tank that allowed direct visual observation of the oxidation process. Homogeneous porous media containing a single DNAPL pool was used to establish understanding of the significant processes. Experiments were designed to observe the oxidative treatment of a DNAPL pool of defined geometry in porous media under a constant flow rate. A pretreatment water flush was designed to establish pretreatment mass transfer rates. A $KMnO_4$ flush was introduced to the system to determine oxidative treatment rates and removal efficiency followed by a post-treatment water flush to establish post-treatment mass transfer rates and effectiveness of treatment. Results were based upon visual observations of important processes that occurred throughout the course of the experiments as well as data from sample analyses. Concentration profiles and observations of reactants/products were used to characterize reactions between PCE/TCE and $KMnO_4$ and calculate mass removal rates.

2   LITERATURE REVIEW

2.1   In Situ Chemical Oxidation

2.1.1   The Oxidation-Reduction Process

An oxidation-reduction reaction or redox reaction, is defined as a chemical transformation in which the oxidation level of a reactant and its reaction partner are equivalently changed, with one substrate gaining electrons and the other losing them (Fox and Whitesell, 1997).

The objective of in situ oxidation technology involves the injection of the oxidizing agent into a contaminated DNAPL zone to convert DNAPL into less harmful species through chemical reactions. Therefore, the oxidant reacts with the organic compound to produce different chemical byproducts and in the process is reduced. Oxidizing agents that have been tested in the laboratory and in the field include ozone, hydrogen peroxide (Fenton's reagent) and $KMnO_4$.

Ozone is a common oxidant used as a disinfection treatment for drinking water. Although extremely reactive, ozone exists primarily in the gas phase and degrades very quickly when dissolved in water (Schnarr, 1992). For that reason, it is non-applicable to a contaminated groundwater system.

Laboratory studies were performed by Gates and Siegrist (1995a) to determine if treating clay soils contaminated with TCE through chemical oxidation by hydrogen peroxide (H_2O_2) was a viable process. Findings revealed

that TCE concentrations were reduced by as much as 98% and that TCE degradation increased with increasing H_2O_2 strength. Gates and Siegrist concluded that H_2O_2 is a feasible oxidant for contaminated soils and is dependent upon the efficient delivery and distribution of H_2O_2 throughout the region to be treated. In later experiments (1995b) comparing H_2O_2 and $KMnO_4$ solutions, they found $KMnO_4$ to be a more effective in situ chemical oxidant.

Vella and Veronda (1992) conducted a series of laboratory experiments to compare the chemical oxidation of TCE in water by $KMnO_4$ and Fenton's reagent. They concluded that both $KMnO_4$ and Fenton's reagent are inexpensive chemical oxidants capable of effectively oxidizing TCE to harmless products in soils. Another important observation was that the reaction rate with $KMnO_4$, while slower than Fenton's reagent, was effective over a wider pH range.

West et al. (1997) found that between the two oxidants, $KMnO_4$ was found to result in higher degradation of PCE/TCE under a wider range of subsurface conditions when compared to H_2O_2. $KMnO_4$ is also more stable than H_2O_2, as the latter will decompose quickly into H_2O and O_2 when contact with organic soil material occurs. This is very important as the oxidant should remain stable when travelling considerable distances to treat large volumes of subsurface media and the contaminated source zone. For that reason, $KMnO_4$ is a more attractive and practical oxidant for application in groundwater treatment.

2.1.2 Potassium Permanganate as an Oxidant

Oxidants used in any in situ treatment of a contaminated area must satisfy several important conditions. Firstly, the oxidant should possess the ability to oxidize the chlorinated compound without the production of harmful products that could have detrimental effects to the groundwater system. The oxidizing agent should be powerful enough to completely oxidize the target contaminant and delivery to the DNAPL source zone must be possible.

Potassium permanganate has a long history of successful use as an oxidant in numerous applications at drinking water treatment plants. Processes where $KMnO_4$ is utilized include coagulation, sedimentation and filtration to remove undesired taste and odour, iron, manganese, phenols, trihalomethane precursors and organic material from the water (Schnarr et al., 1998).

While $KMnO_4$ will readily and completely oxidize chlorinated alkenes, it cannot treat chlorinated compounds containing single carbon bonds such as trichloroethane (LaChance et al., 1998). As a strong oxidizing agent, $KMnO_4$ will not only react with chlorinated alkenes such as PCE and TCE but with any other organics that are present in the soil.

Characteristics of $KMnO_4$ in addition to being an indiscriminant oxidant include a high aqueous solubility, easy handling in solid form and a relatively low current cost of approximately $4 CDN/kg (Schnarr et al., 1998). High aqueous solubility is important as this will allow significant amounts of the oxidant to be injected to treat a contaminated zone. Successful delivery of $KMnO_4$ solutions in

12

the field to treat sites contaminated by chlorinated compounds has been accomplished.

In oxidation using $KMnO_4$, pH is considered a primary variable because it strongly influences the redox potential in a system (Schwartz and Yan, 1998). In general, the overall redox potential tends to increase with a decrease in pH. However, in normal groundwater systems, the pH allows the oxidation reaction to occur. Of the three criteria stated for chemical oxidants, $KMnO_4$ meets all the requirements as a suitable oxidant for contaminated soils.

2.1.3 Oxidation Reactions and Stoichiometry

Through oxidative degradation, the oxidizing agent, $KMnO_4$, readily cleaves the double carbon bond (C=C) of the chlorinated alkene which results in new carbon-oxygen bonds. Stoichiometrically, there is a 2:1 molar ratio for the species $KMnO_4$ and either PCE or TCE (Huang et al., 1999). Reactions between PCE and TCE with $KMnO_4$ are irreversible second-order reactions (Huang et al., 1999; Schwartz and Yan, 1998). Due to the different number of chlorine substituents, reactions between PCE and $KMnO_4$ proceed more slowly compared to the relatively rapid reaction between TCE and $KMnO_4$ (Schwartz and Yan, 1998).

The complete reactions, ignoring intermediate products, for PCE and TCE with $KMnO_4$ are given from Schnarr et al. (1998) respectively:

$$C_2Cl_4 + 2MnO_4^- \rightarrow 2CO_2 + 2MnO_2(s) + Cl_2 + 2Cl^-$$

$$C_2Cl_3H + 2MnO_4^- \rightarrow 2CO_2 + 2MnO_2(s) + 3Cl^- + H^+$$
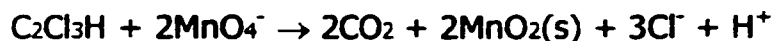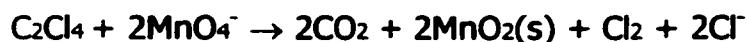
The half-cell reactions for PCE are as follows (half-cell reactions are similar for TCE):

$$MnO_4^- + 4H^+ + 3e^- \rightarrow MnO_2(s) + 2H_2O$$

$$0.5C_2Cl_4 + 2H_2O \rightarrow CO_2 + 4H^+ + 0.5Cl_2 + Cl^- + 3e^-$$
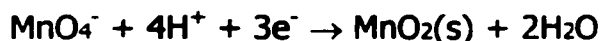
From reactions between PCE/TCE and $KMnO_4$, it is inevitable that various chemical byproducts will be released into the groundwater. Complete oxidation of PCE/TCE yields the products carbon dioxide (CO_2), chlorine (Cl_2), chloride (Cl^-) and manganese dioxide (MnO_2). CO_2 will combine with water thereby lowering the pH of the water. A separate CO_2 vapour phase will form within the soil if the reaction rate exceeds the carrying capacity of the water (LaChance et al., 1998). If the CO_2 vapour phase accumulates, it can interfere with injection of $KMnO_4$ solution into a treatment zone. The formation of a brown precipitate, manganese dioxide, and other manganese oxides produced by the reaction have both oxidative and adsorptive properties that contribute to controlling and minimizing any byproducts (Schnarr, 1992). However, MnO_2 may coat the soil grains and result in reduced permeability of the porous medium (LaChance et al., 1998). Therefore, reduction of $KMnO_4$ yields insoluble byproducts, such as MnO_2, that tend to plug the treated zones and may be detrimental to treatment efficiency.

Properties for PCE, TCE and KMnO₄ are listed below in Table 2.1.

Chemical products produced from oxidation reactions with PCE and TCE are less dangerous and harmful to an aquifer than the original compounds. Therefore, it can be reasoned that the byproducts of in situ oxidation are more favourable than the contaminants PCE and TCE.

Table 2.1: Properties of In Situ Oxidation Compounds
(from Pankow et al., 1996)

Compound	Solubility @ 20 °C (mg/L)	Density @ 20 °C (g/mL)	Molecular Weight (g/mol)
PCE (C_2Cl_4)	200	1.63	165.8
TCE (C_2Cl_3H)	1100	1.46	131.4
Permanganate ($KMnO_4$)	74.3×10^3	N/A	158

2.1.4 Research Investigating the Use of KMnO₄ to Oxidize DNAPL in Porous Media

Since experiments conducted by Vella and Veronda, numerous researchers have completed similar laboratory and field studies to evaluate the effectiveness of KMnO₄ as a possible remediation technology. Results of these experiments are described herein.

In a series of batch tests, Schwartz and Yan (1998) investigated the oxidative treatment of five chlorinated ethylenes: Tetrachloroethylene (PCE),

trichloroethylene (TCE), and three isomers of dichloroethylene (DCEs) using KMnO₄. The study revealed that the degradation process was rapid in aqueous solution and the rate increased with a decreasing number of chlorine substituents on the ethylene. They also found that TCE oxidation is a second-order reaction with the rate constant independent over the pH range of 4-8. Both chloride and hydrogen ions were monitored throughout experiments and levels suggested essentially complete dechlorination. Schwartz and Yan concluded that the degradation products of chlorinated ethylenes are much less harmful than the parent compounds and are miscible with water. Degradation products would therefore be easily removed from the groundwater with flushing at an actual site.

Researchers McKay et al. (1998) performed pilot-scale testing at the U.S. Army Cold Regions Research & Engineering Laboratory in Hanover, New Hampshire to evaluate the effectiveness and feasibility of treating TCE in low permeability layers of soil using a concentrated solution of KMnO₄. Two residual phase TCE contaminated sites are currently undergoing treatment by the injection of 1.5% KMnO₄ solution into unsaturated soil. Oxidation of TCE is indicated by increases of chloride in pore water and by analysis of post-injection soil samples. The study has so far concluded that in order for complete remediation of the site to be achieved, significantly larger volumes of KMnO₄ solution or higher concentrations of KMnO₄ are needed.

Investigation of in situ oxidation conducted by Schnarr (1992) and Schnarr

et al. (1998) involved one-dimensional column experimentation and controlled

field experimentation at Canadian Forces Base (CFB) Borden near Alliston,

Ontario. Objectives of treatment with solutions of $KMnO_4$ included evaluating:

products of PCE and to a lesser extent TCE, destruction rate in porous media

with varying concentrations and flow rates of $KMnO_4$, extent of oxidation using

mass balances of chloride and finally a planned field trial involving PCE and

$KMnO_4$. Laboratory results indicated nearly complete destruction of residual PCE

and TCE in soil columns with flushing of aqueous concentrations of $KMnO_4$

ranging from 7.5 – 10 g/L. Oxidation processes deteriorated when the pH of the

solution was raised to 8.2 and increased significantly at a pH of 4.2. Primary

conclusions that were drawn from the column studies indicated that the

destruction rate of TCE is approximately six times greater than PCE and that the

dissolution rate of DNAPL was the main factor affecting oxidation. Field trials

indicated destruction of a PCE contamination source based on observed chloride

production. Results from field experiments at CFB Borden suggested that the

subsurface distribution of DNAPL had a notable effect on the rates of mass

removal. In variable DNAPL distributions, the contaminant would be present in

both low and high saturations. Residual saturations would be readily oxidized

but mass removal from zones of high saturation such as pools would be slow due

to the lower aqueous phase permeability and lower surface area to volume ratio.

Schnarr et al. (1998) concluded that the capability of in situ oxidation depends

primarily upon the distribution of DNAPL within the contaminated zone, effectiveness of oxidant delivery and dissolution processes.

In 1997, the Department of Energy/Portsmouth Gaseous Diffusion Plant organized a field study in which $KMnO_4$ was injected into an area known as the X-701B Site contaminated with TCE. Using existing horizontal wells that transected the contaminated area, groundwater was extracted from one well, pumped to an existing pump and treat facility, dosed with $KMnO_4$ and re-injected into a parallel horizontal well approximately 90 feet away (West et al., 1997). This treatment approach which involved injection and recirculation of the oxidant solution into a contaminated aquifer through multiple horizontal and vertical wells is referred to as In Situ Chemical Oxidation through Recirculation (ISCOR). This approach allowed more control over oxidant distribution and less risk of mobilizing contamination compared to oxidant injection alone. Results, based on numerous analyses of TCE from sample cores taken before and after the test, indicated significant reduction in TCE in all locations where $KMnO_4$ reached (Fountain, 1998). While ISCOR was effective at oxidizing TCE in the saturated zone, lateral and vertical heterogeneity interfered with the uniform delivery of the $KMnO_4$ solution throughout the contaminated zone that produced non-uniform TCE reduction. West et al. (1997) concluded that long-term groundwater monitoring would be required to fully assess the impact of this demonstration on the ISCOR test region.

As demonstrated by laboratory and field studies, chemical oxidation of PCE/TCE by KMnO4 has the potential to be a highly effective and viable technology for groundwater remediation. As will be discussed in the following section, mass transfer rates play an important role in the effectiveness of in situ oxidation.

2.2   Mass Transfer

2.2.1   Mass Transfer Mechanisms: An Overview

The rate at which DNAPL is transferred from a contaminated zone to flowing groundwater is typically expressed as a mass transfer rate. The rate of mass transfer from DNAPL to the water phase is a function of the contact area between the two phases, DNAPL solubility, physical distribution of the DNAPL in the porous medium and the rate of groundwater flow through and around DNAPL source areas. The driving force for mass transfer is the concentration difference across the mass transfer boundary layer which is defined as the difference between the effective solubility of the DNAPL and the dissolved concentration in the water in contact with the DNAPL (Feenstra and Guiguer, 1996).

Mass transfer rates are significant to the transport and ultimate fate of contaminants. The rate of mass transfer will determine dissolved phase concentrations in flowing groundwater as well as the persistence of a DNAPL

contaminated zone. Where DNAPL is present as residual zones, pore-scale
dissolution occurs more quickly and readily compared to DNAPL pools that have
a smaller contact area with the groundwater and rely on macro-scale mass
transfer. Therefore, pools dissolve substantially slower than residual zones,
which result as sources of long term contamination.

Extensive experimental research has been conducted to study the mass
transport of DNAPL residual and to a lesser extent pools. These will be
examined in the following sections respectively.

2.2.2 Mass Transfer: Pore-Scale

In residual zones, DNAPL is present as disconnected immobile blobs and
ganglia that may occupy 10% or less of the pore space. As illustrated by Figure
2.1, groundwater flows through the remaining pore space. Although the
presence of DNAPL reduces the relative permeability of the medium to water,
pore-scale dissolution of DNAPL occurs as groundwater flows through the
residual zone (Feenstra and Guiguer, 1996).

Numerous laboratory studies using one-dimensional columns have been
conducted to quantify dissolution rates from residual NAPL saturation and to
examine processes affecting the dissolution of NAPL. Highlights from
experiments are presented as follows.

Powers et al. (1991) investigated dissolution of NAPL in subsurface
systems and found that rates of interfacial mass transfer between NAPL and
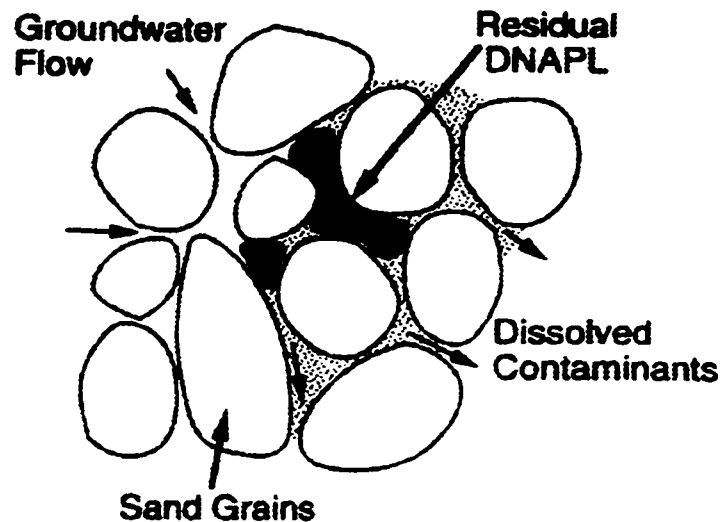
Figure 2.1: Dissolution: Pore-scale.
(from Feenstra and Guiguer, 1996)

water may be a limiting factor in the dissolution of NAPL into groundwater.

Findings also suggested that reduced permeability attributable to reduced mass

transfer rates might be a factor contributing to aqueous phase NAPL

concentrations several orders of magnitude lower than saturation at

contaminated field sites. Further column experimentation by Powers et al.

(1992, 1994) revealed a dependence of dissolution rates on the distribution

pattern of entrapped NAPL in water saturated porous media, porous media

grading, mean grain size, as well as upon aqueous phase velocity.

Geller and Hunt (1993) focused on mechanisms that limit the remediation

of NAPL contaminated aquifers. Through experimental and modelling efforts,

they discovered that there is a complex dependency of groundwater

concentrations on flow velocity; high flow rates reconfigure ganglia into smaller

21

sizes with higher interfacial areas and the length of the mass transfer zone increases at higher velocities. Hunt et al. (1988) also developed analytical solutions for the dissolution of DNAPL residual in a one-dimensional column. Results showed DNAPL residual can persist for long periods releasing low aqueous concentrations as mass transfer rates decrease with time.

One-dimensional column experiments were conducted (Imhoff et al., 1994) to measure changing residual saturations of TCE in a porous medium as clean water was flushed through the column. Results indicated that minimal amounts of separate phase TCE remained trapped within the medium after thoroughly flushing with water. Mass transfer rate coefficients were computed and appeared to be dependent upon Darcy flux, TCE volume and distance into the region of residual TCE.

Dissolved chlorinated contaminants in groundwater are usually at concentrations far below their solubility. Column studies have indicated that saturation concentrations can be achieved rapidly when water is forced to flow through a DNAPL zone. Anderson et al. (1992) conducted a study to examine concentrations and mass removal rates when simulated groundwater was free to flow partially around a zone of stable, residual DNAPL saturation in a sand-filled tank. Possible explanations for lower than solubility aqueous concentrations proposed at the beginning of the study included: 1) mass-transfer limitations on dissolution as water passes through a residual zone; 2) diversion of flow around, rather than through the residual zone; and 3) organic fluids forming flat pools on

top of bedding planes thereby reducing the cross-sectional area available to on-coming water. Results indicated that flow is not affected when flowing through a residual zone and dissolved concentrations quickly approach near-saturation values. Anderson et al. (1992) concluded that low DNAPL concentrations observed in groundwater in the field are not due to limited pore-scale mass transfer from zones of residual DNAPL saturation but rather to mass transfer at the macro-scale.

2.2.3 Mass Transfer: Macro-Scale

Pools of DNAPL may have as much as 50 to 70% of the pore space occupied by DNAPL which results in a significant reduction of groundwater flow through these areas. Dissolution mostly occurs as groundwater passes along the edges of the pooled DNAPL (Feenstra and Guiguer, 1996). Macro-scale processes of dispersion and advection act to transport dissolved chemicals away from a DNAPL pool. Distribution of solute concentration in the aqueous phase is the result of advection and longitudinal and transverse dispersion (Sale, 1998). The concept of mass transfer from a DNAPL pool into flowing groundwater is illustrated in Figure 2.2.

Nearly all mass transfer laboratory experiments have been performed in one-dimensional columns with the exception of a few studies that have employed tanks or cells as the experimental apparatus. One-dimensional columns force water to flow through the DNAPL zone. Realistically, water would also be able to
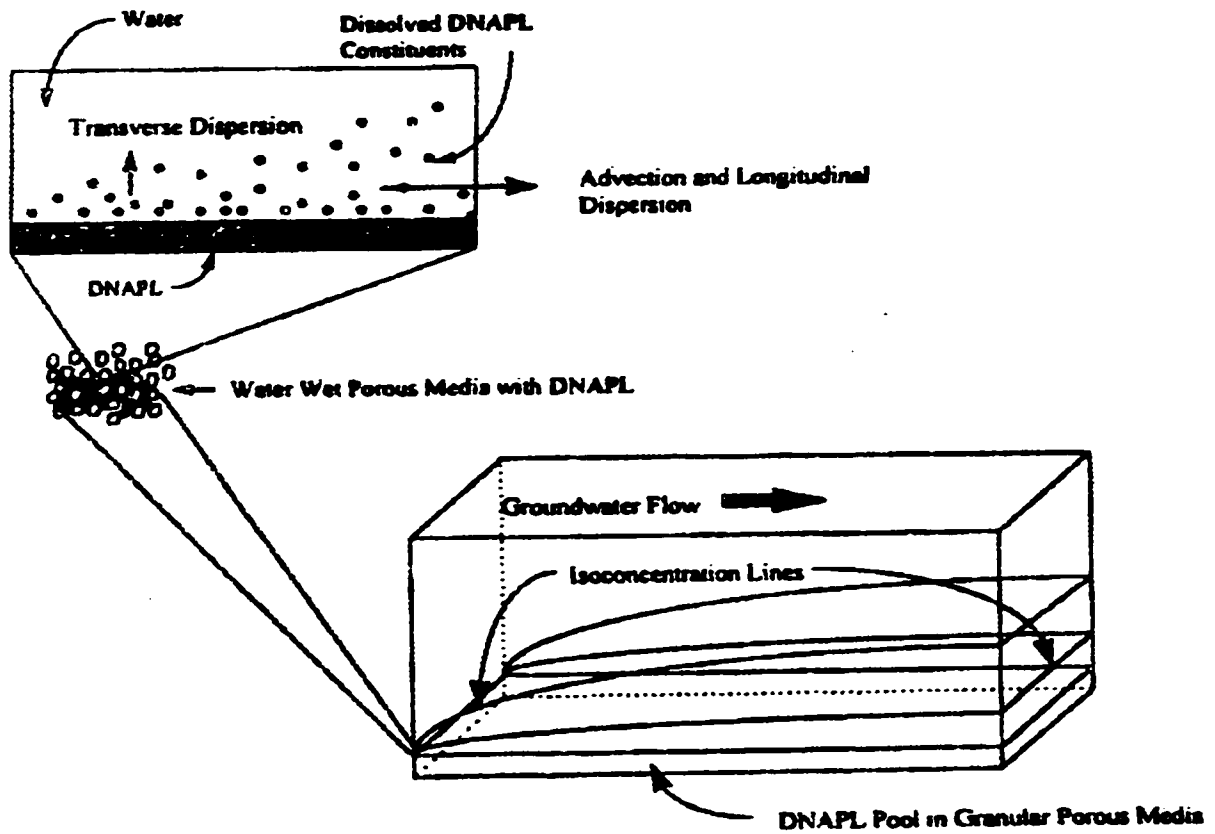
Figure 2.2: Mass transfer into a flowing aqueous phase adjacent to a DNAPL pool. (Sale, 1998)

flow around the contaminated zone. Tank experiments allow contamination scenarios to be better simulated than column experiments. Through tank experiments, two and three-dimensional analysis can also be explored. Research using tank designs to investigate mass transfer from DNAPL pools is discussed below.

Laboratory experiments performed by Schwille (1988) examined water passing over a TCE pool on the bottom of a tank to calculate mass removal rates. The total rate of removal from the TCE/water interface was found to

increase with an increase in flow rate. However, dissolved concentrations of TCE were found to be well below aqueous solubility levels, even when the concentrations were averaged over a short vertical distance above the pool. Schwille (1998) concluded from these experiments that DNAPL pools could persist on the bottom of aquifers for long periods of time.

Pool studies completed by Pearce et al. (1994) and Whelan et al. (1994) involved point sampling of aqueous concentrations of DNAPL around a pool to examine kinetics of dissolution. Results indicated changes in aqueous concentrations over distances of a few centimeters above the pool and the dissolved DNAPL concentrations decreased with increasing vertical distance from the pool resulting in steep concentration gradients. The concentration gradient was found to increase with an increase in groundwater velocity. The pool experiments showed that all measured concentrations were a small fraction of the respective DNAPL solubility due to limited mass transfer rates.

Oostrom et al. (1999) conducted experiments in a flow cell to study the flow of liquid and the transport of dissolved TCE in a saturated heterogeneous porous medium. Visual observations were noted and samples were taken to measure TCE saturations. A simple pool dissolution model was used to predict observed dissolved TCE concentrations. Results showed that the measured concentrations could only be predicted with unrealistically high transverse dispersion values. It was concluded that the observed TCE concentrations were a result of a combination of entrapped residual and pool dissolution.

In another recent study, Powers et al. (1998) conducted experiments to quantify rates of NAPL dissolution from heterogeneous media compared with model simulations. The work addressed processes controlling overall dissolution of NAPL entrapped at a high saturation (pool) in heterogeneous porous media composed of a coarse sand lens surrounded by fine sand in a two-dimensional cell. The study hypothesized that water directly surrounding NAPL is equilibrated with the NAPL phase and that lower concentrations observed downgradient could be accounted for by dilution. Observations suggested that water flowing through the coarse sand lens contaminated with NAPL is predominantly responsible for overall dissolution behaviour. Reductions in the average NAPL saturation due to dissolution occurred over time as water flowed through this region. This in turn increased the relative permeability to water, which led to increased water flow through the NAPL region. The increased water flow through the NAPL zone caused an increase in concentration followed by a rapid decrease when most of the NAPL had been dissolved. Additionally, because of transverse dispersion, dissolution was expected to occur around the periphery of the coarse sand lens. Through model simulations, transverse dispersion to water flowing around a zone of high NAPL saturation was identified as important.

Sale (1998) studied dissolution from a highly saturated column source of NAPL emplaced perpendicular to water flow in an experimental tank. Objectives were to evaluate mass transfer rates as a function of time given constant one-dimensional flow and two-dimensional transport. Near-constant rates of mass

26

transfer were observed shortly after breakthrough of dissolved NAPL occurred at the effluent suggesting individual NAPL subzones or pools achieve steady state mass transfer rates in short periods of time. Rate-limited interphase mass transfer was observed towards the completion of the experiment as the column source of NAPL was depleted and residual NAPL saturation remained. Further experiments indicated that mass transfer rates from a pool are not strongly dependent on pool length. Insensitivity of mass transfer rates to pool length is due to the high rate of mass transfer at the leading edge of the pool. This observation is important to source zone remediation as reducing the length of a NAPL pool by a factor of 25 would only reduce downgradient concentrations by a factor of 2 (Sale, 1998).

2.2.4 Reaction Enhanced Mass Transfer

Previous discussion has established mass transfer rates are crucial in determining the effective removal of DNAPL from a contamination zone. In situ oxidation is a process whereby overall mass transfer rates of DNAPL to the aqueous phase may be enhanced due to the reaction between PCE/TCE and $KMnO_4$. Reactions between $KMnO_4$ and PCE/TCE will tend to increase the mass transfer rate due to increased chemical gradients within the film surrounding the DNAPL/water interface (Schnarr et al., 1998). The increase in the mass transfer rate due to this effect is referred to as an enhancement factor. An enhancement

in mass transfer rates resulting in increased DNAPL solubility would accelerate mass removal rates potentially making in situ oxidation highly effective.

Schnarr et al. (1998) suggested that on a pore-scale level as the aqueous phase PCE/TCE is destroyed directly above the interface, dissolution is enhanced and the mass transfer rate increases from the PCE/TCE residual. This mechanism would rely on improved interphase mass transfer of DNAPL into the surrounding aqueous solution and simultaneous oxidant/DNAPL reaction due to high chemical gradients. This effect is illustrated by Figure 2.3. High concentrations of an oxidant could then be used to increase diffusion rates into low permeability layers.
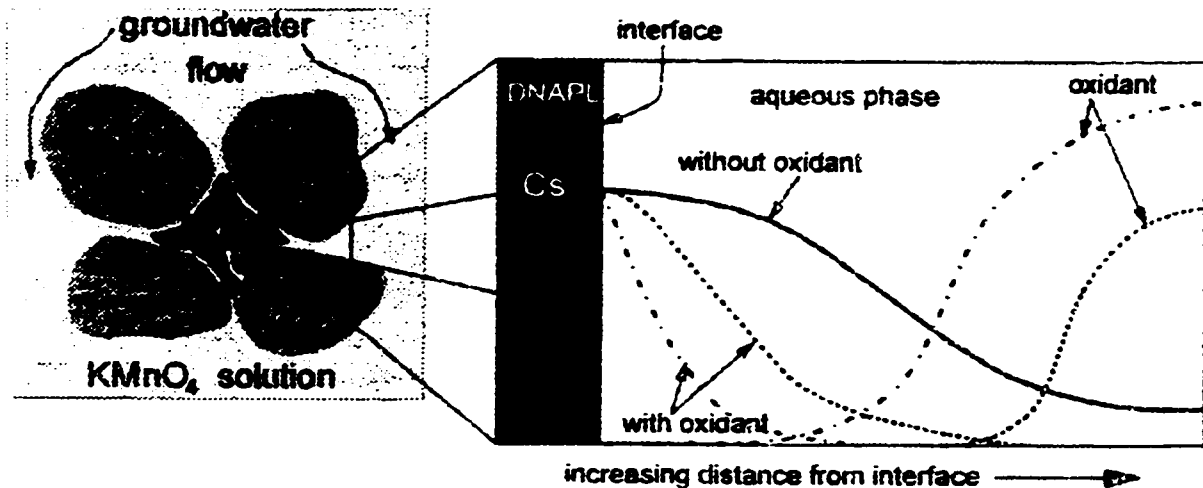
Figure 2.3: Effect of oxidant on aqueous concentrations near the DNAPL/water interface. (from LaChance et al., 1998, modified after Schnarr et al., 1998)

Reitsma and Dai (1999) performed simulations based on theoretical analyses to study reaction induced mass transfer enhancement between $KMnO_4$ and DNAPL in both one and two-dimensional pools. Conclusions that were drawn indicated that $KMnO_4$ would likely not increase pore-scale mass transfer due to slow reaction rates within the film near the DNAPL/water interface. Macro-scale mass removal rates from pools could only be expected to increase based on varying enhancement factors ranging from 5 to 50 depending upon $KMnO_4$ concentration and DNAPL aqueous solubility. Based on these mass removal rates, remediation of contaminated soils by $KMnO_4$ may be enhanced but may still take impractical periods of time to treat (Reitsma and Dai, 1999).

3   MATERIALS AND METHODS

3.1   Introduction

This study was conducted to contribute to the understanding of two-dimensional mass transfer mechanisms and processes that occur during oxidation of pooled DNAPL. Previous laboratory experiments conducted by various researchers (refer to Chapter 2) examined $KMnO_4$ oxidation of residual DNAPL in one-dimensional columns. Two-dimensional tank experiments have been completed to investigate NAPL dissolution without reaction. This research extends one-dimensional oxidation experiments and two-dimensional dissolution experiments to examine mass transfer processes that may not occur in one-dimensional systems.

To determine the importance of various processes that occur during the treatment of DNAPL pools with potassium permanganate, a two-dimensional experiment was designed. In order to achieve this goal, experiments were conducted within a two-dimensional tank that allowed direct visual observation of the oxidation process. Samples were also collected from the tank and analyzed for DNAPL compounds, $KMnO_4$ and Cl^-. A simple porous media and DNAPL pool configuration were used to establish understanding of the significant processes. The experiment was designed to observe the oxidation of a single DNAPL pool of defined geometry under a constant flow rate in homogeneous porous media. DNAPL was injected into a single coarse sand lens surrounded by fine sand to

produce a pool positioned in the centre of the tank. DNAPL saturation (S) in the pool was calculated based on the porosity of the coarse sand lens and volume of DNAPL injected.

The original design procedure called for an initial water flush to establish baseline mass transfer rates from pooled DNAPL prior to treatment. $KMnO_4$ solution would then be introduced at a uniform flow rate at one end of the tank and effluent samples collected from the opposite end. Additional point samples would be collected around the DNAPL pool to establish dissolved DNAPL concentration distributions in the vicinity of the pool. Samples taken would then be analyzed for PCE/TCE, $KMnO_4$ and Cl^-. Chloride concentrations would be used to establish mass transfer rates during the $KMnO_4$ flush. The $KMnO_4$ flush would be followed by an additional water flush to determine post-treatment mass transfer rates. Careful visual records of the experiments were also planned for analysis.

A summary of the experimental conditions is outlined below in Table 3.1. The first experiment employed a volume of 5.0 mL of TCE to create a DNAPL pool with a DNAPL saturation of 0.25. The pool was subject to a pretreatment water flush for 159.5 hours and a $KMnO_4$ treatment flush for 75.0 hours. The concentration of the $KMnO_4$ solution used in experiment 1 was 10.0 g/L. Experiment 2 used 5.0 mL of PCE for pool formation with a DNAPL saturation of 0.25. The pool was treated with a pretreatment water flush for 42.5 hours and a $KMnO_4$ flush for 120 hours. The concentration of $KMnO_4$ injected was reduced to

31

5.0 g/L during experiment 2. A post-treatment water flush was not possible for either experiment 1 or 2. The original volume of PCE injected in experiment 3 was reduced from 5.0 mL to 2.0 mL to create a pool with a DNAPL saturation of 0.10. The pretreatment water flush lasted 45.5 hours and the $KMnO_4$ flush for 422 hours. The PCE pool was treated with a reduced $KMnO_4$ solution with a concentration of 1.0 g/L. A post-treatment water flush was possible in experiment 3 and continued for 432.5 hours. Chapter 4 expands on the logical reasons for changes in the type of DNAPL, $KMnO_4$ concentration and the different duration of treatment.

Table 3.1: Experimental Conditions

Experiment	DNAPL Injected	[$KMnO_4$] (g/L)	Flush Duration (hours)		
			H_2O	$KMnO_4$	Total
1	5.0 mL TCE (S=0.25)	10.0	Pretreatment: 159.5	75.0	234.5
2	5.0 mL PCE (S=0.25)	5.0	Pretreatment: 42.5	120	162.5
3	2.0 mL PCE (S=0.10)	1.0	Pretreatment: 45.5 Post-treatment: 432.5	422	900

3.2 Tank Design

Details of the experimental tank are illustrated in Figure 3.1 and an actual picture of the tank is provided in Figure 3.2. The tank was primarily constructed out of aluminum with a glass front to allow direct visual observation of all visible processes that were occurring within the tank. Viton o-rings ($\varnothing$=2.5 mm) were used to seal the glass and top plate to the tank. A frame made from 2.5 cm width aluminum flat bar was used to secure the glass. A rubber gasket was placed between the glass and the aluminum frame to protect the glass. Figure 3.3 shows a cross-sectional view that illustrates how the front of the tank was assembled. PVC plugs (ID=2.0 mm) located at the inlet and outlet were connected to viton tubing (ID=3.5 mm) leading to influent and effluent containers. The top inlet plug was clamped and was not used for incoming flow. The plug was only unclamped to draw liquid upward at the beginning of a $KMnO_4$ flush to help create uniform flow of $KMnO_4$ into the sand. Stainless steel screens and mesh, both with openings of 1.0 mm, were joined and installed to create open reservoirs at either end of the tank. The open reservoirs were designed to create constant head conditions along either end of the tank and provide uniform flow conditions in the porous medium. Four stainless steel plugs ($\varnothing$=1.7 cm) were placed along the top of the tank to provide openings whereby sand could be added. It was necessary to add a larger aperture positioned in the middle of the top of the tank (26.0 cm x 2.5 cm) to allow more access into the tank. This opening provided an easier means for filling the tank with fine sand and for

Figure 3.1: Experimental tank design.

EFFLUENT

INFLUENT

ALUMINUM FLAT BAR (2.5 cm width)

TEMPERED GLASS (1.0 cm width)

ALUMINUM TOP PLATE (26.0 x 5.1 x 1.3)

PLUGS (∅=1.7 cm)

CLAMPED INLET

FLOW

2.5

2.5

2.5

STAINLESS STEEL SCREENS AND MESH

GLASS BEADS (∅=5.0 mm)

COARSE SAND LENS (15.0 x 2.8 x 1.0)

FINE SAND (76.8 x 2.8 x 30.6)

OVERALL TANK DIMENSIONS (91.7 x 6.6 x 35.8)

PORT A

PVC PLUGS (ID=2.0 mm)
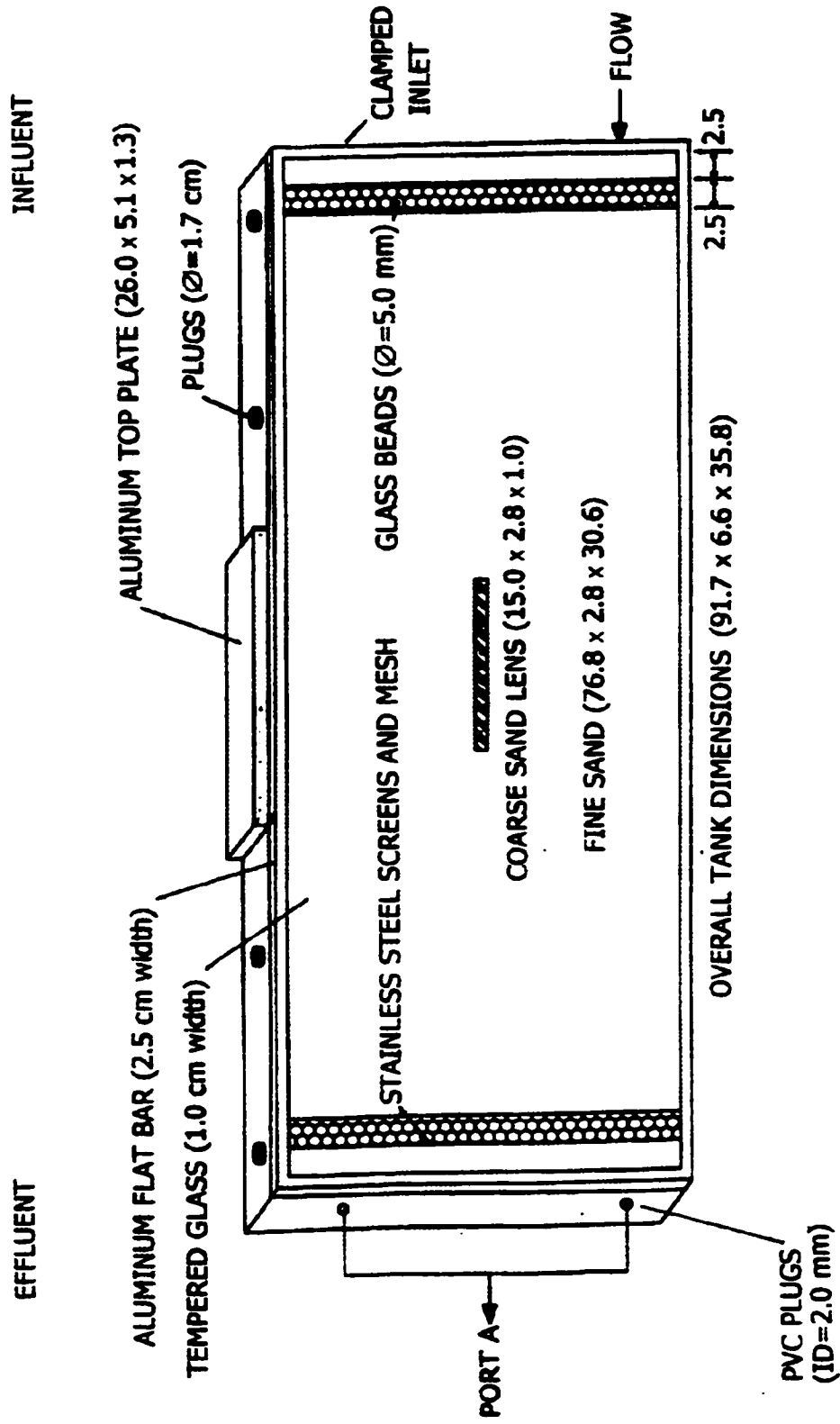
*drawn to scale
*dimensions are given in cm
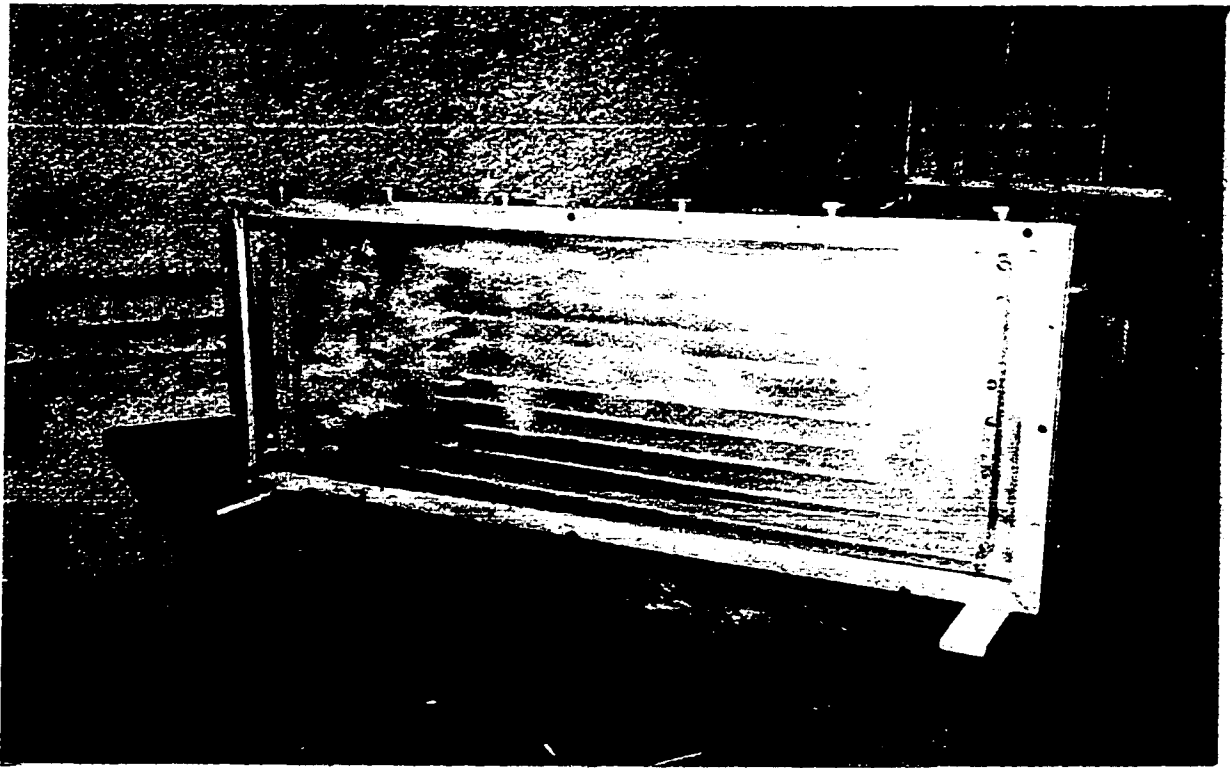
Figure 3.2: Experimental tank.
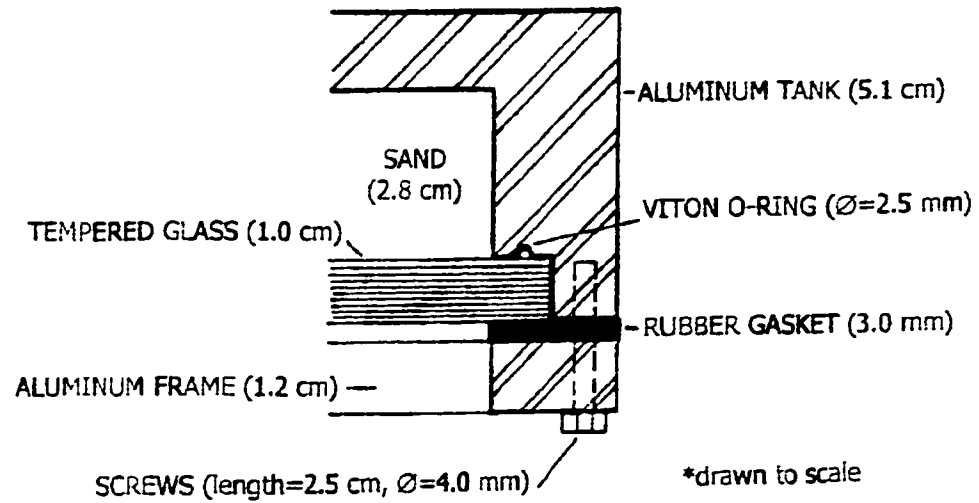
Figure 3.3: Cross-section of tank.

35

positioning the single coarse sand lens (see Section 3.3.3).

Figure 3.4 indicates the location of 10 point sampling ports labelled B-K in the back of the tank. Teflon septa ($\varnothing$=6.0 mm) placed in each sampling port allowed insertion and removal of syringe needles without causing leakage. The sampling ports B-K were placed 2.0 cm above and downstream of the coarse sand lens/DNAPL pool to allow measurement of the aqueous concentrations of species of interest. Effluent samples were collected at port A.

Figure 3.4: Sampling port locations: Back view of tank

*drawn to scale
*dimensions are given in cm

3.3 Experimental Procedures

The following sub-sections describe the procedures that were followed in preparing the tank for an experiment. Minor modifications to these procedures were made as necessary and are discussed.

3.3.1 Leak Testing

After construction of the experimental tank was completed, it was pressure-tested to ensure that neither liquid nor sand could escape. This proved to be a challenging task and several adjustments were made to the tank design to improve the seal of the viton o-ring surrounding the front of the tank. Vacuum grease was used to increase the seal of the o-rings in the top plate and along the front of the tank. Failure at the corners of several pieces of glass necessitated the use of thicker glass. A suitable piece of tempered glass 1.0 cm in thickness was ultimately used to form a tight seal without cracking. A rubber gasket was also positioned between the glass and aluminum frame on the front of the tank to protect the glass when the frame was tightened. Leaks also occurred from the plugs positioned along the top of the tank. Teflon tape wrapped around the plugs provided an effective seal. Experiments did not begin until the tank was adequately tested and proven to be leak-proof.

3.3.2 Sand Characteristics

Two quartz sands employed in all experiments were chosen to provide a flow velocity of approximately 1.0 m/day with reasonably small head drop and low operating pressure. Coarse sand was used for placement of the DNAPL pool and was chosen such that DNAPL would preferentially remain in the coarse sand due to differences in capillary characteristics between the fine and coarse sand. Because the fine-grained sand used in all experiments had a higher capillary entry pressure than the capillary pressure in the coarse sand, DNAPL injected into the coarse sand lens remained in the lens and did not enter the fine sand. This created a single well-defined DNAPL pool in the centre of the tank that could then be studied.

To produce a more uniform grain size and homogeneous packing, all sand was sifted before use in experiments. Fine quartz sand was sifted through a #50 sieve to remove coarse grains and a #60 sieve to remove fine particles. Similarly, coarse silica sand was sifted through a #20 sieve to remove coarse grains and a #30 sieve to remove fine grains.

Sand porosity was calculated based on a laboratory procedure outlined in Fetter (1994). A known volume of sand was placed in an oven at 105°C for 24 hours to remove all moisture. The mass of this sample was measured and used to determine the bulk density. The porosity was then calculated as outlined in Appendix A. Six sand samples for both fine and coarse sand were tested and results averaged. The porosity of the fine quartz sand was found to be 0.44 and

39

the coarse silica sand was 0.49 with standard deviations of 0.80% and 1.67% respectively.

3.3.3 Experimental Preparation

Following successful leak testing, the tank was filled in approximately 2 cm lifts of fine sand to a depth 0.5 cm below the DNAPL injection port; after each lift was added, the tank was lightly tapped to compact the sand. Two vertical barriers, constructed of stiff cardboard, were then placed 15.0 cm apart and 1.0 cm above the fine sand to assist in positioning the coarse sand lens. The coarse sand was then placed between the two barriers to a thickness of 1.0 cm and the same thickness of fine sand was placed outside of the barriers. The barriers were then removed from the tank, leaving a coarse sand lens (15.0 cm x 2.8 cm x 1.0 cm) positioned 2.0 cm below sampling ports I-K and 2.0 cm upstream of sampling ports B-H (refer to Figure 3.4). Upon careful placement of the coarse sand lens, the remaining top half of the tank was filled with fine sand in the same manner as the lower half. Glass beads placed at either end of the tank provided constant head conditions by distributing liquid to produce uniform flow. Glass wool and coarse sand were also tested for this task in experiment 2 but the glass beads were found to be the most effective. Due to passage of fine sand into the influent and effluent glass bead packs during experiment 1, stainless steel mesh was coupled with the stainless steel screens. This

combination provided a more effective barrier to the sand. Figure 3.5 shows the tank prepared for experimentation.

The sand was flushed with carbon dioxide (CO_2) for a minimum of one hour to displace air in the sand. CO_2 dissolves into water more readily than nitrogen (N_2), which comprises 79% of air (88.0 mL CO_2 will dissolve in 100.0 mL of water compared to 1.6 mL N_2 at 20°C and 760 mm pressure) (Budavari et al., 1989). The sand was then saturated with de-ionized, de-aired water for a minimum of 5 days to ensure complete saturation. This process ensured that all gas originally in the tank dissolved in the water and was removed.
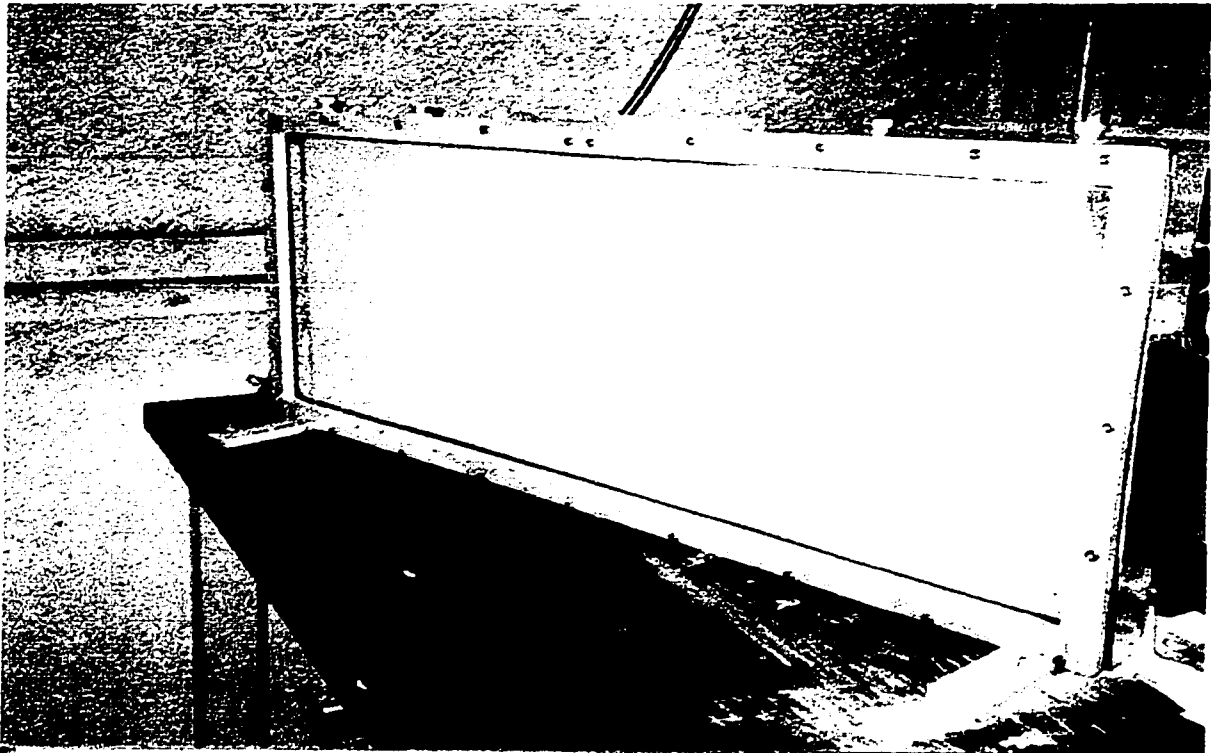
Figure 3.5: Tank filled with sand prior to experimentation.

During the initial saturation of the sand, settling of the fine sand occurred and gaps developed along the top of the tank. To correct for this, fine sand was added through the openings along the top of the tank and compacted as much as possible.

Solutions of $KMnO_4$ of the desired concentration were prepared by dissolving $KMnO_4$ crystals in de-ionized, de-aired water. Solutions were thoroughly mixed at a rate of 100 rpm using a Philips and Bird Stirrer Model 7790-400. Mixing was continued at the same rate during the entire course of $KMnO_4$ injection. $KMnO_4$ solutions held in 45 L glass containers were covered with aluminum foil to protect the liquid from halodecomposition.

3.3.4   Flow Rate

Flow rates were maintained using a Cole-Parmer peristaltic pump equipped with a Masterflex PTFE Tubing Pump Head Model 77390-00 employing 4.0 mm OD PTFE tubing. A flow rate of 2.26 mL/min was maintained to establish an average flow velocity of 0.001 cm/s in the sand representative of a realistic groundwater velocity. This flow rate produced approximately 1 pore volume of flow through the tank per day or 3.0 L/day. Measurements of flow were checked at the tank effluent at least 2 times per day using a graduated cylinder. Influent volumes were recorded and verification of this measurement was made with an overall mass analysis to ensure the accuracy of the flow rates and volume of solution injected. The mass analysis measured the weight of the

effluent exiting the tank over a certain period of time and this measurement was compared to the volume of solution injected and volumetric flow measurements made daily. The verification and accuracy of all flow measurements was within 4%. This small difference can be accounted for by unweighed liquid remaining in the tank. The pump speed was held constant throughout the duration of the experiment but daily flow rates fluctuated slightly between 2.17 and 2.50 mL/min. Refer to Appendix B for flow rates and flush volumes associated with each experiment and a flow rate profile from the $KMnO_4$ flush of experiment 3.

3.3.5 DNAPL Emplacement

In all experiments, DNAPL was introduced into the coarse sand lens to establish a DNAPL saturation representative of a pool. Injection of DNAPL into the centre of the coarse sand layer was accurately accomplished using a Harvard Apparatus Pump 22 equipped with a Becton Dickinson 20 mL glass syringe (19.13 mm gauge) inserted through a port in the back of the tank. TCE and PCE were evenly injected at a rate of 10.0 mL/hr for experiments 1 and 2, respectively, and a rate of 4.0 mL/hr was used for PCE injection in experiment 3. At these injection rates, disruption of the sand was not observed and there was no indication of DNAPL outside of the coarse sand lens. Injection of DNAPL was performed after the sand was completely saturated; the experiment began after injection was completed and the water flush was resumed.

3.3.6 Sampling Procedures

Sampling procedures were similar for all experiments. Effluent and point samples taken downstream and above the coarse sand/DNAPL lens were collected during water and $KMnO_4$ flushes. Airtight glass syringes ranging in volume from 10.0 μL to 500 μL were used for sampling. Syringe samples extracted from sampling ports B-K were withdrawn slowly over a period of 3 minutes to reduce volume averaging of the sample. Needles were inserted into the port to a depth corresponding to the centre of the sand thickness to withdraw each sample; a mark on the needle served as a depth gauge in order to achieve this. No disturbance of the sand or liquid was observed during sampling. Syringe volumes of 0.0010-0.050 mL were taken for TCE analysis and 0.010-0.25 mL for PCE analysis. All PCE/TCE samples were diluted to 10.0 mL with de-ionized water, placed in headspace vials sealed with Teflon septa and refrigerated in the absence of light. Volumes ranging from 0.10-1.0 mL were diluted to 100.0 mL for titration to determine $KMnO_4$ concentration. Small volumes of $KMnO_4$ solution were taken at the beginning of each experiment from the influent to verify the concentration of $KMnO_4$ solution injected. Samples 1.0 mL in volume were diluted to 100.0 mL for chloride electrode analysis.

3.4 Analytical Methods

Analysis of PCE and TCE was completed with a Hewlett Packard 5890A Flame Ionization Detector (FID) Gas Chromatograph (GC) equipped with a 30 m

DB1 column using N_2 carrier gas with a flowrate of 1.5 mL/min. Concentrations

of samples were determined using a calibration curve prepared from the

integrated area of external standard solutions as specified by US EPA Method

3810 (1986). Initially, analysis of PCE and TCE was to be completed using a

Varian CP-3800 GC equipped with an Electron Capture Detector (ECD) with

sample introduction via a Genesis Headspace Autosampler. ECD techniques are

superior to FID techniques because of the high selectivity to halogens resulting

in low detection limits. However, due to numerous problems that were

encountered when trying to apply the ECD technique, this instrument could not

be used.

Concentrations of $KMnO_4$ were determined by titrimetry using sodium

thiosulfate ($Na_2S_2O_3$). $Na_2S_2O_3$ was first standardized with potassium iodate

(KIO_3) according to Standard Methods 4500-Cl⁻ B (Eaton et al., 1995). Titration

of $KMnO_4$ by $Na_2S_2O_3$ was based on a procedure from Kolthoff and Sandell

(1946).

An Orion Model 94-17B Chloride Ion Selective Electrode (ISE) with a

double junction reference electrode was used to analyze chloride concentrations.

Standards were prepared according to Standard Methods 4500-Cl⁻ D (1995).

Addition of Ion Strength Adjustor (ISA) was based on 2.0 mL per 100.0 mL of

standard or sample. The pH of all samples was adjusted from approximately pH

5 to pH 12-13 prior to analysis by adding 0.5 mL of 5 M sodium hydroxide

(NaOH) to quench the reaction between $KMnO_4$ and the chlorinated organic.

This step was critical in order to obtain readings without damaging the chloride electrode.

Several methods including dilution of samples, removal of $KMnO_4$ by titration with $Na_2S_2O_3$ and consumption of $KMnO_4$ by ethanol were tried in the attempt to analyze chloride by the ISE technique without success. An argentometric titration with silver nitrate was also attempted to analyze chloride but this also proved unsuccessful. Researcher M. Schnarr (1992), who measured chloride in a similar solution matrix using the ISE technique, was contacted for advice; it was reported that many electrodes were damaged through this method of analysis and readings that were published were in fact estimations. A further attempt was made to analyze chloride by first quenching the $KMnO_4$ reaction through the addition of NaOH before submerging the electrode in the sample, which initially seemed promising. However, interference proved to make the chloride readings highly uncertain.

It was finally decided that the available equipment was not capable of accurately measuring chloride in the presence of $KMnO_4$ and chloride concentration measurements were abandoned. Therefore, determination of mass transfer rates during the $KMnO_4$ flush was not possible due to the inability to measure chloride. The original objectives to measure pretreatment, treatment and post-treatment mass transfer rates proved too difficult at this time. However, other observations provided very interesting results with significant implications as discussed in Chapter 4. Original objectives also included the

development of a data set for verification of numerical models. However, due to the complexity of the system and difficulties with chemical analyses, the data set for mass transfer rates and removal efficiency was not collected and is unavailable for model development.

3.5 Materials

$KMnO_4$ (99+% purity) was purchased from BDH Inc., Toronto, Ontario. Research grade PCE and TCE were both purchased from Aldrich Chemical Co., Milwaukee, WI (99+% and 99.5+% purity respectively).

Chemicals used in titrimetry included $Na_2S_2O_3$ which was Certified American Chemical Standard (A.C.S.) supplied by Fisher Scientific, Fairlawn, N.J. and KIO_3 and potassium iodide (KI) which were both acquired from BDH Inc.

Chemicals used to prepare chloride standards included sodium chloride (NaCl) purchased from BDH Inc.; ISA was prepared from 5 M sodium nitrate ($NaNO_3$) supplied by Fisher Scientific; NaOH was prepared from reagent provided by BDH Inc.; pH indicator strips assisted in pH adjustment.

All water used in chemical preparation was de-ionized. Water used in experiments was also de-ionized and de-aired for approximately 5 days prior to use.

Glass beads ($\emptyset$=5.0 mm) obtained from Fisher Scientific were used to distribute flow at the tank inlet and outlet. Fine quartz sand (#56 mesh) was

supplied by Barnes Environmental Int., Waterdown, Ontario and coarse silica

sand (#25 mesh) was supplied by Sunrise Pools Co., Windsor, Ontario.

3.6 Sources of Error

As with any experiment, errors inevitably occur that affect the reliability of

the results. Errors may be systematic due to analytical techniques and

instrumentation or random which are of a human nature.

Calibration curves for GC analysis were repeated several times and

verified for accuracy. Standards were analyzed with all sample runs to check the

accuracy of a given calibration curve. Blanks were always analyzed with all

sample runs. Each $KMnO_4$ titration was performed using 3 replicates to check

repeatability with the average used as the reported value. This was also done

for the chloride analysis, however these values were highly unreliable as

discussed in Section 3.4.

Chapter 4 provides a more detailed analysis of errors associated with

experimental conditions and chemical analysis.

4   RESULTS AND DISCUSSION

4.1   Introduction

This chapter presents results and discussion for the three two-dimensional tank experiments discussed in Chapter 3. Results are based on interesting visual observations and processes that occurred throughout the course of the experiments as well as data from sample analyses. Discussion will relate experimental results to observed phenomena.

As previously mentioned, three individual experiments were performed, each with varying conditions. This chapter will elaborate on the rationale for the changes implemented in each experiment with respect to $KMnO_4$ concentration, volume of DNAPL injected and the duration of each experimental flush.

4.2   Dissolution: Pretreatment Water Flush

4.2.1   Saturation of Sand Prior to DNAPL Introduction

Figure 4.1 shows the initial saturation of sand with de-ionized, de-aired water. The figure illustrates the preferential pathway of flow, which was typical for all three experiments. Due to differences in capillary characteristics between the fine and coarse sand, water was drawn only into the fine sand through capillary suction. Once the fine sand below the coarse sand lens was at positive pressure, water began to enter the coarse sand lens as shown in Figure 4.2.

Figure 4.1: Experiment 1: Initial saturation of sand prior to DNAPL introduction.
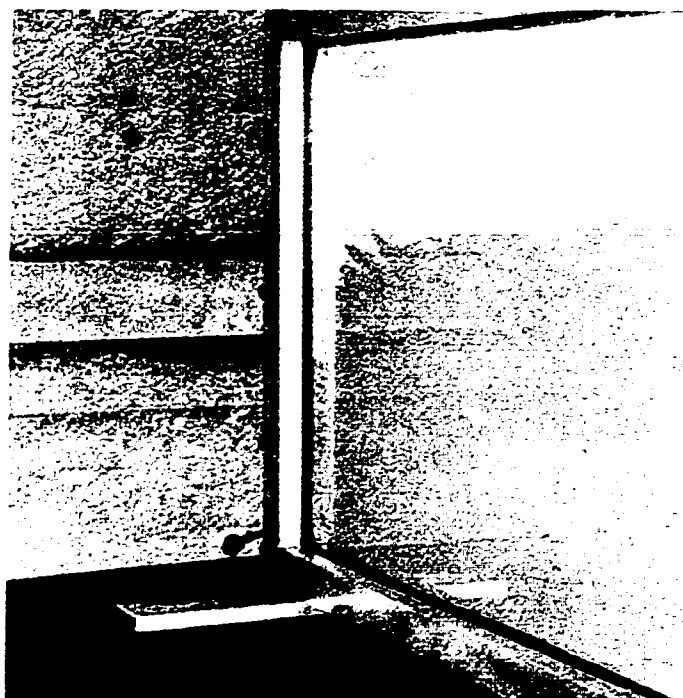
Figure 4.2: Initial saturation of sand prior to DNAPL introduction: Water entering the coarse sand lens.

Initially, the coarse sand remained partially saturated because gases from the coarse sand lens were trapped by imbibed water in the fine sand. Continued water injection wetted the remainder of the fine sand. Trapped gases in the fine sand and coarse sand slowly dissolved and disappeared after several days of flushing.

After complete saturation of the sand was accomplished, DNAPL was injected and the flush of de-ionized, de-aired water began. PCE/TCE concentrations were measured from effluent port A and sampling ports B-K during the water flush. Results are grouped accordingly for each experiment in the following sections.

4.2.2 Dissolution: Effluent

Approximate volumes of water injected into the tank for the pretreatment water flush were: 18.0 L or approximately 6 pore volumes in experiment 1, 4.15 L or approximately 1.4 pore volumes in experiment 2 and 5.11 L or approximately 1.7 pore volumes in experiment 3. Effluent PCE concentrations obtained from samples taken during the pretreatment water flush of experiment 2 and experiment 3 were below the detection limit of 0.01875 $\mu g/mL$. Results from samples taken during the pretreatment water flush of experiment 1 provided the only source of information associated with DNAPL effluent concentrations and dissolution processes.

Effluent TCE concentrations for the pretreatment water flush from

experiment 1 are shown in Figure 4.3. Measured concentrations were less than

55.0 µg/mL (55.0 mg/L) but varied as the flush progressed. Fluctuations in

concentration may have been caused by variations in flow rate. The dissolved

aqueous phase concentrations measured were considerably lower than the TCE

solubility limit of 1100 mg/L (Pankow et al., 1996) due to dilution. Results are

similar to results obtained from solubilization experiments conducted by Schwille

(1988) who measured TCE concentrations from a pool in a flat trough; measured

concentrations were below 90 mg/L. PCE concentrations obtained from effluent

samples taken during the post-treatment water flush of experiment 3 are

presented in Section 4.5.1.
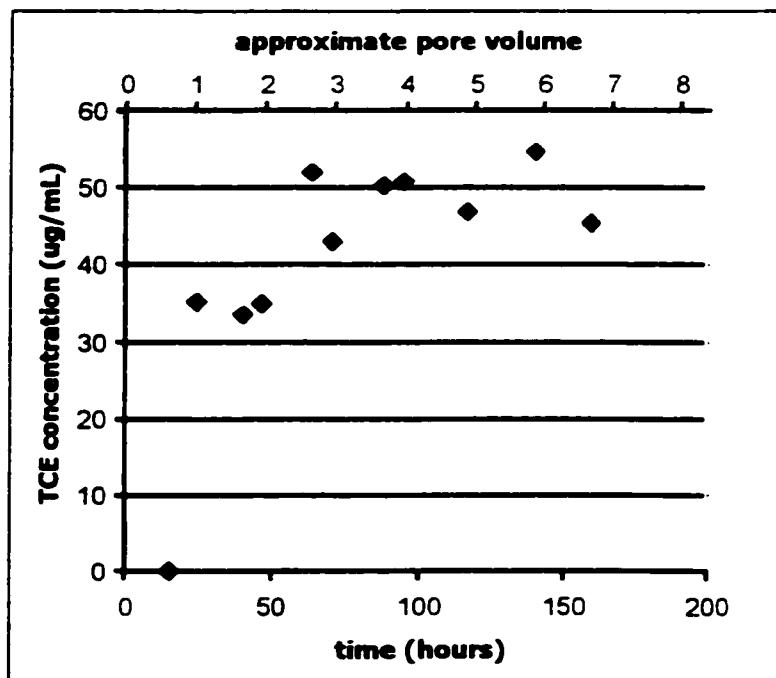
Figure 4.3: Experiment 1: Effluent TCE concentrations for pretreatment water flush.

4.2.3 Dissolution: Point Samples

Point samples were obtained downstream and above the DNAPL pool to provide DNAPL concentration data in the vicinity of the pool as water flowed past the DNAPL pool. This data provided estimates of transverse dispersion that influence mass transfer rates from the pool. Refer to Figure 3.4 for sampling port locations. Several sets of point samples were obtained during experiment 1 while relatively few samples were taken for experiment 3 due to the short pretreatment water flush. Point samples were not taken during the brief pretreatment water flush of experiment 2.

TCE concentrations analyzed during the pretreatment water flush of experiment 1 from sampling ports B-H downstream of the pool are given in Figure 4.4. Concentrations fluctuated for each individual port with respect to time. Concentrations for ports B, C and D were similar and within the range of 57.0-67.0 μg/mL. Ports B, C and D were located downstream and below the level of the coarse sand lens. Because concentrations of TCE below and downstream of the pool were not elevated, it appeared that TCE remained in the coarse sand lens and did not migrate into the fine sand due to gravity. TCE concentrations measured at ports E-H were between the range of 398–956 μg/mL.

Figure 4.5 illustrates experiment 1 TCE concentrations for sampling ports I, J and K located above the TCE pool. Dissolved aqueous concentrations
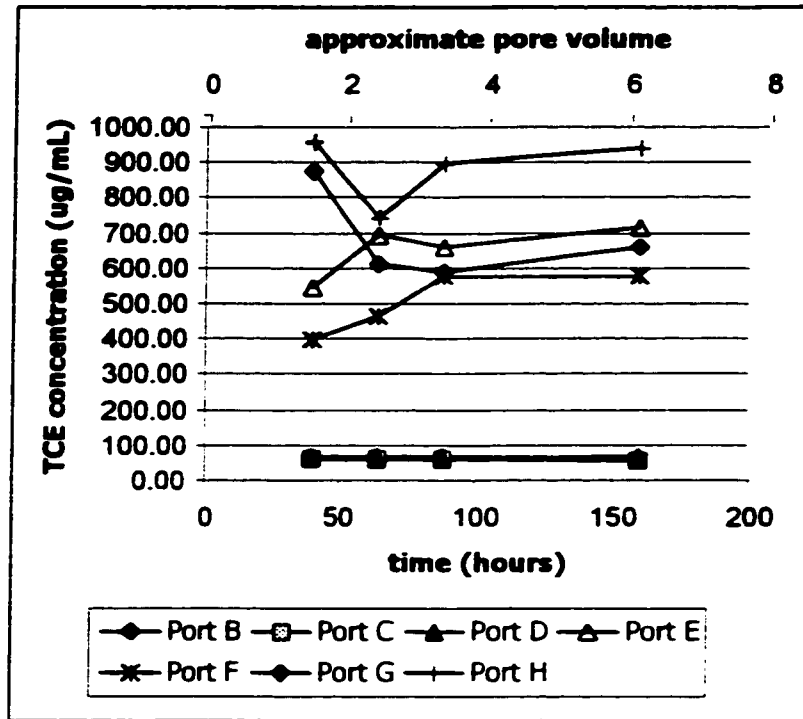
Figure 4.4: Experiment 1: TCE concentrations for sampling ports B-H for pretreatment water flush.
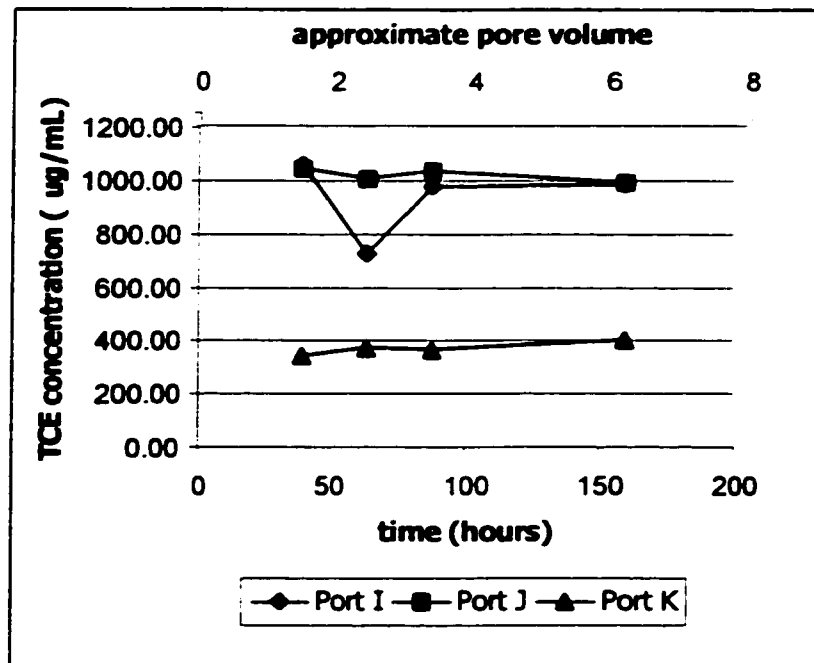
Figure 4.5: Experiment 1: TCE concentrations for sampling ports I-K for pretreatment water flush.

measured at ports I and J were near the TCE solubility limit indicating that concentrations equal to the aqueous solubility of TCE existed within the pool.

Figure 4.6 shows the average TCE concentrations from point sample locations in relation to the DNAPL pool. Concentrations appeared to increase as the vertical distance increased from ports F to H, with the highest concentration detected at port H. This result was not expected and appeared to indicate that water flow was not strictly horizontal but was also moving vertically within the vicinity of the pool. The figure shows the elevated TCE concentrations at ports I and J. TCE concentrations around the pool approached aqueous solubility, which indicates that pore-scale mass transfer within the pool was rapid enough to achieve TCE solubility within the pool.

H • 883

G • 684

372   1019   936

• K   • J   • I   F • 504

Flow

→   DNAPL Pool   E • 652

D • 62

C • 59

B • 64
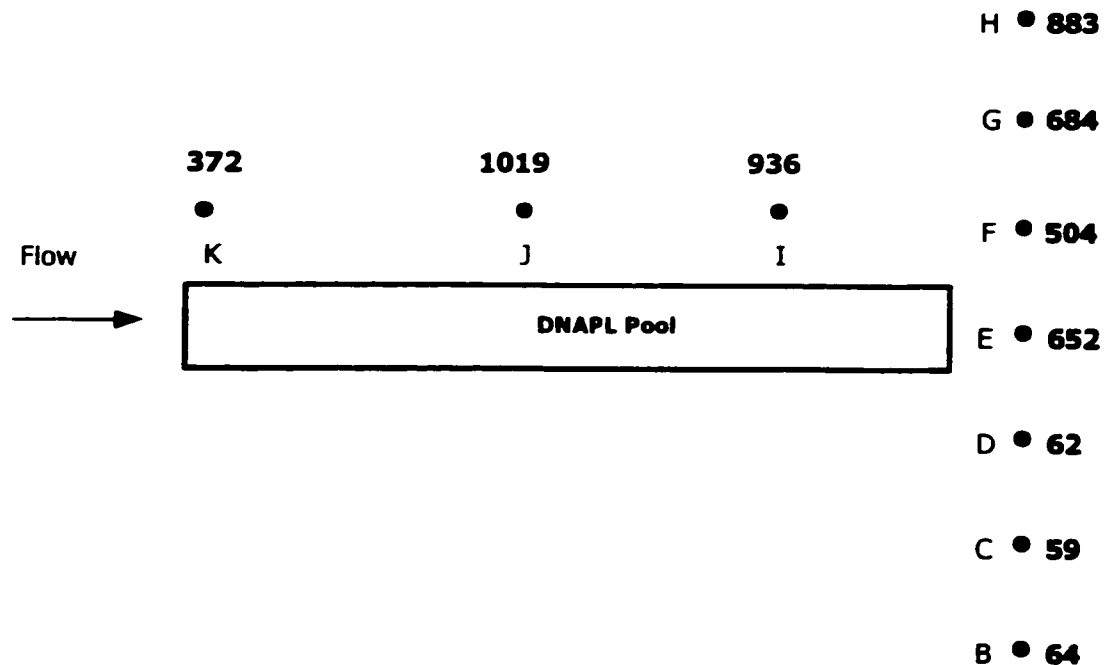
Figure 4.6: Experiment 1: Average TCE concentrations for all sampling ports for pretreatment water flush.

Therefore, results from the pretreatment water flush of experiment 1 suggest that macro-scale mass transport from the DNAPL pool to the surrounding water limits overall mass transport rates rather than pore-scale mass transfer within the pool. This in turn indicates that mass transfer into flowing water will tend to occur along the long edges of a DNAPL pool and this process will control dissolved aqueous concentrations.

Samples taken from vertical ports C, F and G during the pretreatment water flush of experiment 3 yielded very low PCE concentrations while ports D and E located directly behind the pool yielded higher concentrations (refer to Figure 4.7 and Figure 4.8). Measured PCE concentrations for ports D and E were approximately 100 μg/mL (100 mg/L), which approached half of the PCE solubility limit of 200 mg/L (Pankow et al., 1996). Samples from ports I, J and K were not taken. The point sample results for experiment 3 differed significantly from experiment 1 as only points located directly downgradient of the DNAPL pool showed elevated PCE concentrations. This indicates that flow in experiment 3 was essentially horizontal whereas in experiment 1 this likely was not the case. The difference in flow direction could possibly be attributed to subtle heterogeneity in the fine sand. Figure 4.1 taken from experiment 1 shows that heterogeneity existed in the fine sand at the upper side and downgradient end of the coarse sand lens, which may have created a vertical flow component at that location during the flushing. Evidence of heterogeneity that caused upward flow behind the pool is shown in Figure 4.1 where water, indicated by darker coloured

56
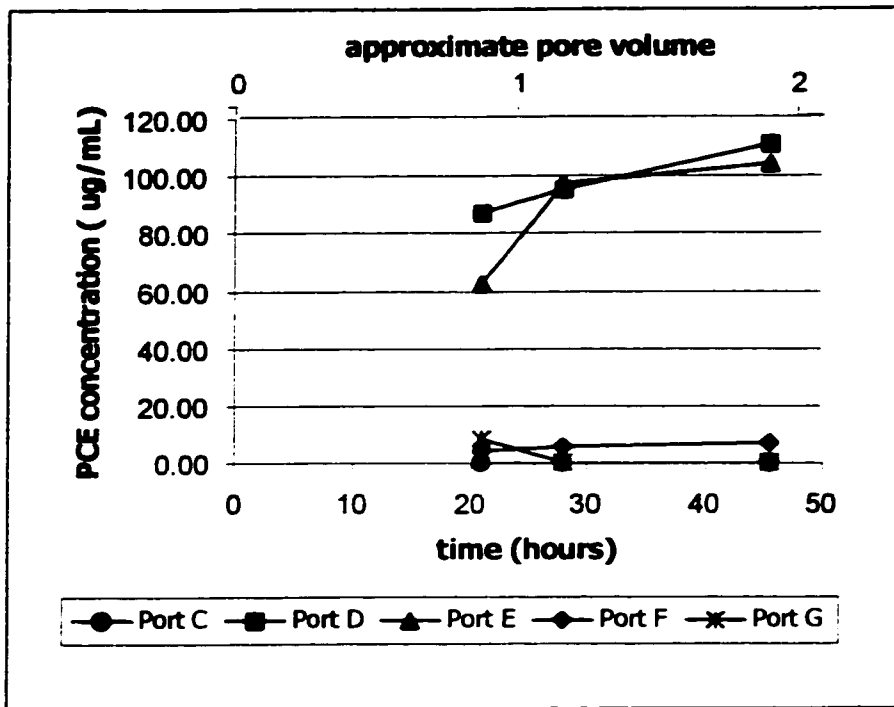
Figure 4.7: Experiment 3: PCE concentrations for sampling ports C-G for pretreatment water flush.
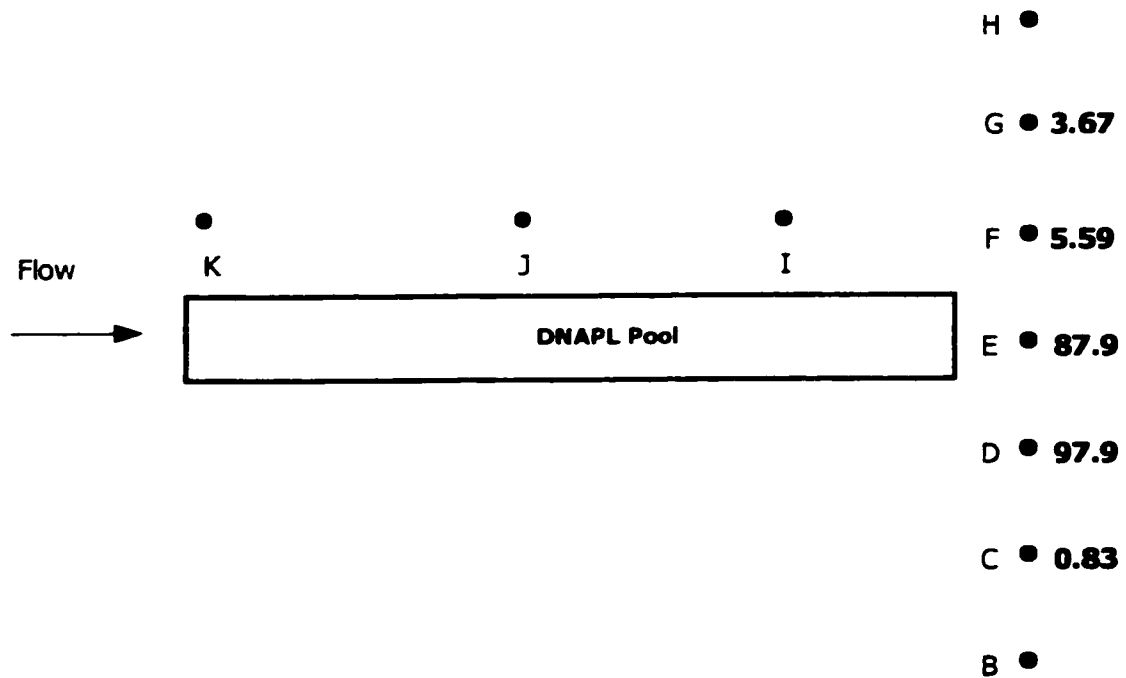
Figure 4.8: Experiment 3: Average PCE concentrations for sampling ports C-G for pretreatment water flush.

saturated sand, was moving in a wedge at the downgradient end of the coarse sand lens. There was no particular evidence of this phenomenon in experiments 2 and 3.

4.3 In Situ Oxidation: KMnO₄ Flush

This section describes observations noted during each $KMnO_4$ flush that followed the pretreatment water flush. Findings from the $KMnO_4$ flush for each experiment will be given chronologically. Discussion will focus on a number of important processes that occurred during $KMnO_4$ oxidation that may impact mass removal rates.

The beginning of each $KMnO_4$ flush was closely observed to monitor the progression of the flush. Visual observation of the initial progression of $KMnO_4$ flow was obvious due to the intense purple colour of the potassium permanganate. Figure 4.9 shows the beginning of a flush and the $KMnO_4$ front. Pathways associated with $KMnO_4$ flow as the flush reached the DNAPL pool provided clues as to what type of processes occurred. The coarse sand lens/DNAPL pool and fine sand immediately surrounding the lens were observed for reaction products such as MnO_2 and CO_2, which would visually indicate oxidation reactions. MnO_2 precipitated leaving a dark black discolouration in the sand (see Figure 4.10) and where significant amounts of CO_2 were produced, gas bubbles in the sand were observed. Visual observations were noted throughout the duration of a given $KMnO_4$ flush and time-lapsed pictures were taken.

Figure 4.9: Experiment 1: The beginning of the KMnO$_4$ flush.

Figure 4.10: Experiment 1: KMnO$_4$ flush at 19.0 hours.

Breakthrough of KMnO₄ occurred approximately 24 hours or 1 pore volume after the flush began in every experiment.

4.3.1 Experiment 1: KMnO₄ Flush

Experiment 1 employed a $KMnO_4$ flush of concentration 10.0 g/L to treat a DNAPL pool containing 5.0 mL of TCE. Figures 4.10 to 4.13, taken during the initial stages of experiment 1, illustrate the progression of the $KMnO_4$ flush and oxidation reactions occurring within and around the TCE pool. Initially, most of the flow was diverted around the pool due to reduced permeability of the coarse sand lens caused by the relatively high TCE saturation in the lens. As evidenced by Figure 4.10, reaction of $KMnO_4$ with the front of the TCE pool occurred and small amounts of MnO_2 were deposited inside the pool and around the front edges. MnO_2 also contributed to a reduction in permeability at the front of the pool. Reactions mostly took place at the top, bottom and front of the pool, where MnO_2 reduced permeability and diverted more flow around the pool. Therefore, most of the reaction between $KMnO_4$ and the TCE pool occurred around the perimeter of the pool and reaction inside the pool was minimal.

The production of CO_2 gas was observed in all three experiments, most notably for experiment 1. In experiment 1, CO_2 gas production was rapid and led to nearly immediate de-saturation of the coarse sand lens, along with a subsequent reduction of sand permeability to the $KMnO_4$ solution. The gas tended to travel in an upward direction and was easily recognized as bubbles

Figure 4.11: Experiment 1: KMnO₄ flush at 21.25 hours.
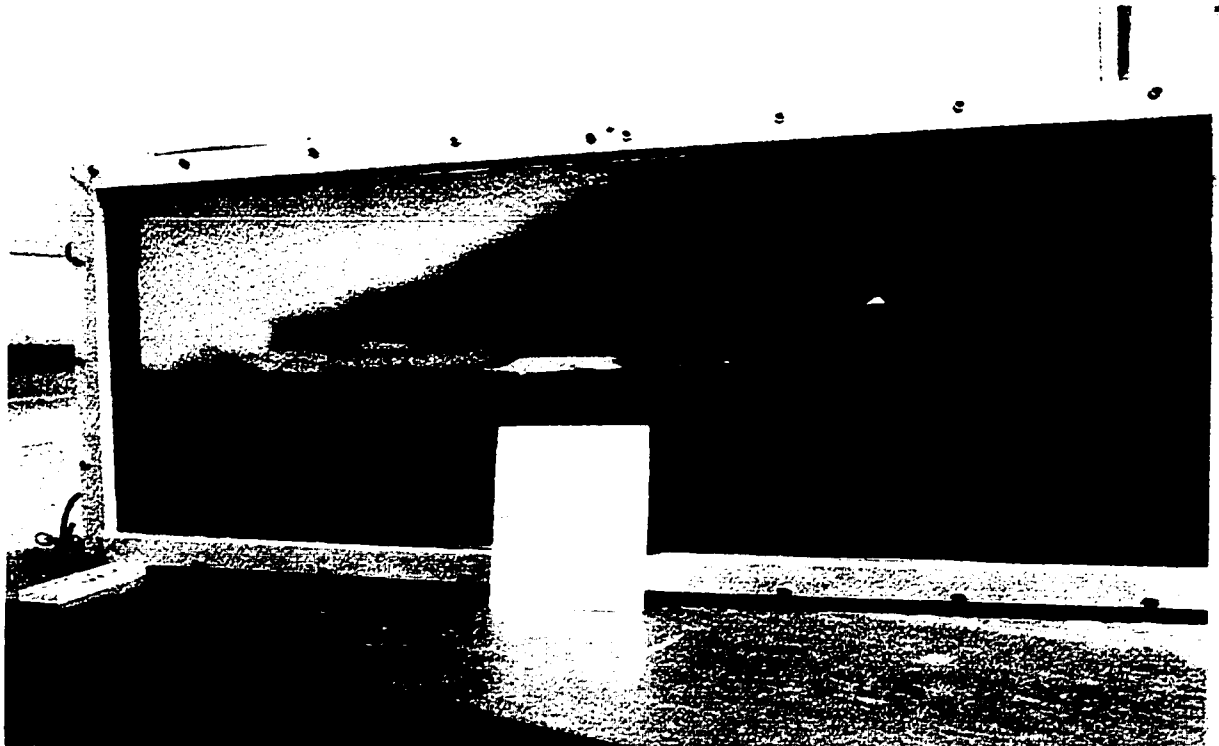
Figure 4.12: Experiment 1: KMnO₄ flush at 24.25 hours.

Figure 4.13: Experiment 1: $KMnO_4$ flush at 26.25 hours.

distributed in a vertical path above the coarse sand lens. Figure 4.13 shows

clearly that no reaction took place in the posterior half of the coarse sand lens

due to CO_2 de-gassing, MnO_2 plugging and presence of TCE. As the experiment

proceeded, MnO_2 formation was observed above the coarse sand lens coinciding

with zones of de-saturation where CO_2 had previously been noted. This effect

suggests that the CO_2 gas played a role in the transport of TCE vapour from the

coarse sand lens into the fine sand located above the lens. The CO_2 gas likely

served as a "carrier" for the TCE vapour and potentially may have enhanced

mass transfer by providing an additional mass transport mechanism from the

TCE pool. Figure 4.14 taken at 44.25 hours shows black zones of MnO_2 situated
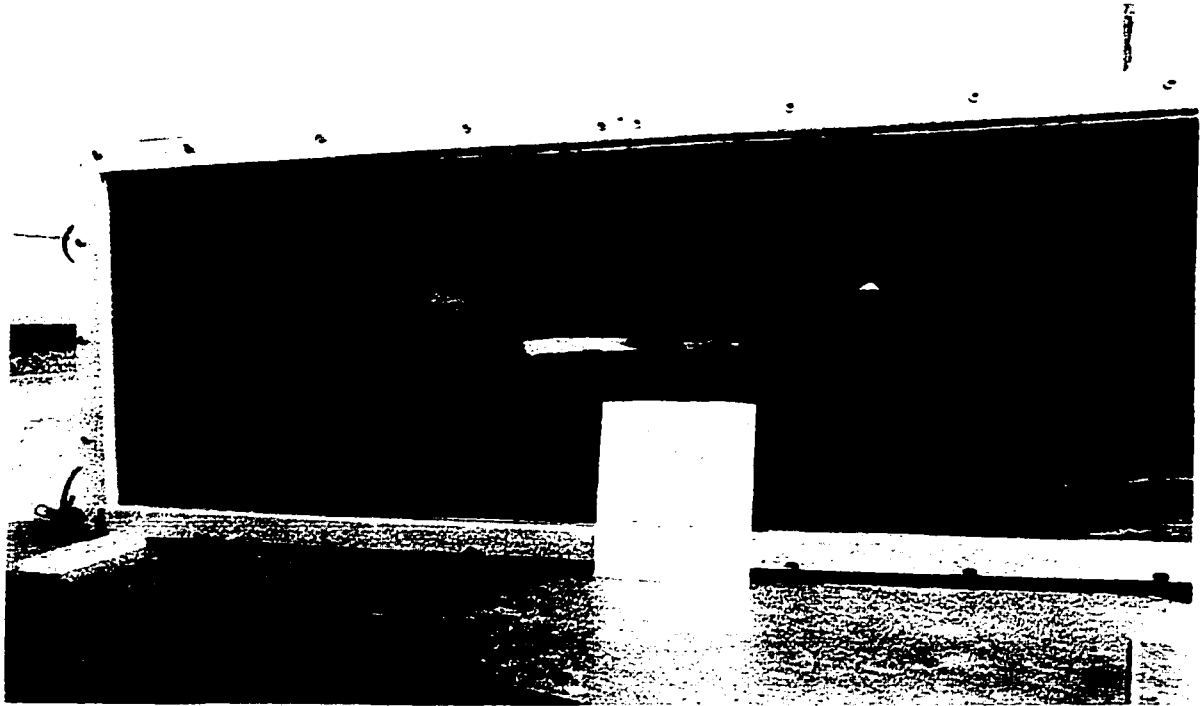
Figure 4.14: KMnO₄ flush at 44.25 hours.

directly above the TCE pool that coincided with zones of de-saturation and CO_2

gas. Fluctuation of flow rates during the $KMnO_4$ flush were observed and

attributed to CO_2 gas production and pressure in the tank.

Manganese dioxide served as an excellent indicator of where reactions

between $KMnO_4$ and TCE were occurring. MnO_2 solids were deposited around

the periphery of the coarse sand lens as oxidation occurred. Fine sand directly

surrounding the coarse sand lens/TCE pool turned a very dark brown and had a

crystal-like appearance. Figure 4.14 illustrates MnO_2 around the perimeter of the

TCE pool. Reduction in permeability around the pool due to MnO_2 may have

caused a decrease in mass transfer rates. As the flush progressed and mass

transfer from the TCE pool continued, a light brown MnO_2 plume was highly

visible downstream from the pool (refer to Figure 4.12 and 4.13). The slender shape of the plume extended outward from the pool in the direction of the flow. Figure 4.13 also illustrates MnO_2 extending as a thin dark brown strand downgradient of the coarse sand lens associated with a CO_2 zone at the upper side of the lens, which further indicates that CO_2 had a significant role in mass transfer.

Later in the experiment, MnO_2 was noted in the effluent glass bead pack along the screens and to a lesser extent, along the influent screens. Eventually, the accumulation of MnO_2 (approximately 1.0 cm thick) along the effluent screens and in the glass bead pack caused severe plugging. It was therefore reasonably concluded that the $KMnO_4$ solution had oxidized the stainless steel screens and mesh. Due to pressure that built in the tank as a result of plugging, leaks developed along the bottom of the tank and from sampling port septa 75 hours after the $KMnO_4$ flush had begun. Because of serious leakage, experiment 1 was ended and a post-treatment water flush was not possible.

Accumulation of CO_2 within the coarse sand lens likely caused the de-saturation of the coarse sand lens and subsequent mobilization of TCE. Several pieces of evidence substantiate this fact including the appearance of MnO_2 in unexpected areas of the tank and the strong odour of TCE in the effluent bead pack when the tank was disassembled. MnO_2 solids not associated with either CO_2 gas or expected aqueous transport processes from the pool were observed directly downgradient of the pool and in the bottom of the effluent bead pack.

DNAPL mobilization was also noted in experiment 2 and experiment 3 which is discussed in Section 4.3.2 and Section 4.3.3, respectively.

The high rate of CO_2 production resulted in a dramatic reduction in permeability of the coarse sand lens in experiment 1. This may have significant implications for $KMnO_4$ treatment because DNAPL tends to pool in coarse-grained porous media. During a $KMnO_4$ flush, if the coarse media contains large volumes of CO_2 gas, flow will be diverted around the DNAPL pools, thereby reducing treatment efficiency. Injection of $KMnO_4$ solution may become very difficult due to the significant production of CO_2, and in addition, flow may be restricted to fine-grained layers with lower permeability as observed by LaChance et al. (1998).

4.3.2 Experiment 2: $KMnO_4$ Flush

Several variables were altered for experiment 2 in the attempt to avoid complete MnO_2 plugging, CO_2 de-gassing and DNAPL mobilization that were encountered in experiment 1. To reduce the amount of MnO_2 produced and eliminate potential plugging, the concentration of the $KMnO_4$ solution was reduced by a factor of 2. PCE, which has a slower reaction rate with $KMnO_4$ than TCE and therefore slower production of CO_2 gas, was used to reduce potential DNAPL mobilization. A second set of stainless steel screens and mesh were added to the tank. Glass wool and coarse sand were tested and used for flow distribution.

A DNAPL pool containing 5.0 mL of PCE was flushed with 5.0 g/L $KMnO_4$ during experiment 2. As illustrated by Figure 4.15, some $KMnO_4$ penetrated the coarse sand lens/PCE pool as opposed to experiment 1 where almost all flow was diverted around the lens. The relatively slow reaction rate between PCE and $KMnO_4$ enabled $KMnO_4$ solution to enter the lens whereas reactions in experiment 1 proceeded quickly, oxidation occurred at the front of the pool and prevented further penetration of $KMnO_4$ into the pool. Also due to the slower reaction rate, CO_2 production in experiment 2 was slower than in experiment 1, which allowed more flow into the DNAPL pool during experiment 2. After 24 hours, the presence of MnO_2 was observed in the PCE pool, indicating that oxidation of the PCE pool had already begun. At this time, CO_2 gas was not observed.

Figure 4.16 was taken at 47.5 hours. Advancement of oxidation of the PCE pool was evident by the increase in MnO_2 precipitation. The inside of the pool was light brown in colour, which indicated that some reaction was occurring inside the pool. A dark, thin layer of MnO_2 had formed around the perimeter of the pool and small plumes of MnO_2 could be detected upstream and downstream of the pool. Upon closer inspection of the pool, it was noted that areas of de-saturation were intermittently spaced throughout the coarse sand lens/PCE pool. Small amounts of CO_2 gas were observed above and upstream of the pool.
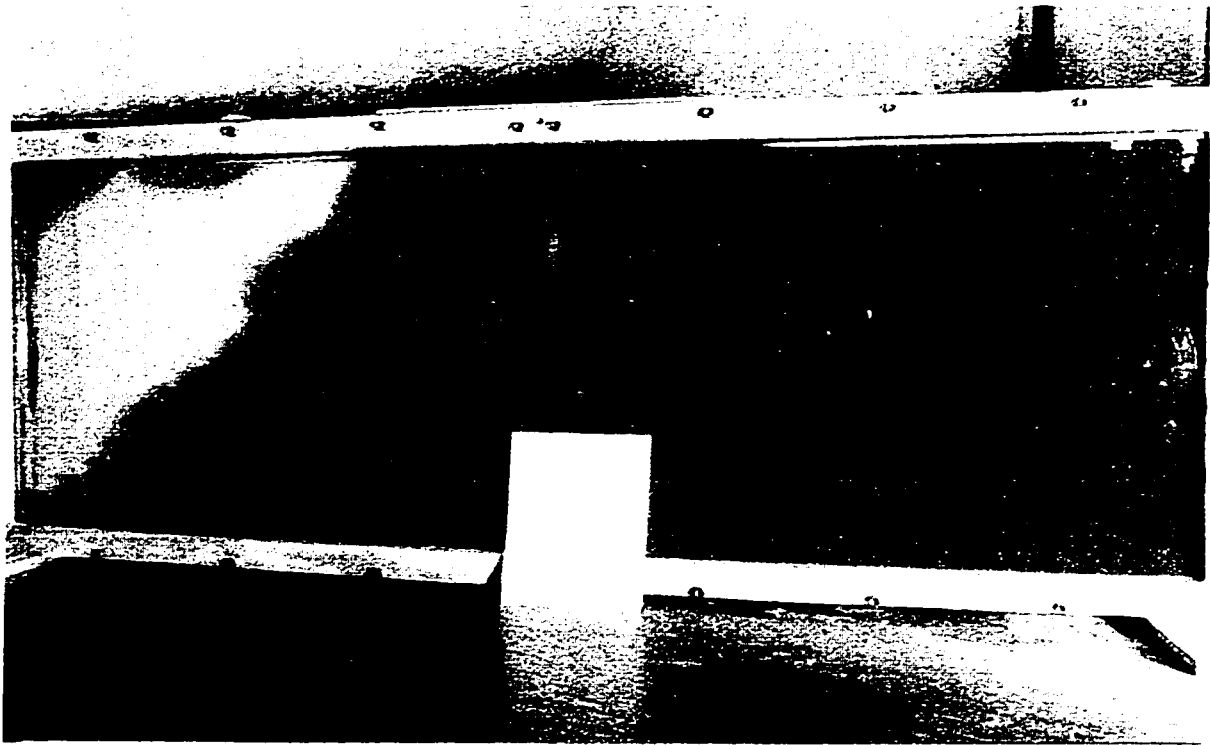
Figure 4.15: Experiment 2: KMnO$_4$ flush at 24.0 hours.
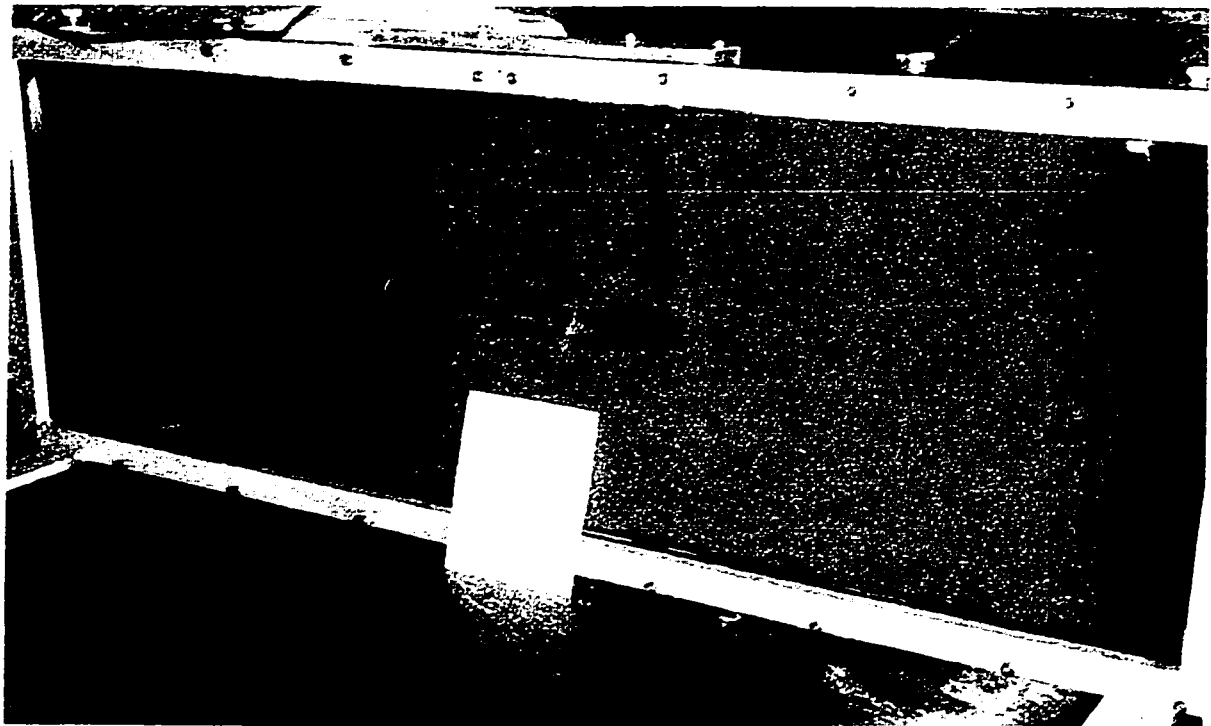
Figure 4.16: Experiment 2: KMnO$_4$ flush at 47.5 hours.

These observations suggest that like experiment 1, CO_2 production resulted in vapour transport of PCE and subsequent adsorption of vapour phase PCE coupled with reaction in the aqueous phase.

Figures 4.17, 4.18 and 4.19 illustrate the progression of experiment 2. Figure 4.17 shows MnO_2 formation as a vertical trail situated above the front of the PCE pool. CO_2 gas pressure in the pool caused a vertical fracture in the fine sand, which served as an escape route for the gas. Figure 4.18 reveals a darker, thicker layer of MnO_2 deposited around the pool indicating further oxidation of the PCE pool at 78 hours. The plume of MnO_2 downstream from the pool had lengthened. MnO_2 formation became more pronounced along the vertical fracture as CO_2 gas carried PCE vapour generated around the pool to the fracture and subsequent oxidation of the vapour occurred. Both Figures 4.18 and 4.19 reveal areas of MnO_2 located downstream of the pool extending from the pool to the effluent end of the tank. This MnO_2 zone is likely an indication of PCE migration due to CO_2 de-gassing in the coarse sand lens.

Experiment 2 was terminated at 120 hours. Severe accumulation of MnO_2 in the effluent glass wool area occurred as a result of oxidation of the screens. The effluent end of the tank became completely plugged and subsequently the tank developed leaks due to pressure buildup. Despite the reduction in $KMnO_4$ concentration and use of PCE, experiment 2 ultimately suffered the same problems as experiment 1. A post-treatment water flush was not possible.
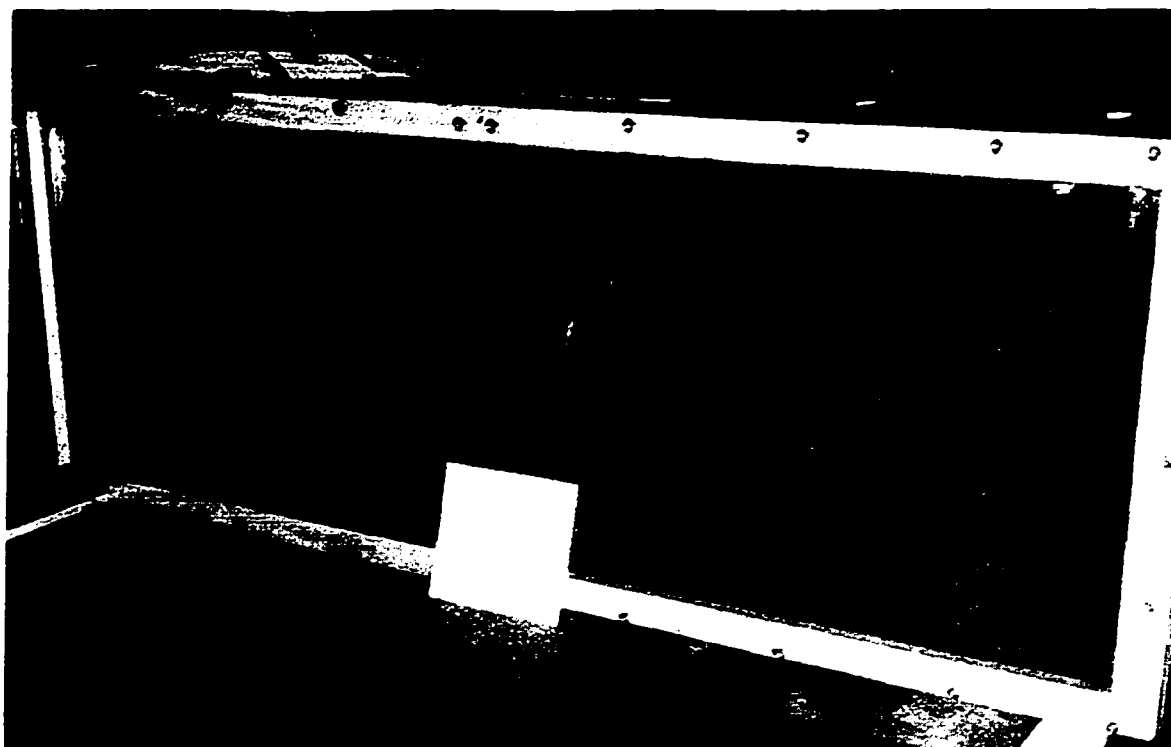
Figure 4.17: Experiment 2: $KMnO_4$ flush at 54.0 hours.
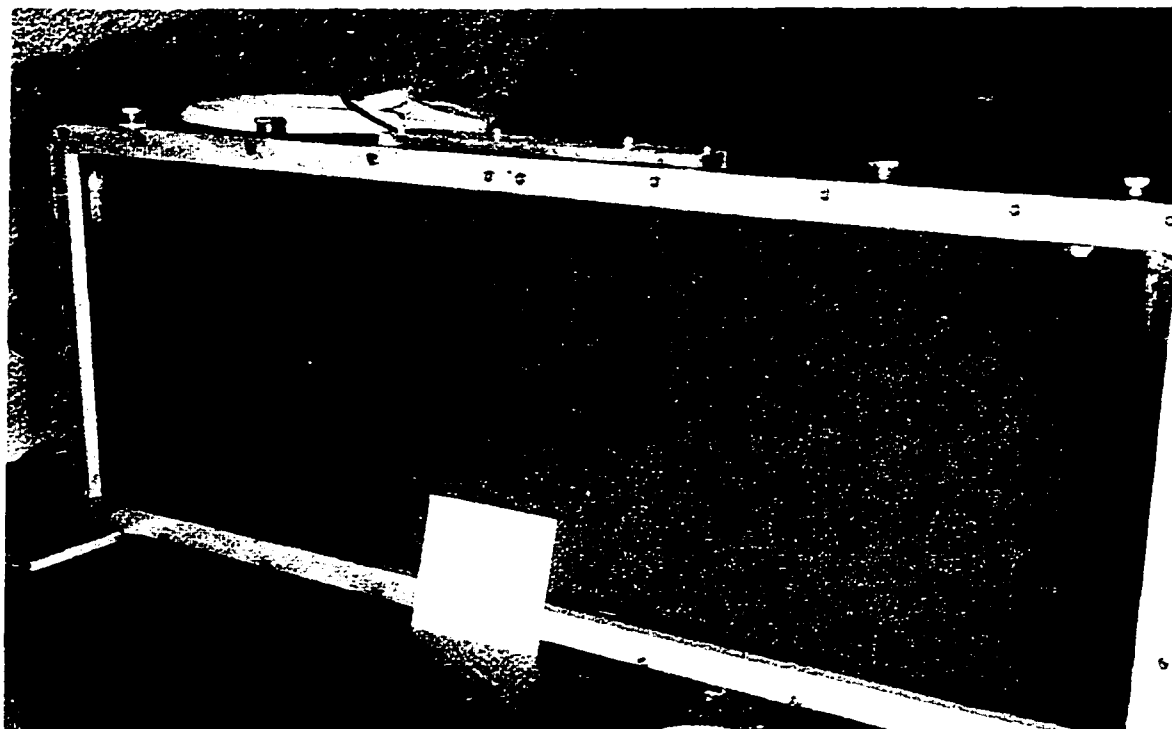
Figure 4.18: Experiment 2: $KMnO_4$ flush at 78.0 hours.
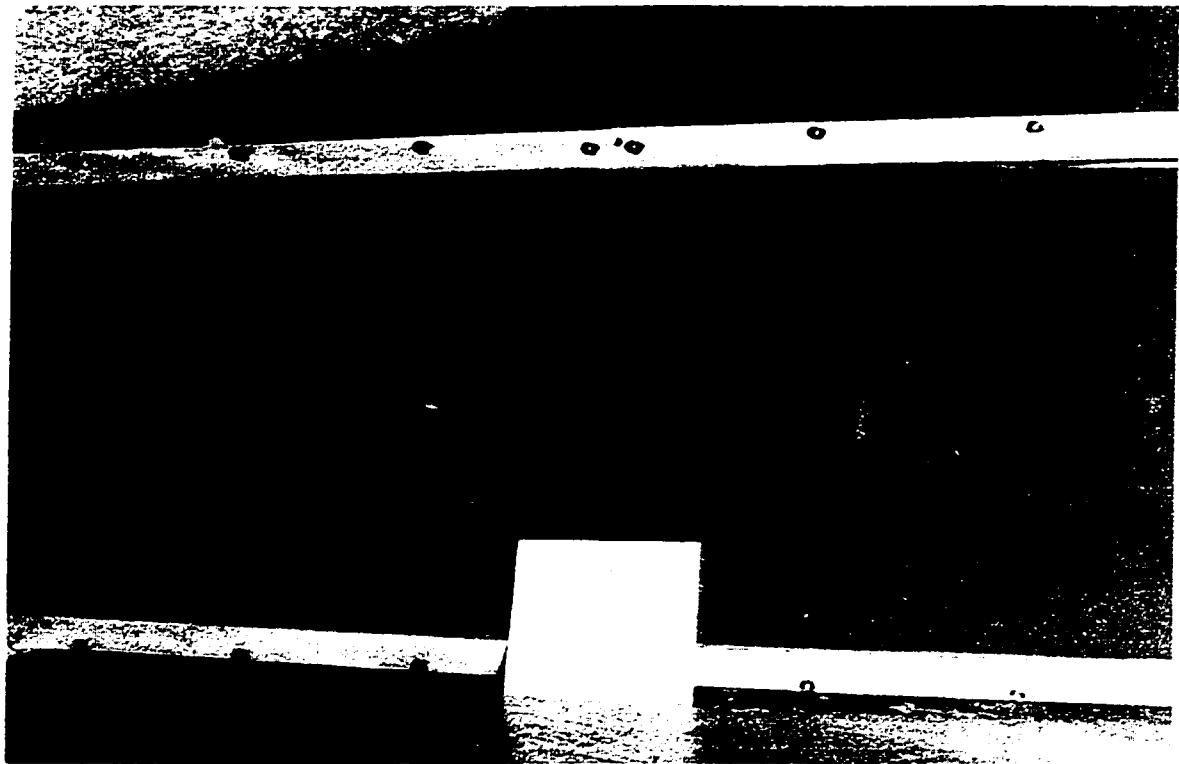
Figure 4.19: Experiment 2: $KMnO_4$ flush at 120 hours.

Experiments 1 and 2 provided the opportunity to observe interesting

processes that occur during $KMnO_4$ oxidation of DNAPL. In particular,

mobilization of DNAPL during oxidation has not been previously reported in any

literature and represents an important finding. Generally, mobilization of DNAPL

during treatment is undesirable, particularly where no controls are in place to

capture the mobilized DNAPL. In the case of in situ oxidation using $KMnO_4$, the

extent of mobilization is unknown and requires further investigation. In some

instances, minor mobilization may be helpful since the DNAPL will diffuse and

improve mass transfer rates and increase contact with $KMnO_4$. However, caution

is recommended before large-scale applications are undertaken until this phenomenon and possible implications are better understood.

4.3.3 Experiment 3: $KMnO_4$ Flush

Changes implemented in experiment 3 proved to be effective in preventing complete plugging of the tank due to MnO_2 precipitation. This provided the opportunity to perform a $KMnO_4$ flush of 422 hours and complete the experiment with a post-treatment water flush of 432.5 hours. Experimental changes included reduction of the original PCE volume of 5.0 mL to 2.0 mL and the reduction of $KMnO_4$ concentration from 5.0 g/L to 1.0 g/L. The reduced volume of PCE was designed to minimize mobilization of the PCE and prevent complete de-saturation of the pool in the event of CO_2 production. A lower concentration of $KMnO_4$ was used to decrease the reaction rate and ultimately decrease the rate of CO_2 production. Reduction of PCE mobilization from CO_2 production would enable the study of mass transfer from the PCE pool without the complexity of these additional phenomena. Because of MnO_2 plugging in the glass wool during the previous experiment, glass beads were again used in the influent and effluent reservoirs.

Figure 4.20 from experiment 3 shows the front of $KMnO_4$ solution at 15 hours approaching the middle of the tank and $KMnO_4$ beginning to infiltrate the PCE pool. Preferential flow occurred in the coarse sand lens due to the higher permeability of the lens. This is in contrast to experiment 1 where much of the
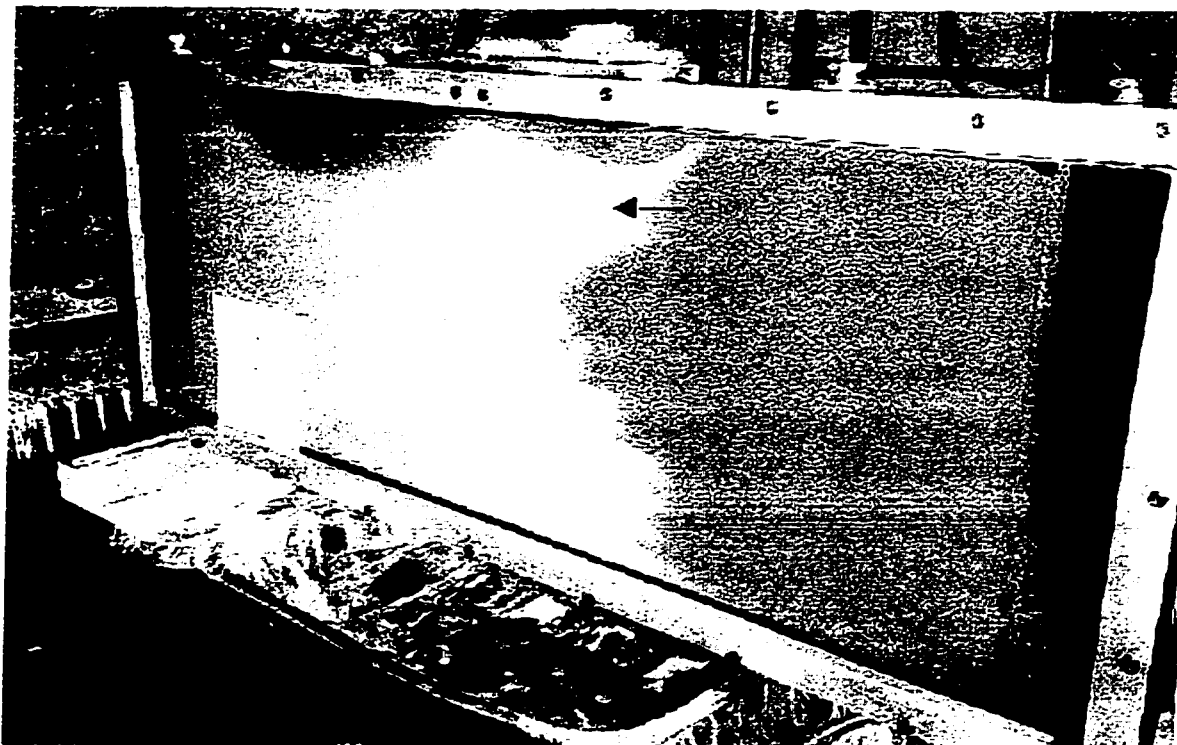
Figure 4.20: Experiment 3: KMnO₄ infiltration of PCE pool at 15.0 hours.

flow was diverted around the pool. Differences in the flow are due to the lower

DNAPL saturation of the pool in experiment 3 and therefore a smaller decrease in

the effective permeability of the coarse sand lens. Note that the glass was

stained from MnO_2 in the previous experiment and can be seen as a brown

vertical stain near the top of the tank, as indicated by the arrow in the figure.

Figure 4.21 shows the front of the KMnO₄ flush exiting the PCE pool.

Oxidation of the PCE pool was closely monitored during the KMnO₄ flush.

At 34 hours, significant precipitation of MnO_2 was observed throughout the PCE

pool and in a plume extending downstream from the pool as indicated in Figure

4.22. The presence of MnO_2 inside the pool verified that reactions occurred
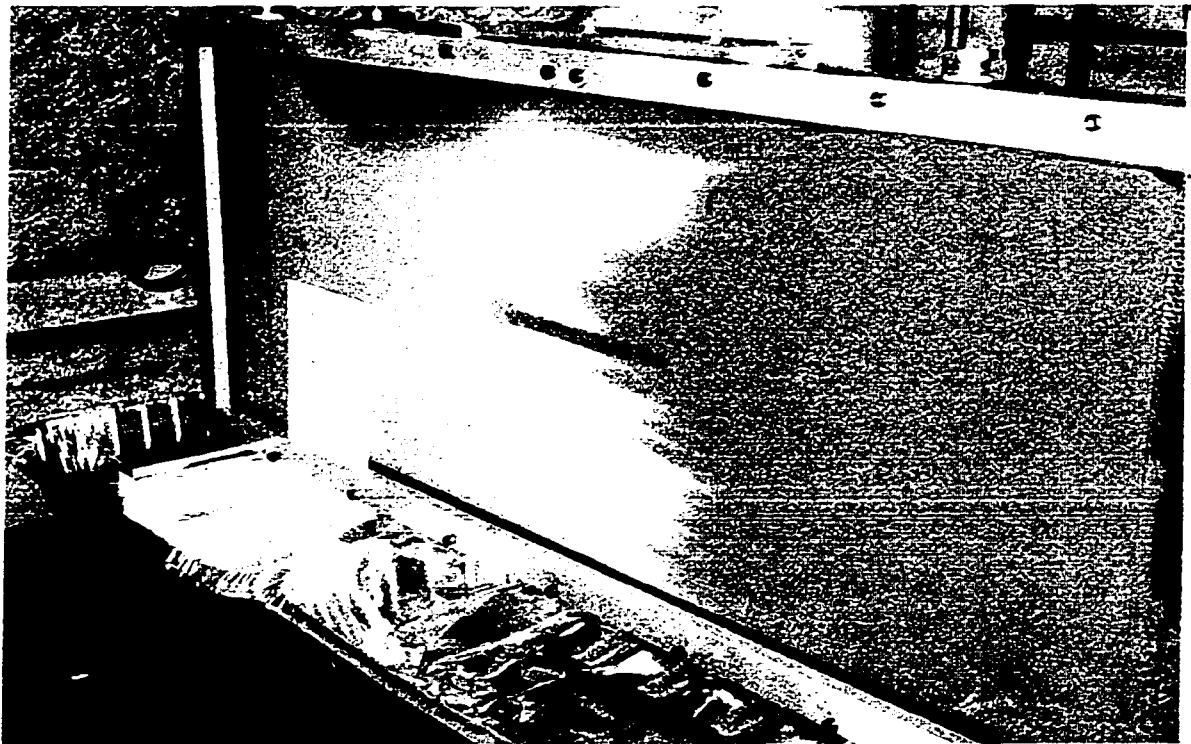
Figure 4.21: Experiment 3: KMnO₄ exiting PCE pool at 17.0 hours.

Figure 4.22: Experiment 3: KMnO₄ flush at 34.0 hours.

inside the pool as well as around the pool. Conditions inside and surrounding the PCE pool remained essentially steady until about 66 hours (refer to Figure 4.23). Significant reduction of permeability within the coarse sand lens did not occur and did not appear to affect $KMnO_4$ flow through the pool. MnO_2 inside the pool darkened and thicker layers formed around the perimeter of the pool, particularly along the front edges of the pool where oxidation first occurred. The plume was also stained a darker brown but retained the same shape. The plume downgradient of the pool was very different than the plume observed during experiment 1 due to differences in the reaction rate between TCE and PCE with $KMnO_4$ and flow in and around the pool. In experiment 1, the rate of reaction was approximately 50 times greater than that in experiment 3 (Schwartz and Yan, 1998). As a result, during experiment 1 reaction took place along the edge of the trailing plume (refer to Figure 4.12) leaving a zone where no $KMnO_4$ was present directly downgradient from the pool (indicated by the absence of purple colour) and MnO_2 solids formed along the edges of the plume. In comparison, the MnO_2 plume observed in experiment 3 was more dispersed and extended from the pool to the effluent end of the tank. It also revealed that $KMnO_4$ coexisted with MnO_2 in and around the plume, which indicated that $KMnO_4$ remained unreacted after travelling through and beyond the PCE pool. Figure 4.24 shows changes associated with increased MnO_2 formation and widening of the plume at 107 hours.
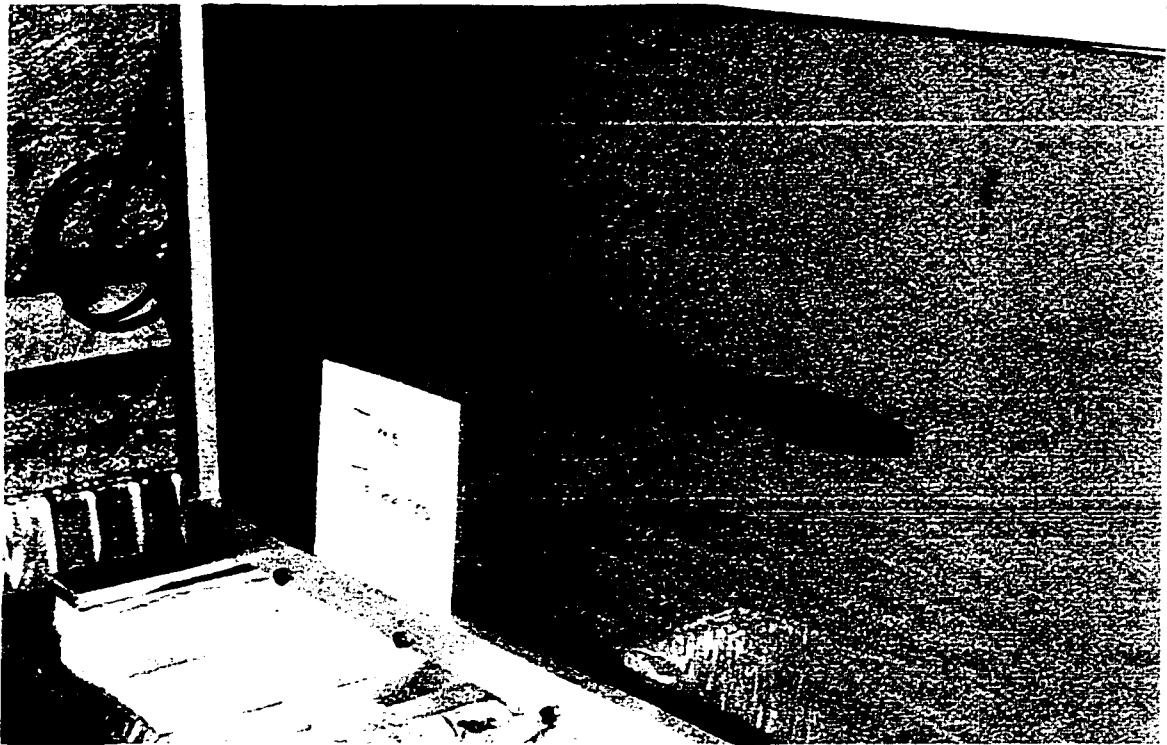
Figure 4.23: Experiment 3: $KMnO_4$ flush at 66.0 hours.
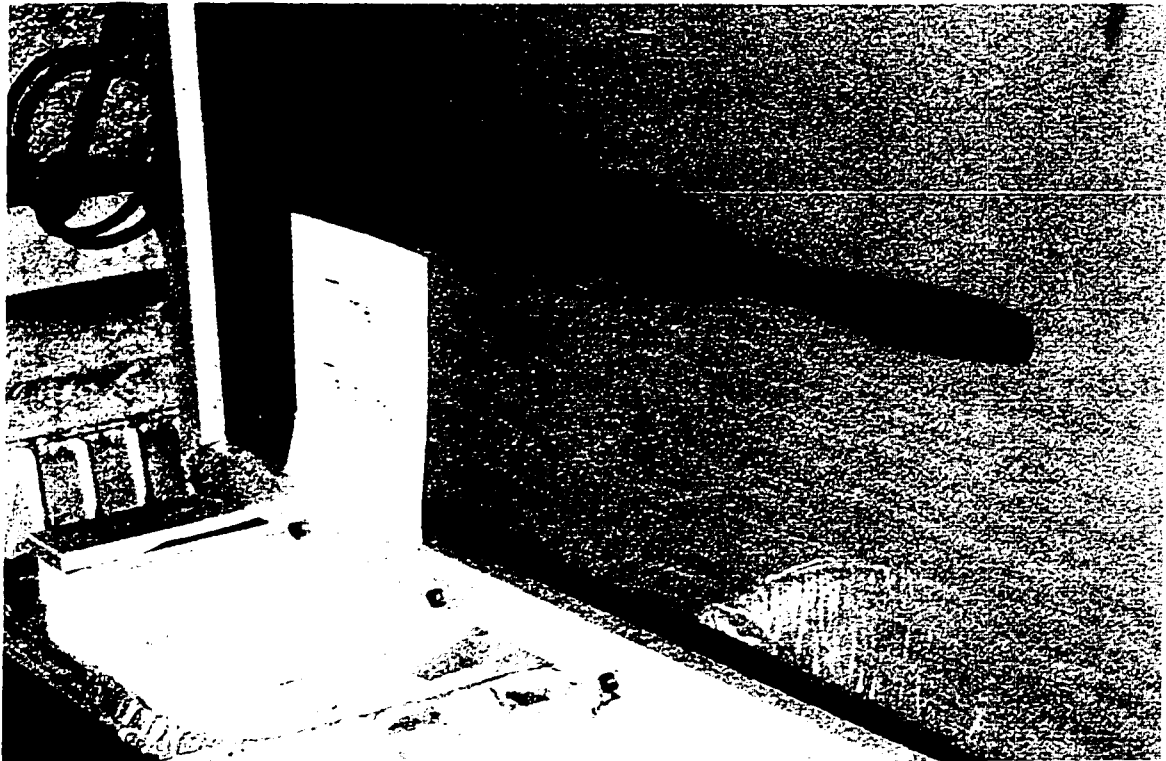
Figure 4.24: Experiment 3: $KMnO_4$ flush at 107 hours.

Changes inside the pool were noted again at approximately 130 hours after onset of the flush. At this time, trace amounts of CO_2 gas were visible in the pool and de-saturation of the PCE pool had begun. By 150 hours, CO_2 production increased as indicated by gas bubbles in the coarse sand and extensive de-saturation of the PCE pool had occurred. Although de-saturation of the pool had occurred at this time, the presence of CO_2 / MnO_2 zones were not apparent above the pool, as was the case in experiments 1 and 2. The plume had lengthened and de-saturation of the plume tail was observed which indicated movement or de-gassing of CO_2 downstream from the pool. Figure 4.25 exhibits the development of MnO_2 zones at the same elevation as the PCE pool downstream near the effluent reservoir screens at 156 hours. The appearance of these MnO_2 zones supports arguments for mobilization of DNAPL due to CO_2 production. Figure 4.26 represents conditions in the tank near the completion of the $KMnO_4$ flush. As oxidation continued, MnO_2 formed a layer around the pool that was approximately twice as thick as the coarse sand lens. CO_2 gas production in the coarse sand lens resulted in the upward migration of PCE vapour at the front of the pool, which was the main transport mechanism that caused the broad zone of MnO_2 above the pool. Zones of MnO_2 downstream from the pool continued to develop during the remainder of the $KMnO_4$ flush. MnO_2 was noted throughout the glass beads and provided evidence of oxidation of the influent and effluent screens. However, the screens
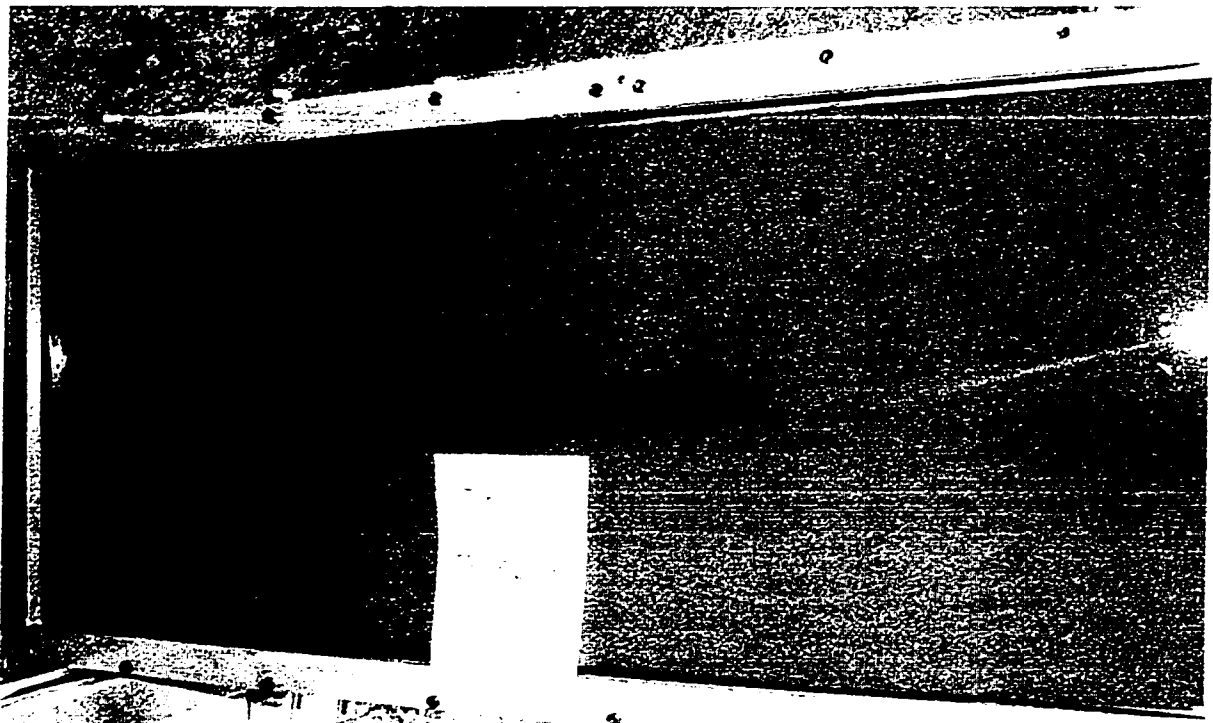
Figure 4.25: Experiment 3: $KMnO_4$ flush at 156 hours.
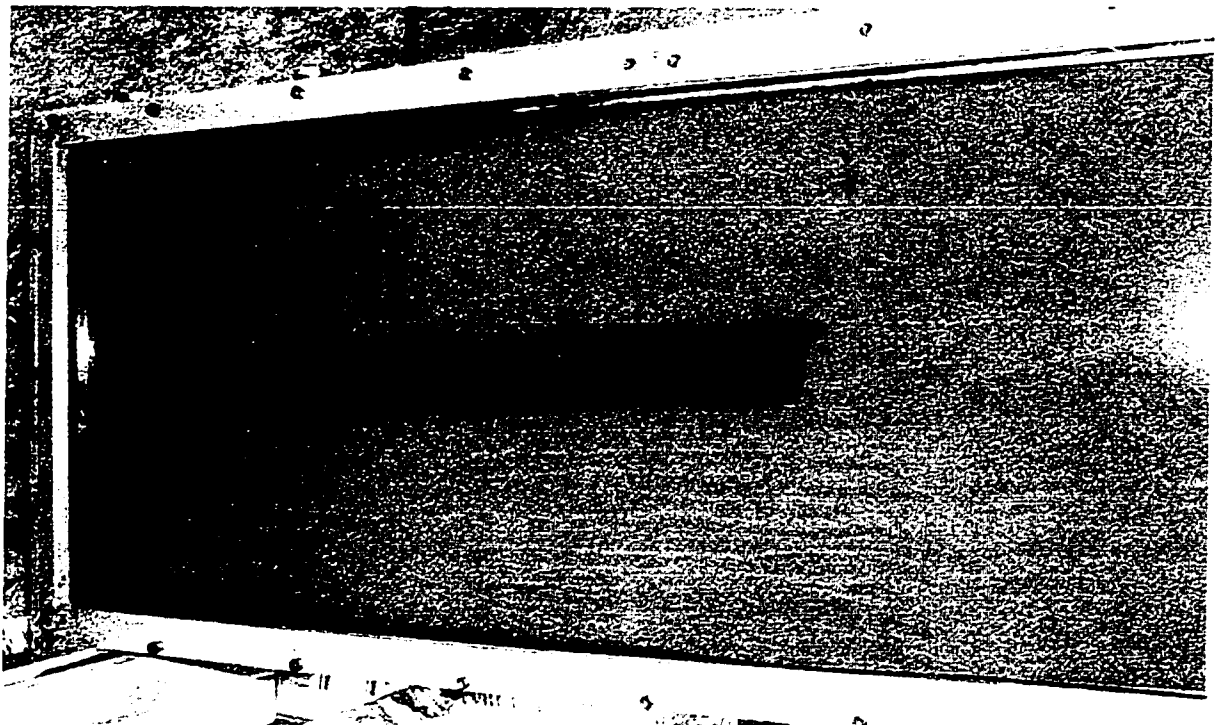
Figure 4.26: Experiment 3: $KMnO_4$ flush at 397 hours.

and glass bead pack were not plugged and flow through the tank was maintained.

Successful modifications led to reduced plugging of the effluent reservoir during experiment 3. Experiment 3, like experiments 1 and 2, demonstrated CO_2 and MnO_2 production to be significant in altering the flow pattern around a DNAPL pool and for having the potential to cause DNAPL migration and contribute to changes in mass transfer rates from DNAPL pools.

4.4 KMnO₄ Concentration

As previously discussed in Chapter 3, the concentration of $KMnO_4$ was determined by titrimetry for all samples taken from the effluent of the tank. A number of single samples were taken from the point sampling ports as well. Due to CO_2 gas production and cementation of the fine sand by MnO_2, point samples could not be obtained throughout the entire duration of the experiments. The results for each experiment are presented sequentially below.

4.4.1 KMnO₄: Effluent

Effluent samples were collected for experiment 1 for a total of 75 hours. Approximately 6.31 L (2.1 pore volumes) of $KMnO_4$ solution was injected through the tank. Figure 4.27 depicts the concentration for samples collected during that time period. As the graph illustrates, $KMnO_4$ breakthrough was detected at 24 hours. The maximum effluent concentration of 7.64 g/L was found at 68 hours,
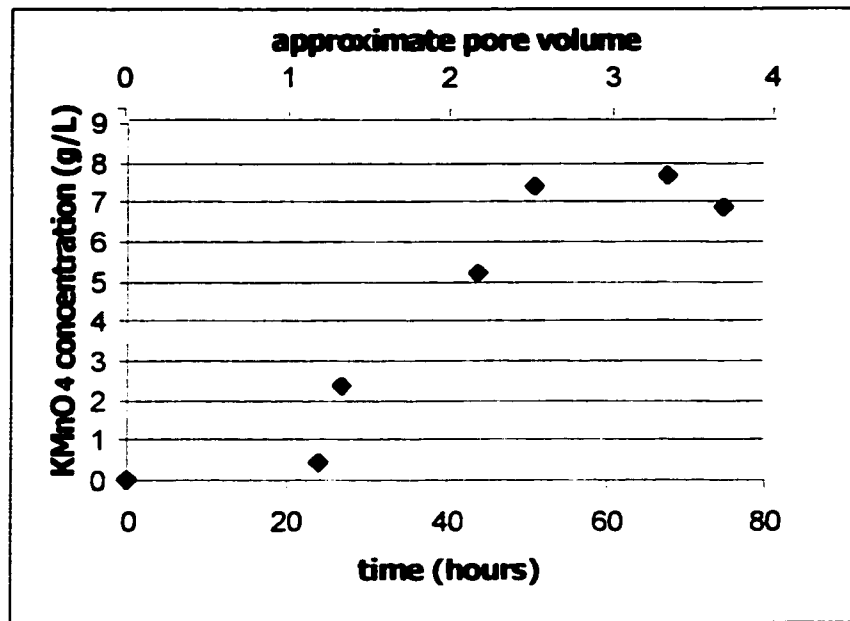
Figure 4.27: Experiment 1: Effluent KMnO4 concentrations.

which was less than the influent concentration of 10.0 g/L. KMnO4

concentrations could not be further investigated due to plugging and leaks that

developed which prevented the experiment from continuing.

During experiment 2, 10.6 L (approximately 3.5 pore volumes) of KMnO4

solution was injected through the tank. Figure 4.28 shows KMnO4 concentrations

for experiment 2 over the duration of 102 hours. KMnO4 was again initially

detected in the effluent after about 24 hours. Concentrations leveled off at

about 47.5 hours with the maximum concentration recorded as 3.73 g/L at 102

hours. Effluent concentrations did not achieve the influent concentration of 5.0

g/L. Like experiment 1, plugging and leaks caused early termination of the

experiment and KMnO4 concentrations could no longer be measured.
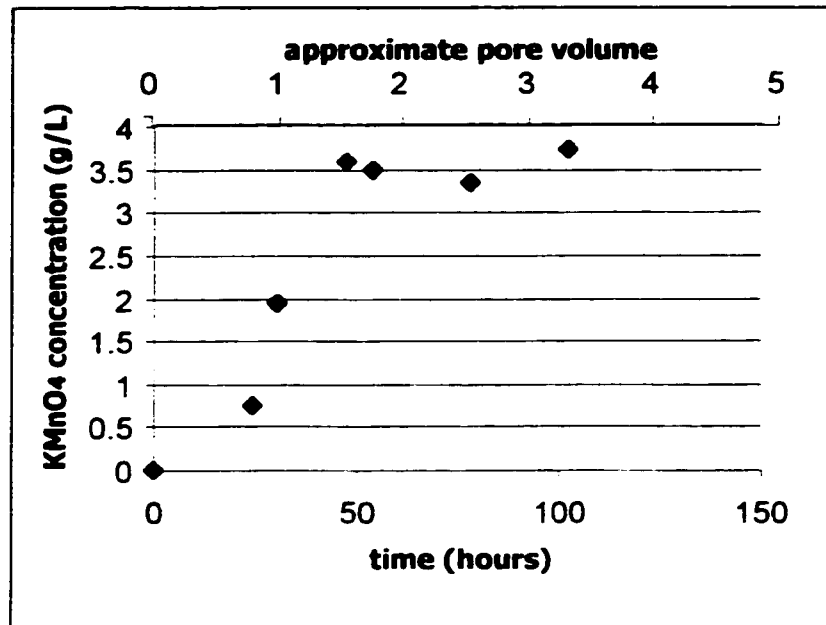
Figure 4.28: Experiment 2: Effluent KMnO₄ concentrations.

A comprehensive KMnO₄ concentration profile for a period of 467 hours was achieved in experiment 3. Approximately 40.5 L (13.5 pore volumes) of KMnO₄ solution was injected through the tank over the course of experiment 3. Figure 4.29 illustrates the detection of KMnO₄ at the effluent after about 30 hours followed by a quick increase in concentration, which then leveled off at about 100 hours. Effluent concentrations remained fairly stable for the remainder of the experiment. The maximum concentration of 0.76 g/L was detected 401.5 hours after the KMnO₄ flush began. The influent concentration of KMnO₄ solution in experiment 3 was 1.0 g/L. Note that the second water flush began at 423 hours and the last three samples where taken as KMnO₄ solution remaining in the tank was flushed out.
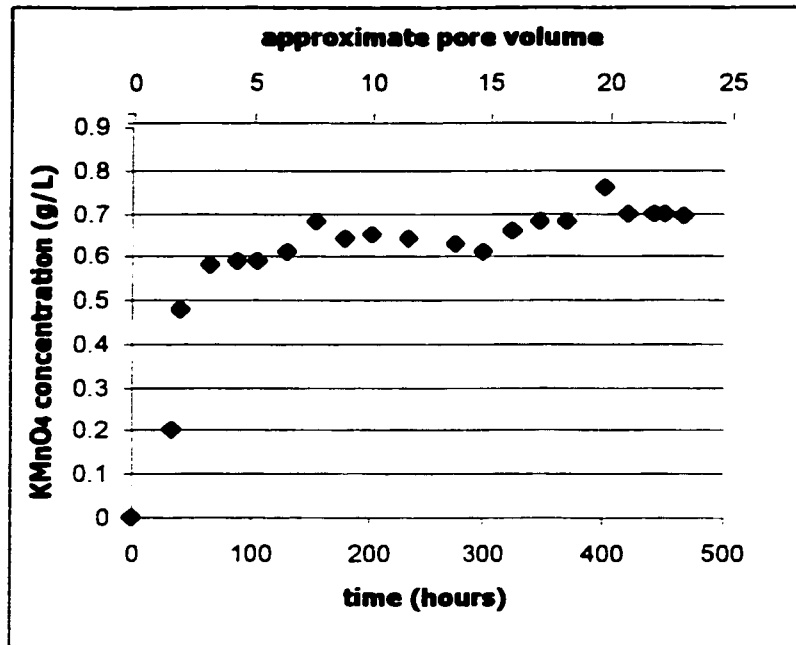
Figure 4.29: Experiment 3: Effluent KMnO4 concentrations.

Results revealed that for all three experiments, effluent KMnO4 concentrations were less than the respective influent concentrations. Some loss of KMnO4 was likely due to oxidation of the stainless steel screens and mesh as evidenced by MnO2 formation at both ends of the tank and plugging at the effluent end of the tank. Possible reaction of KMnO4 and the aluminum tank may have resulted in loss of KMnO4. Reaction of KMnO4 with previously precipitated MnO2 also contributed to the loss of KMnO4 (Schnarr, 1992). Reaction between KMnO4 and PCE/TCE also reduced KMnO4 effluent concentrations.

4.4.2 KMnO₄: Point Samples

KMnO₄ port samples were obtained for experiment 1 at 44 and 68 hours after the beginning of the KMnO₄ flush. In some cases, samples could not be taken because of MnO_2 that plugged the port and/or CO_2 gas interference. Results indicated that at 44 hours, concentrations of KMnO₄ were slightly less than the influent concentration of 10.0 g/L at all ports, except for ports D and F which had concentrations of 8.76 g/L and 8.00 g/L respectively. Concentrations were likely lower at these ports, located within close proximity to the TCE pool, because reactions took place in front of the pool and along the edges, thereby consuming the KMnO₄. Concentrations of KMnO₄ at 66 hours appeared to decrease slightly, due to continuing oxidation of TCE and possible reactions between KMnO₄ and MnO_2. At 66 hours, port E located directly behind the TCE pool exhibited a low KMnO₄ concentration of 2.29 g/L due to reaction of KMnO₄ at the front and edges of the pool. Figure 4.30 shows the average KMnO₄ concentration during experiment 1 for each sampling port.

Only one set of KMnO₄ port samples for experiment 2 could be taken because of the short duration of the experiment. KMnO₄ concentrations closely approached the influent concentration of 5.0 g/L approximately 48 hours after the flush began, possibly due to the slow reaction rate between PCE and KMnO₄. Point samples for experiment 3 were not taken for KMnO₄ analysis because of difficulties that were encountered.

H ● **9.51**

G ● **9.32**

10.1   **9.98**   **10.0**
●   ●   ●

Flow   K   J   I

→

| DNAPL Pool |

F ● **8.00**

E ● **2.29**

D ● **8.76**

C ● **9.93**

B ● **8.64**
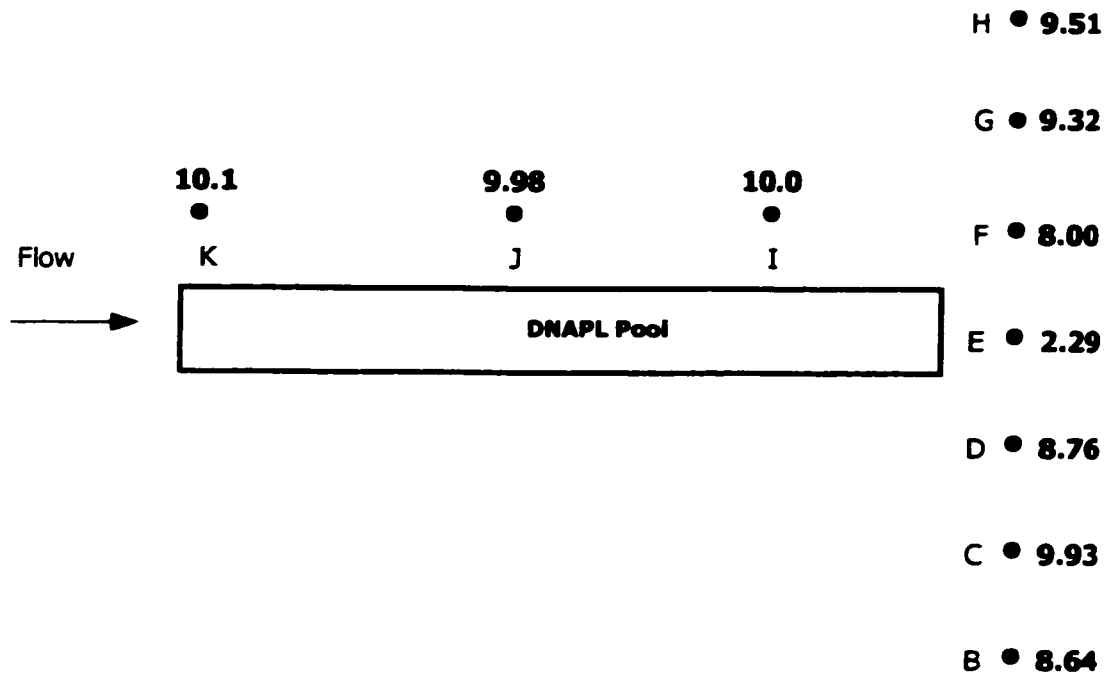
Figure 4.30: Experiment 1: Average KMnO₄ concentrations for all sampling ports.

4.5   Mass Removal Rate and Mass Balance

While experiments 1, 2 and 3 provided information from sample analyses and some important visual observations, rates of mass removal could not be established nor mass balances calculated due to the numerous difficulties that were encountered in attempting to measure chloride. Mass balance and mass transfer rates could not accurately be determined using KMnO₄ effluent concentrations because losses of KMnO₄ were not due solely to oxidation reactions between DNAPL and KMnO₄. Rough estimates for experiment 3 of PCE removed using a KMnO₄ mass balance suggest 200% to 300% recovery which clearly is not possible.

4.5.1 Dissolution: Post-treatment Water Flush

Experiment 3 was the only experiment where a post-treatment water flush was performed after completion of the $KMnO_4$ flush. Approximately 41.3 L or 13.8 pore volumes of water was injected into the tank over 432.5 hours. The post-treatment water flush was conducted to observe if PCE could be detected after the pool had undergone treatment of $KMnO_4$ for 422 hours. The tank was also observed for any changes with respect to the MnO_2 solids that surrounded the coarse sand lens, the MnO_2 plume and CO_2 gas present in the fine and coarse sand.

PCE concentrations from effluent samples taken are given in Figure 4.31. PCE concentrations were detected in the effluent 194.5 hours after the post-treatment water flush began and concentrations were less than 10.5 µg/mL. Post-treatment PCE concentrations in the effluent were detected while pretreatment PCE concentrations were not. Mass transfer of PCE into the aqueous phase during the post-treatment water flush could have been maintained by residual PCE in the coarse sand lens. As previously discussed in Section 2.2.1, for a given volume of DNAPL, residual DNAPL has a greater contact surface area compared to a DNAPL pool. These results suggest that because of DNAPL mobilization that occurred during the $KMnO_4$ flush, the DNAPL occupied a greater volume during the post-treatment water flush than during the pretreatment water flush.
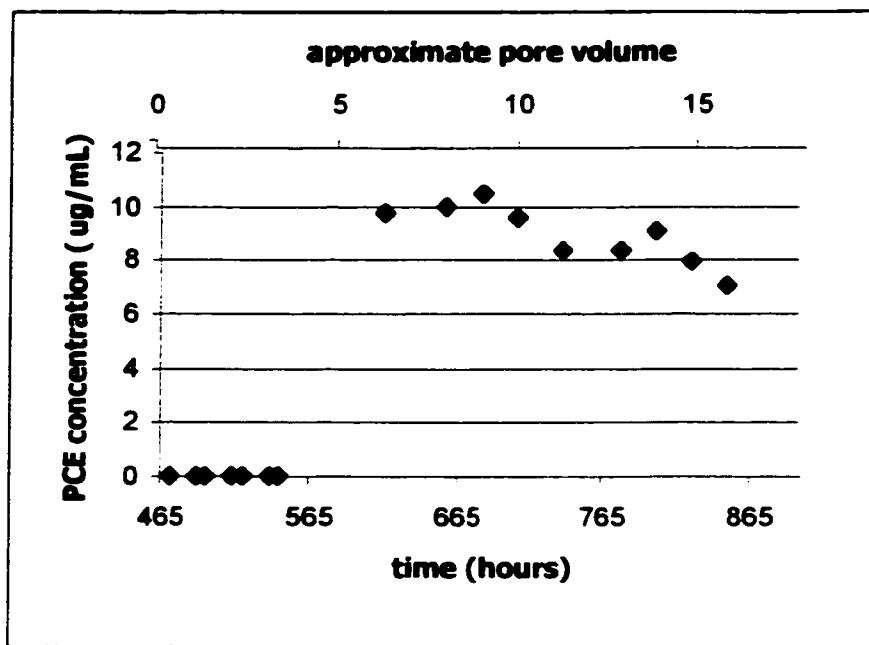
Figure 4.31: Experiment 3: Effluent PCE concentrations for post-treatment water flush.

Figure 4.32 taken during the post-treatment water flush, shows that after treatment PCE was very likely present at locations other than the coarse sand lens. Significant zones of MnO_2 indicate these locations. In particular, the area directly downgradient of the coarse lens near the effluent end of the tank most likely contained PCE. Figure 4.33 is a close-up of this area. The "spotty" pattern of MnO_2 precipitation reflects a typical distribution of DNAPL as it migrates through mildly heterogeneous porous media. The increased volume of porous media containing PCE would have increased effluent concentrations during the post-treatment water flush. The presence of CO_2 gas may also have increased PCE effluent concentrations during the post-treatment flush. The CO_2 gas likely

85
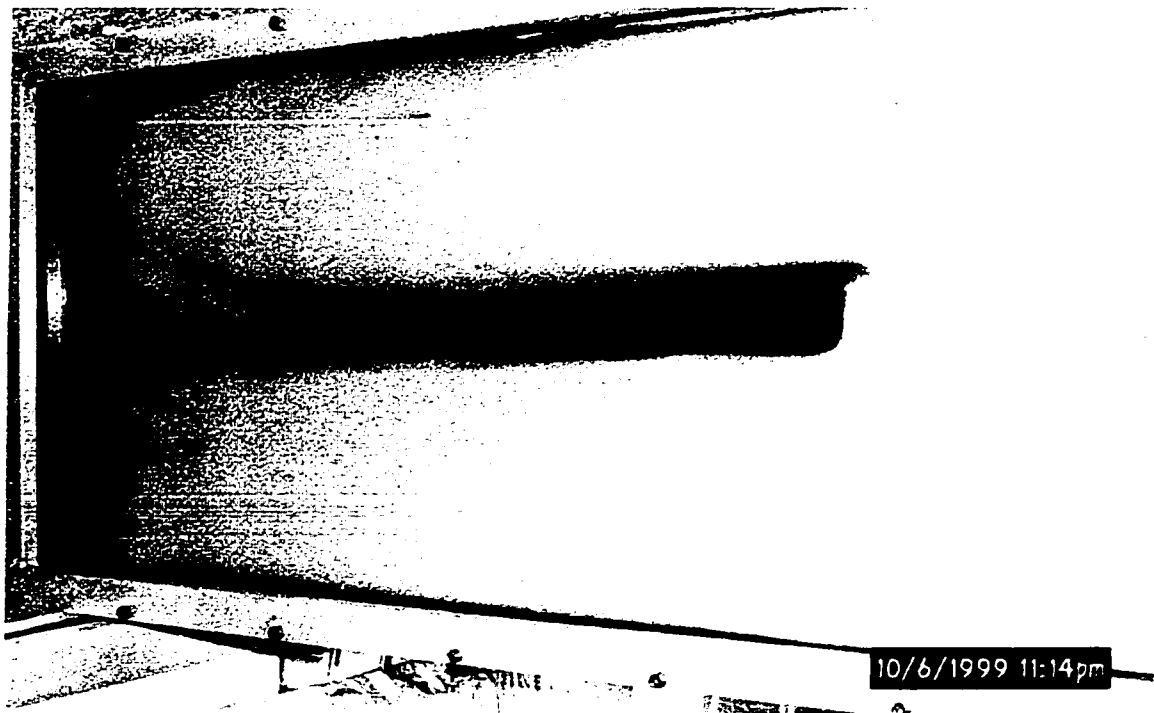
Figure 4.32: Experiment 3: Post-treatment water flush.

One possible migration
pathway of PCE

Possible locations of mobilized PCE
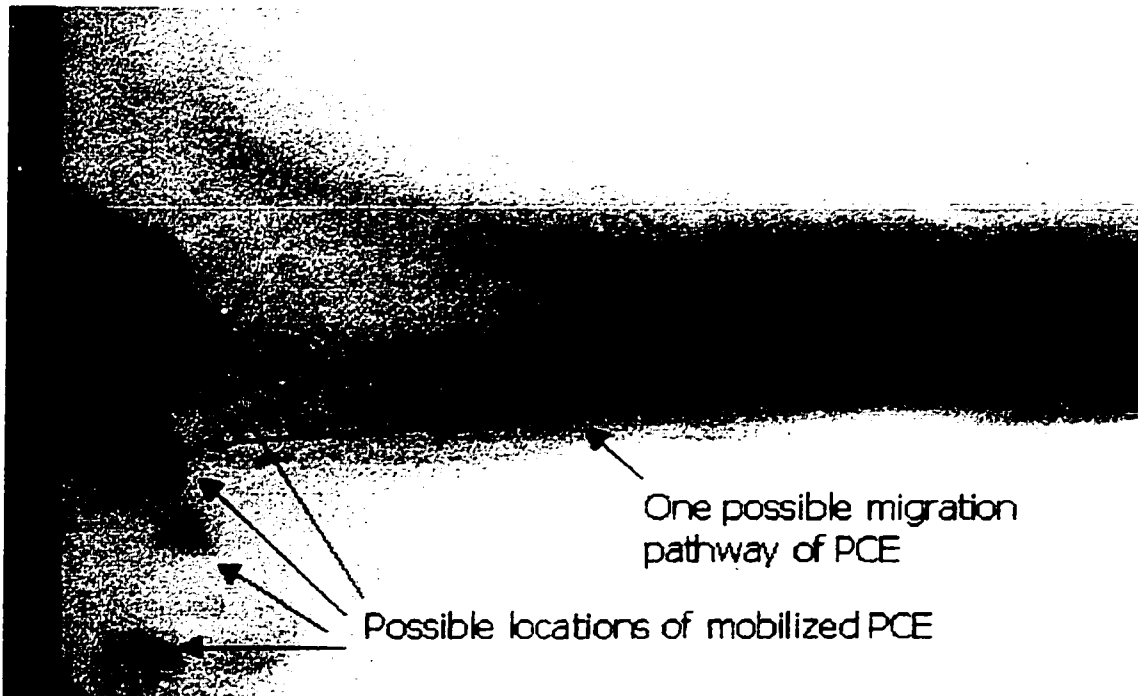
Figure 4.33: Experiment 3: Close-up of MnO₂ plume and MnO₂ zones during
post-treatment water flush.

contained PCE vapour that would have dissolved into the flowing water. As CO_2

gas dissolved into the water during the post-treatment flush, PCE concentrations

would decrease as observed in Figure 4.31. CO_2 dissolved and disappeared

following several days of flushing with water.

In addition to obtaining effluent samples for PCE analysis, a single syringe

sample was withdrawn from the centre of the coarse sand lens through the

DNAPL injection port. The PCE concentration for this sample was found to be

145 $\mu g/mL$, which strongly suggests that pure-phase PCE remained in the coarse

sand lens after the $KMnO_4$ flush. The PCE concentration of 145 $\mu g/mL$ also

suggests that pore-scale mass transfer within the pool was sufficiently rapid such

that the aqueous solubility of PCE was approached within the pool.

The MnO_2 distribution during the post-treatment water flush is shown in

Figure 4.32. No changes were observed as the post-treatment water flush

proceeded with respect to the presence of MnO_2, suggesting that in field sites,

MnO_2 could potentially remain in the soil for indefinite periods of time following

treatment.

5   CONCLUSIONS AND RECOMMENDATIONS

5.1   Conclusions

The results of this study have demonstrated the applicability of in situ chemical oxidation for treating DNAPL contamination sites. Pools of PCE and TCE were treated using various concentrations of $KMnO_4$ and duration of treatment. This research has resulted in several conclusions.

The volume of DNAPL in a pool or residual zone, which directly related to the degree of DNAPL saturation, influenced the flow domain in the pretreatment water flush. This factor also influenced $KMnO_4$ flow in and around a DNAPL pool and ultimately affected the treatment rate.

Significant productions of manganese dioxide and carbon dioxide were identified as important issues. MnO_2 is an inevitable product resulting from the oxidation of DNAPL by $KMnO_4$. MnO_2 may interfere with $KMnO_4$ treatment by reducing the permeability of the porous media and reducing the amount of $KMnO_4$ that reaches the DNAPL pool. Manganese dioxide impacts the mass removal rate of DNAPL from a pool; the magnitude of this effect is unknown and requires further investigation. As well, MnO_2 adheres to the soil grains and will remain in the soil for indefinite periods of time.

While CO_2 gas has been recognized as a product of in situ oxidation using $KMnO_4$ in previous literature, CO_2 was not identified as an important issue. This

research has revealed the production of CO_2 gas to be very important during in situ $KMnO_4$ oxidation for a number of reasons. Significant production of CO_2 gas can cause de-saturation of the porous media containing the DNAPL and subsequently reduce flow of $KMnO_4$ into this area. This in turn causes a reduction in the effectiveness of $KMnO_4$ treatment at that particular location. Mobilization of DNAPL pools was also observed and identified as an important issue related to CO_2 production. Due to notable amounts of CO_2 gas produced, DNAPL was mobilized from the coarse sand lens to the surrounding fine sand. Therefore, CO_2 provided an additional mechanism of mass transfer through the movement of DNAPL vapour in the gas phase, which ultimately affected overall mass transfer rates from the pool. Mobilization may create an enhancement of mass transfer from DNAPL pools due to an increased volume of porous media containing DNAPL that results in greater contact between the DNAPL and $KMnO_4$ solution. However, mobilization may also be undesirable, particularly where no controls are in place to capture the mobilized DNAPL. In the case of in situ oxidation using $KMnO_4$, the extent of mobilization is unknown and quantification of this mechanism will require further investigation.

Point TCE concentrations taken during the pretreatment water flush of experiment 1 from the 10 sampling port locations provided an indication of the dominating process for mass transfer. Results suggest that macro-scale mass transfer from the DNAPL pool to the surrounding water limits the overall mass transport rate rather than pore-scale mass transfer within the pool. TCE

concentrations indicated that the TCE aqueous solubility of 1100 mg/L (Pankow et al., 1996) was approached inside the pool and therefore pore-scale mass transfer was not restricted. The PCE concentration measured inside the DNAPL pool during the post-treatment water flush of experiment 3 also indicated that the PCE aqueous solubility of 200 mg/L (Pankow et al., 1996) was approached within the pool.

Results from the post-treatment water flush of experiment 3 suggest that, for a given volume of DNAPL, mass transfer rates might be greater from residual DNAPL than from DNAPL pools. Due to the greater contact surface area, mass transfer from residual DNAPL into the aqueous phase may result in higher concentrations downstream.

5.2 Recommendations

The results of these experiments have demonstrated in situ $KMnO_4$ oxidation to be reasonably effective in treating PCE and TCE pools. Several factors should be considered in applying this technique.

MnO_2 and CO_2 are important issues that need to be addressed. Further experimentation should be conducted to fully investigate and understand the effects of MnO_2 and CO_2 on mass transfer and mass removal rates from DNAPL pools, as well as residual DNAPL. Experiments should focus on the examination of the reduction of permeability of a porous medium to flow due to MnO_2

formation. In addition, mobilization of DNAPL due to CO_2 gas and the effect on mass transfer and removal rates should be thoroughly investigated.

Potential toxicity of manganese dioxide and other manganese oxides produced during $KMnO_4$ oxidation should be investigated since these solids will remain in treated soil for long periods of time. The duration that MnO_2 could subsist in a porous medium should also be quantified.

When treating any contaminated site, time and cost are important factors. Results from these experiments and others conducted by various researchers have indicated the strong possibility of long periods of time and an associated expense using $KMnO_4$ as an in situ oxidant to treat DNAPL contaminated sites. The duration of treatment must be considered when using $KMnO_4$ as an oxidant as related to the effectiveness of treatment and removal rates to be achieved.

The measurement of chloride proved to be a difficult task in this research. The chloride electrode (ISE) technique is not applicable for solutions containing $KMnO_4$. Further techniques to accurately measure chloride in a solution matrix containing $KMnO_4$ should be tested or developed. The measurement of hydrogen ions by pH could also possibly be used as an indicator of reaction rates. This technique should also be tested.

Changes to the experimental tank design would also have been beneficial to this study. As the experiments progressed, it became very obvious that materials used in the tank construction must be carefully selected to ensure that the various chemicals do not react with the tank itself. The tank must be made

out of a non-reactive material, such as glass, as $KMnO_4$ reacts with aluminum and stainless steel and there was possible reaction with PCE and TCE and the tank materials as well.

Visual observations were very helpful in understanding mechanisms that occurred during the in situ oxidation process. They may also provide quantitative information related to the amount of MnO_2 precipitation or CO_2 saturation. Imaging techniques may provide information for the development and testing of numerical models or design criteria.

REFERENCES

American Conference of Governmental Industrial Hygienists (ACGIH), Threshold Limit Values for Chemical Substances and Physical Agents and Biological Exposure Indices. Cincinatti, Ohio, 1995.

Anderson, M. R., Johnson, R. L. and Pankow, J. F., Dissolution of Dense Chlorinated Solvents into Ground Water: 1. Dissolution from a Well-Defined Residual Source. Ground Water, Vol. 30, No. 2, pgs. 250-256, March-April, 1992.

Budavari, S., O'Neil, M.J., Smith, A. and Heckelman, P.E., editors, The Merck Index, Merck & Co., Inc, Rahway, N.J., 1989.

Eaton, D. A., Clesceri, L. S. and Greenburg, A. E., editors, Standard Methods for the Examination of Water and Wastewater 19th Edition. American Public Health Association, Washington, D.C., 1995.

Feenstra, S. and Guiguer, N., Dissolution of Dense Non-Aqueous Phase Liquids (DNAPLs) in the Subsurface. In:Dense Chlorinated Solvents and other DNAPLs in Groundwater:History, Behaviour and Remediation, Waterloo Press, Portland, Oregon, 1996.

Fetter, C. W., Applied Hydrogeology, Third Edition. Prentice-Hall, Upper Saddle River, New Jersey, 1994.

Fountain, J. C., Technologies for Dense Nonaqueous Phase Liquid Source Zone Remediation. Prepared for: Ground-Water Remediation Technologies Analysis Center, December, 1998.

Fox, M. and Whitesell, J. K., Core Organic Chemistry. Jones and Bartlett Publishers, Inc., 1997.

Gates, D. D. and Siegrist, R. L., In-Situ Chemical Oxidation of TCE using Hydrogen Peroxide. Journal of Environmental Engineering, Vol. 121, No. 9, September, 1995a.

Gates, D. D., Siegrist, R. L. and Cline, S. R., Chemical Oxidation of Contaminants in Clay of Sandy Soil. Proceedings of the 88th Annual Meeting and Exhibition, San Antonio, Texas, 1995b.

Geller, J. T. and Hunt, J. R., Mass Transfer from Nonaqueous Phase Organic Liquids in Water-saturated Porous Media. Water Resources Research, Vol. 29, No. 4, pgs. 833-845, April, 1993.

Huang, K., Hoag, G. E., Chheda, P., Woody, B. A., and Dobbs, G. M., Kinetic Study of Oxidation of Trichloroethylene by Potassium Permanganate. Environmental Engineering Science, Vol. 16, No. 4, pgs. 265-274, 1999.

Hunt, J. R., Sitar, N. and Udell, K. S., Nonaqueous phase liquid transport and cleanup. 1. Analysis of Mechanisms. Water Resources Research, Vol. 24, pgs. 1247-1259, 1988.

Imhoff, P. T., Jaffe, P. R. and Pinder, G. F., An Experimental Study of Complete Dissolution of a Nonaqueous Phase Liquid in Saturated Porous Media. Water Resources Research, Vol. 30, No. 2, pgs. 307-320, February, 1994.

Kolthoff, I. M. and Sandell, E. B., Textbook of Quantitative Inorganic Analysis, Revised Edition. The MacMillan Company, New York, 1946.

Kueper, B. H., The Behaviour of Dense, Non-Aqueous Phase Liquid Contaminants in Heterogeneous Porous Media. Ph.D. Thesis, University of Waterloo, Waterloo, Canada, 1989.

LaChance, J. C., Reitsma, S., McKay, D. and Baker, R., In Situ Oxidation of Trichloroethene using Potassium Permanganate Part 1: Theory and Design. Proceedings of the First International Conference on Remediation of Chlorinated and Recalcitrant Compounds, Monterey, California, 1998.

McKay, D., Hewitt, A., Reitsma, S., LaChance, J. and Baker, R., In Situ Oxidation of TCE using $KMnO_4$ Part 2: Pilot Study. Proceedings of the First International Conference on Remediation of Chlorinated and Recalcitrant Compounds, Monterey, California, 1998.

McWhorter, D. B. and Kueper, B. H., Mechanics and Mathematics of the Movement of Dense Non-Aqueous Phase Liquids (DNAPLs) in Porous Media. In:Dense Chlorinated Solvents and other DNAPLs in Groundwater:History, Behaviour and Remediation, Waterloo Press, Portland, Oregon, 1996.

Oostrom, M., Hofstee, C., Walker, R. C. and Dane, J. H., Movement and Remediation of Trichloroethylene in a Saturated Heterogenous Porous Medium 1. Spill Behavior and Initial Dissolution. Journal of Contaminant Hydrology, Vol. 37, pgs. 159-178, 1999.

Pankow, J. F., Feenstra, S., Cherry, J. A. and Ryan, C., Dense Chlorinated
Solvents in Groundwater: Background and History of the Problem.
In:Dense Chlorinated Solvents and other DNAPLs in Groundwater:History,
Behaviour and Remediation, Waterloo Press, Portland, Oregon, 1996.

Pearce, A. E., Voudrias, E. A. and Whelan, M. P., Dissolution of TCE and TCA
Pools in Saturated Subsurface Systems. Journal of Environmental
Engineering, Vol. 120, No. 5, pgs. 1191-1206, 1994.

Powers, S. E., Loureiro, C. O., Abriola, L. M. and Weber Jr., W. J., Theoretical
Study of the Significance of Nonequilibrium Dissolution of Nonaqueous Phase
Liquids in Subsurface Systems. Water Resources Research, Vol. 27, No. 4,
pgs. 463-477, April, 1991.

Powers, S. E., Abriola, L. M. and Weber Jr., W. J., An Experimental Investigation
of Nonaqueous Phase Liquid Dissolution in Saturated Subsurface Systems:
Steady State Mass Transfer Rates. Water Resources Research, Vol. 28, No.
10, pgs. 2691-2705, October, 1992.

Powers, S. E., Abriola, L. M. and Weber Jr., W. J., An Experimental Investigation
on Nonaqueous Phase Liquid Dissolution in Saturated Subsurface Systems:
Transient Mass Transfer Rates. Water Resources Research, Vol. 30, No. 2,
pgs. 321-332, February, 1994.

Powers, S. E., Nambi, I. M. and Curry Jr., G. W., Non-aqueous Phase Liquid
Dissolution in Heterogeneous Systems: Mechanisms and a Local Equilibrium
Modeling Approach. Water Resources Research, Vol. 34, No. 12, pgs. 3293-
3302, December, 1998.

Reitsma, S. and Dai, Q. L., Reaction Enhanced Mass Transfer During Potassium
Permanganate Treatment of Porous Media Containing a Chlorinated Solvent.
Submitted to Journal of Contaminant Hydrology, May 1999.

Sale, T., Interphase Mass Transfer from Single Component DNAPLs. Dissertation
for Colorado State University, Fort Collin, Colorado, 1998.

Schnarr, M., An In-Situ Oxidative Technique to Remove Residual DNAPL from
Soils. M.A.Sc. Thesis, University of Waterloo, Waterloo, Canada, 1992.

Schnarr, M., Truax, C., Farquhar, G., Hood, E., Gonullu, T. and Stickney, B.,
Laboratory and Controlled Field Experiments using $KMnO_4$ to Remediate TCE
and PCE DNAPLs in Porous Media. Journal of Contaminant Hydrology, Vol.
29, pgs. 205-224, 1998.

Schwartz, F. W. and Yan, Y. E., Oxidative Degradation of Chlorinated Ethylenes by Potassium Permanganate. Ohio State University. Proceedings of the First International Conference on Remediation of Chlorinated and Recalcitrant Compounds, Monterey, California, 1998.

Schwille, F., Dense Chlorinated Solvents in Porous and Fractured Media. Translated by James F. Pankow, Lewis Publishers, Boca Raton, Florida, 1988.

Toon, E. R. and Ellis, G. L., Foundations of Chemistry. Holt, Rinehart and Winston of Canada, Limited, Toronto, Canada, 1978.

United States Environmental Protection Agency (US EPA), Office of Solid Waste, Third Edition (SW- 846). Washington, D.C. 20460, 1986.

Vella, P. A. and Veronda, B., Oxidation of TCE: A Comparison of $KMnO_4$ and Fenton's Reagent. Presented at the Third International Symposium on Chemical Oxidation Technology for the Nineties, Vanderbuilt University, Nashville, TN., 1992.

West, O. R., Cline, S. R., Holden, W. L., Gardner, F. G., Schlosser, B. M., Thate, J. E. and Pickering, D. A., A Full-Scale Demonstration of In Situ Chemical Oxidation Through Recirculation at the X-701B Site: Field Operations and TCE Degradation. Prepared by: Oak Ridge National Laboratory, Oak Ridge, TN., Environmental Sciences Division, Publication No. 4727, December, 1997.

Whelan, M. P., Voudrias, E. A. and Pearce, A., DNAPL Pool Dissolution in Saturated Porous Media: Procedure Development and Preliminary Results. Journal of Contaminant Hydrology, Vol. 15, pgs. 223-237, 1994.

APPENDIX A

Sand Porosity

1. General

Flow velocity calculations required estimations of sand porosity. Porosity was calculated for the fine quartz sand and coarse silica sand based on a procedure obtained from Fetter (1994).

2. Procedure

Laboratory porosity is determined by taking a known volume of sand (V). The sample is then dried in an oven at 105°C until it reaches a constant mass (m) after approximately 24 hours. The sample is thoroughly dried in an oven to remove all moisture clinging to the sand surface. The bulk density (ρ_b) of the sand is the mass of the sample after oven drying divided by the original sample volume. The particle density (ρ_d) for most rock and soil is about 2.65 g/cm^3 (Fetter, 1994). The porosity (n) for the sample is then calculated.

3. Calculation

i) Calculate the bulk density (g/cm^3) of the sand.

$$\rho_b = \frac{m}{V}$$

ii) Calculate the porosity of the sand.

$$n = 1 - \frac{\rho_b}{\rho_d}$$

The porosity can then be calculated as a percentage by multiplying by 100. The average porosity for the fine and coarse sand was calculated by summing the porosity for the six samples and dividing by six.

iii)   The standard deviation for the fine and coarse sand was calculated and found to 0.80% and 1.67% respectively.

Sand	Sample	Mass (g)	Volume (mL)	Bulk Density (g/cm^3)	Porosity	Porosity (average)
Fine	1	72.49	50.0	1.450	0.453	0.44
	2	73.71	50.0	1.474	0.444	
	3	73.12	50.0	1.462	0.448	
	4	73.55	50.0	1.471	0.445	
	5	75.62	50.0	1.513	0.429	
	6	73.83	50.0	1.477	0.443	
Coarse	1	65.74	50.0	1.315	0.504	0.49
	2	64.47	50.0	1.289	0.513	
	3	70.77	50.0	1.415	0.466	
	4	66.08	50.0	1.322	0.501	
	5	68.35	50.0	1.367	0.484	
	6	66.84	50.0	1.337	0.496	

APPENDIX B

Flush Volume and Flow Rate

1. General

The volume of each flush was recorded using the volume of influent injected. A mass analysis of the effluent was used to verify this volume. The mass analysis measured the weight (g) of the cumulative effluent exiting the tank over a certain period of time, which was then divided by the density (ρ) of water to give a volume (V). Note that the density of the $KMnO_4$ solution was not taken into account. The effluent volume was compared to the volume of solution injected with the effluent volume recorded as the volume of the flush that had passed through the tank (expressed in L). Approximate pore volumes passing through the tank for a given flush were calculated based on the elapsed time, average flow rate (Q_{avg}) and approximate pore volume/day (3.0 L/day). Flow rate measurements (mL/min) were made daily. To illustrate the slight fluctuations in flow, a profile of the flow rates from the $KMnO_4$ flush of experiment 3 is graphed below as measured flow rate/average flow rate VS time where the average flow rate is 2.26 mL/min.

2. Calculation

i)   Calculate the cumulative volume of the flush using the mass of the effluent over a given period of time. The density for water is 1.00 g/mL at 25°C.

$$V \ (L) = \frac{m}{\rho}$$

ii)   Calculate the approximate pore volume for a given flush. First calculate the total volume of flush through the tank at a given time. Use the approximate pore volume through the tank of 3.0 L/day to calculate the pore volumes through the tank.

$$\text{Volume (L)} = \text{elasped time (h)} \times Q_{avg} \left(\frac{mL}{min}\right) \times \frac{60\,min}{h} \times \frac{L}{1000mL}$$

$$\text{Approximate pore volume of flush through tank} = \frac{\text{Volume(L)}}{3.0L}$$

3.   Flow Rate Profile: KMnO₄ Flush – Experiment 3
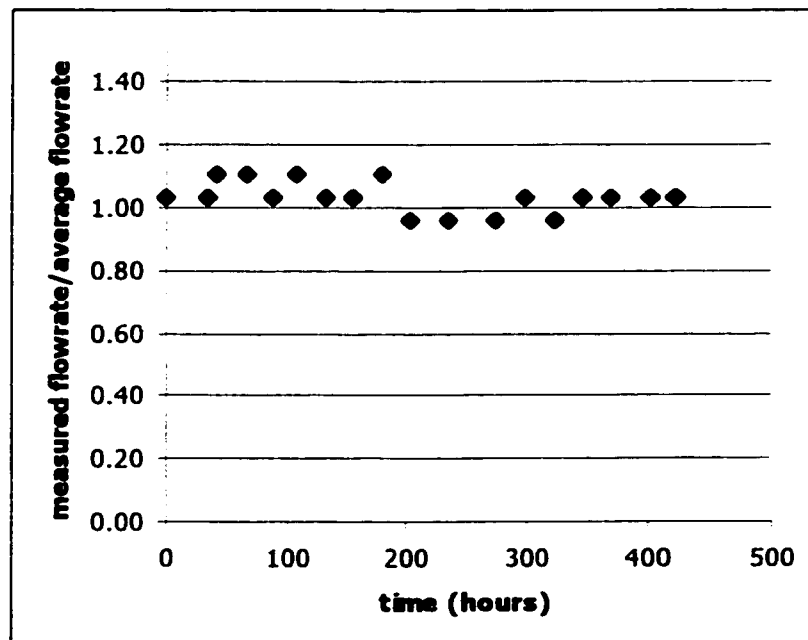
EXPERIMENT #1   Start Date = 12-Jul 1999 @ 5:30pm
TCE Injected = 5.0 mL
[KMnO₄] = 10.0 g/L

Pretreatment Water Flush

		INFLUENT	EFFLUENT	
Date	Time	Injected H$_2$O (L)	Flow (mL/min)	Collected H$_2$O (L)
12-Jul	5:30pm	0	2.26	*
13-Jul	9:00am	2.5	3.00	*
13-Jul	5:30pm	3.0	3.00	*
14-Jul	9:30am	3.5	3.00	*
14-Jul	4:00pm	4.5	2.33	*
15-Jul	9:30am	6.5	2.33	*
15-Jul	4:30pm	7.5	2.00	*
16-Jul	9:30am	9.5	2.17	*
16-Jul	4:30pm	10.0	2.50	9.81
17-Jul	2:30pm	12.0	2.33	*
18-Jul	1:30pm	14.5	2.33	*
19-Jul	9:00am	15.5	2.33	*
19-Jul	1:05pm	16.0	2.33	8.22

Total Effluent Collected= 18.0 L
Average Flowrate= 2.45 mL/min
* Cumulative Volume was not measured at this time

KMnO₄ Flush

		INFLUENT	EFFLUENT	
Date	Time	Injected KMnO$_4$ (L)	Flow (mL/min)	Collected KMnO$_4$ (L)
19-Jul	1:30pm	0	2.17	*
20-Jul	11:30am	3.5	4.67	*
20-Jul	1:30pm	4.5	2.67	*
20-Jul	4:30pm	4.8	3.33	*
21-Jul	9:30am	5.5	1.70	*
21-Jul	4:30pm	6.0	3.20	*
22-Jul	9:30am	6.5	2.25	*
22-Jul	4:30pm	6.0	0.45	*
22-Jul	6:00pm	7.0	N/A	6.30

Total Effluent Collected= 6.30 L
Average Flowrate= 2.55 mL/min
* Cumulative Volume was not measured at this time

EXPERIMENT #2   Start Date = 9-Aug 1999 @ 2:30pm
PCE Injected = 5.0 mL
[KMnO₄] = 5.0 g/L

Pretreatment Water Flush

Date	Time	INFLUENT Injected H₂O (L)	EFFLUENT Flow (mL/min)	EFFLUENT Collected H₂O (L)
9-Aug	2:30pm	0	2.00	*
10-Aug	9:15am	2.0	2.33	*
10-Aug	4:00pm	2.5	2.17	*
11-Aug	9:15am	4.0	2.33	4.15

Total Effluent Collected= 4.15 L
Average Flowrate= 2.21 mL/min
* Cumulative Volume was not measured at this time

KMnO₄ Flush

Date	Time	INFLUENT Injected KMnO₄ (L)	EFFLUENT Flow (mL/min)	EFFLUENT Collected KMnO₄ (L)
11-Aug	10:00am	0	2.17	*
11-Aug	4:00pm	1.8	2.17	*
12-Aug	10:00am	4.8	2.33	*
12-Aug	4:00pm	5.3	2.33	*
13-Aug	9:30am	6.0	2.50	4.69
13-Aug	3:45pm	6.3	2.33	*
14-Aug	4:10pm	8.0	2.33	*
15-Aug	4:15pm	10.3	2.33	*
16-Aug	10:00am	11.8	N/A	5.92

Total Effluent Collected= 10.6 L
Average Flowrate= 2.31 mL/min
* Cumulative Volume was not measured at this time

EXPERIMENT #3   Start Date = 13-Sep 1999 @ 12:00pm
PCE Injected = 2.0 mL
[KMnO4] = 1.0 g/L

Pretreatment Water Flush

Date	Time	INFLUENT Injected H_2O (L)	EFFLUENT Flow (mL/min)	EFFLUENT Collected H_2O (L)
13-Sep	12:00pm	0	2.17	*
14-Sep	9:15am	2.5	2.17	*
14-Sep	4:15pm	3.0	2.00	*
15-Sep	9:45am	4.5	2.17	*
15-Sep	2:45pm	5.0	2.00	5.11

Total Effluent Collected= 5.11 L
Average Flowrate= 2.10 mL/min
* Cumulative Volume was not measured at this time

KMnO4 Flush

Date	Time	INFLUENT Injected $KMnO_4$ (L)	EFFLUENT Flow (mL/min)	EFFLUENT Collected $KMnO_4$ (L)
15-Sep	11:00pm	0	2.33	*
16-Sep	5:00pm	4.0	2.33	*
17-Sep	9:10am	5.3	2.33	*
17-Sep	4:00pm	5.8	2.50	4.27
18-Sep	5:15pm	7.5	2.50	*
19-Sep	3:30pm	9.5	2.33	*
20-Sep	9:30am	11.5	2.50	*
20-Sep	4:15pm	12.5	2.33	7.52
21-Sep	10:00am	14.5	2.33	*
22-Sep	9:30am	16.5	2.50	*
23-Sep	10:00am	19.0	2.17	*
24-Sep	10:00am	21.5	2.17	8.82
25-Sep	5:30pm	24.5	2.17	*
27-Sep	9:30am	28.0	2.33	*
28-Sep	10:00am	30.5	2.17	8.70
29-Sep	10:30am	33.0	2.33	*
30-Sep	9:30am	35.0	2.33	*
1-Oct	9:30am	37.5	2.33	*
2-Oct	4:30pm	40.5	2.33	9.33
3-Oct	12:00pm	42.0	N/A	1.76

Total Effluent Collected= 40.5 L
Average Flowrate= 2.33 mL/min
* Cumulative Volume was not measured at this time

Post-treatment Water Flush

Date	Time	INFLUENT Injected H2O (L)	EFFLUENT Flow (mL/min)	Collected H2O (L)
3-Oct	1:00pm	0	2.50	*
4-Oct	9:30am	3.5	2.33	*
4-Oct	6:00pm	4.0	2.33	*
5-Oct	10:00am	4.8	2.17	*
5-Oct	4:00pm	5.0	2.33	*
6-Oct	10:00am	7.0	2.33	*
6-Oct	3:30pm	7.5	2.33	*
7-Oct	9:30am	9.0	2.33	8.89
7-Oct	4:30pm	9.5	2.30	*
8-Oct	10:00am	11.5	2.33	*
8-Oct	4:00pm	12.0	2.33	*
11-Oct	2:30pm	19.0	2.33	9.61
12-Oct	10:00am	20.5	2.50	*
13-Oct	9:30am	23.0	2.50	*
14-Oct	10:00am	25.5	2.17	*
15-Oct	10:00am	28.0	2.00	8.81
16-Oct	5:00pm	31.0	2.17	*
18-Oct	10:30am	35.0	2.17	*
19-Oct	10:00am	37.5	2.17	*
20-Oct	10:00am	40.0	2.17	9.55
21-Oct	10:00am	42.5	2.17	*
21-Oct	1:30pm	43.0	2.17	4.43

Total Effluent Collected= 41.3 L
Average Flowrate= 2.28 mL/min
* Cumulative Volume was not measured at this time

APPENDIX C

KMnO$_4$ Concentration

1. General

Concentrations of KMnO₄ were determined by titrimetry. Solutions of $Na_2S_2O_3$ were first standardized with the primary standard KIO_3 according to Standard Methods 4500-Cl⁻ B (Eaton et al., 1995). KMnO₄ samples were then titrated with $Na_2S_2O_3$ to determine the concentration of KMnO₄. Titration of KMnO₄ by $Na_2S_2O_3$ was based on a procedure from Kolthoff and Sandell (1946).

2. Procedure

Dilute the KMnO₄ sample with de-ionized water to 100.0 mL in a volumetric flask. Add 1.0 mL sulfuric acid and 3.0 g of KI. After mixing thoroughly, titrate with $Na_2S_2O_3$, adding starch towards the end of the titration when the reddish-brown colour fades into a pale yellow. The endpoint of the titration occurs when the entire brown colour is discharged and the solution becomes clear. Calculate the mass and the concentration of the KMnO₄ sample.

3. Calculation

i)   Calculate the mass of the KMnO₄ sample. The equivalent weight (EW) of KMnO₄ is the molecular weight of KMnO₄ (158.03 g/mol) divided by 5 (Toon and Ellis, 1978). The normality (n) of the $Na_2S_2O_3$ is 0.025 N. The volume (V) of $Na_2S_2O_3$ used for the titration is expressed in L.

$$mass\ (g) = n \times V \times EW$$

ii)   Calculate the concentration (g/L) of the $KMnO_4$ sample as the mass (g) divided by the volume (L) of the original sample (V_s).

$$[KMnO_4] = \frac{mass}{V_s}$$

.

EXPERIMENT #1   Start Date = 12-Jul 1999 @ 5:30pm
TCE Injected = 5.0 mL
$[KMnO_4]$ = 10.0 g/L

EFFLUENT

Date	Time	Elasped time (h)	Sample V (ml)	$[KMnO_4]$ (g/L)
20-Jul	Influent	0	0.10	10.0
20-Jul	1:30pm	24	1.00	0.44
20-Jul	4:30pm	27	1.00	2.37
21-Jul	9:30am	44	0.50	5.20
21-Jul	4:30pm	51	0.10	7.40
22-Jul	9:30am	68	0.025	7.64
22-Jul	4:30pm	75	0.10	6.84

SAMPLING PORTS

Port B

21-Jul	9:30am	44	0.10	9.46
22-Jul	9:30am	68	0.10	7.82

Port C

21-Jul	9:30am	44	0.10	10.4
22-Jul	9:30am	68	0.10	9.46

Port D

21-Jul	9:30am	44	0.10	8.76
22-Jul	9:30am	68	0.10	N/A

Port E

21-Jul	9:30am	44	0.10	N/A
22-Jul	9:30am	68	0.10	2.29

Port F

21-Jul	9:30am	44	0.10	8.00
22-Jul	9:30am	68	0.10	N/A

Port G

21-Jul	9:30am	44	0.10	9.32
22-Jul	9:30am	68	0.10	N/A

EXPERIMENT #1   Start Date = 12-Jul 1999 @ 5:30pm
TCE Injected = 5.0 mL
$[KMnO_4]$ = 10.0 g/L

SAMPLING PORTS

Port H

Date	Time	Elasped time (h)	Sample V (ml)	$[KMnO_4]$ (g/L)
21-Jul	9:30am	44	0.10	9.60
22-Jul	9:30am	68	0.10	9.42

Port I

21-Jul	9:30am	44	0.10	9.87
22-Jul	9:30am	68	0.10	10.2

Port J

21-Jul	9:30am	44	0.10	10.1
22-Jul	9:30am	68	0.10	9.87

Port K

21-Jul	9:30am	44	0.10	9.91
22-Jul	9:30am	68	0.10	10.3

EXPERIMENT #2   Start Date = 9-Aug 1999 @ 2:30pm
                       PCE Injected = 5.0 mL
                       $[KMnO_4]$ = 5.0 g/L

EFFLUENT

Date	Time	Time (hours)	Sample V (ml)	$[KMnO_4]$ (g/L)
11-Aug	Influent	0	0.50	5.00
12-Aug	10:00am	24	0.50	0.74
12-Aug	4:00pm	30	0.50	1.93
13-Aug	9:30am	48	0.50	3.58
13-Aug	4:00pm	54	0.25	3.49
14-Aug	4:00pm	78	0.25	3.34
15-Aug	4:00pm	102	0.25	3.73

SAMPLING PORTS

Port B

13-Aug	9:30am	48	0.10	4.94

Port C

13-Aug	9:30am	48	0.10	4.59

Port D

13-Aug	9:30am	48	0.10	N/A

Port E

13-Aug	9:30am	48	0.10	N/A

Port F

13-Aug	9:30am	48	0.10	N/A

Port G

13-Aug	9:30am	48	0.10	4.66

Port H

13-Aug	9:30am	48	0.10	4.62

Port I

13-Aug	9:30am	48	0.10	4.97

EXPERIMENT #2 Start Date = 9-Aug 1999 @ 2:30pm
PCE Injected = 5.0 mL
$[KMnO_4]$ = 5.0 g/L

SAMPLING PORTS

Port J

Date	Time	Elasped time (h)	Sample V (ml)	$[KMnO_4]$ (g/L)
13-Aug	9:30am	48	0.10	4.87

Port K

13-Aug	9:30am	48	0.10	5.04

EXPERIMENT #3   Start Date = 13-Sep 1999 @ 12:00pm
PCE Injected = 2.0 mL
[KMnO₄] = 1.0 g/L

EFFLUENT

Date	Time	Elasped Time (h)	Sample V (mL)	[KMnO₄] (g/L)
17-Sep	Influent	0	0.50	1.00
17-Sep	9:10am	34	2.0	0.19
17-Sep	4:00pm	41	2.0	0.48
18-Sep	5:00pm	66	0.50	0.58
19-Sep	3:00pm	88	0.50	0.59
20-Sep	9:30am	107	0.50	0.59
21-Sep	10:00am	131	0.50	0.61
22-Sep	9:30am	155	0.50	0.68
23-Sep	10:00am	179	0.50	0.64
24-Sep	10:00am	203	0.50	0.65
25-Sep	5:30pm	235	0.50	0.64
27-Sep	9:30am	275	0.50	0.63
28-Sep	10:00am	299	0.50	0.60
29-Sep	10:30am	324	0.50	0.66
30-Sep	9:30am	347	0.50	0.68
1-Oct	9:30am	371	0.50	0.68
2-Oct	4:30pm	402	0.50	0.76
3-Oct	12:00pm	421	0.50	0.70
4-Oct	9:30am	443*	0.50	0.70
4-Oct	6:00pm	451*	0.50	0.70
5-Oct	10:00am	467*	0.50	0.70

* indicates beginning of post-treatment water flush

APPENDIX D

PCE and TCE Concentration

1.   General

Analysis of PCE and TCE was completed with a Hewlett Packard 5890A

Flame Ionization Detector (FID) Gas Chromatograph (GC) equipped with a 30 m

DB1 column using N_2 carrier gas with a flowrate of 1.5 mL/min.   Concentrations

of samples were determined using a calibration curve prepared from the

integrated area of external standard solutions as specified by EPA Method 3810

(1986). The limit of detection (LOD) for the instrument was determined from the

standard solutions for the compounds PCE and TCE respectively.

2.   Procedure

PCE and TCE samples for GC analysis were prepared in the same manner.

Syringe samples were diluted with de-ionized water to 10.0 mL in a volumetric

flask. Solutions were then transferred to 22 mL headspace vials and immediately

sealed with teflon septa. The GC then analyzed samples. Results from the GC

were expressed as the integrated area of the peak associated with the particular

compound.

3.   Calculation

i)   Using the appropriate standard curve (Appendix E), convert area readings

into concentration (μg/mL). This value represents the concentration of the

diluted 10.0 mL solution.

ii)   Calculate the concentration (μg/mL) of the PCE or TCE sample by multiplying by the dilution factor of 10 and dividing by the original sample volume (V_s) in mL.

$$\text{concentration of sample} = \text{concentration from curve} \times \frac{10.0\text{mL}}{V_s}$$

EXPERIMENT #1   Start Date = 12-Jul 1999 @ 5:30pm
TCE Injected = 5.0 mL
[KMnO₄] = 10.0 g/L

Pretreatment Water Flush

EFFLUENT

Date	Time	Elasped Time (h)	Flowrate (mL/min)	Sample V (mL)	[TCE] (ug/mL)
13-Jul	9:00am	16	3.00	0.010	N/A
13-Jul	5:30pm	24	3.00	0.010	35.3
14-Jul	9:30am	40	3.00	0.010	33.5
14-Jul	4:00pm	47	2.33	0.010	34.9
15-Jul	9:30am	64	2.33	0.010	52.0
15-Jul	4:30pm	71	2.00	0.010	43.1
16-Jul	9:30am	88	2.17	0.010	50.4
16-Jul	4:30pm	95	2.17	0.010	50.8
17-Jul	2:30pm	117	2.50	0.010	46.9
18-Jul	1:30pm	140	2.33	0.010	54.7
19-Jul	9:00am	160	2.33	0.010	45.5

SAMPLING PORTS

Port B

Date	Time	Elasped Time (h)	Flowrate (mL/min)	Sample V (mL)	[TCE] (ug/mL)
13-Jul	9:00am	16	3.00	0.0050	N/A
14-Jul	9:30am	40	3.00	0.0050	63.6
15-Jul	9:30am	64	2.33	0.0050	67.3
16-Jul	9:30am	88	2.17	0.0050	63.8
19-Jul	9:00am	160	2.33	0.0050	62.1

Port C

Date	Time	Elasped Time (h)	Flowrate (mL/min)	Sample V (mL)	[TCE] (ug/mL)
13-Jul	9:00am	16	3.00	0.0050	N/A
14-Jul	9:30am	40	3.00	0.0050	59.8*
15-Jul	9:30am	64	2.33	0.0050	61.1
16-Jul	9:30am	88	2.17	0.0050	58.4*
19-Jul	9:00am	160	2.33	0.0050	57.6*

N/A - sample not available
N/D - not detected
* estimated value - below LOD
LOD= Limit of Detection = 0.001385 ug/mL

EXPERIMENT #1   Start Date = 12-Jul 1999 @ 5:30pm
                     TCE Injected = 5.0 mL
                     [KMnO₄] = 10.0 g/L

Pretreatment Water Flush

SAMPLING PORTS

Port D

Date	Time	Elasped Time (h)	Flowrate (mL/min)	Sample V (mL)	[TCE] (ug/mL)
13-Jul	9:00am	16	3.00	0.0050	N/A
14-Jul	9:30am	40	3.00	0.0050	63.9
15-Jul	9:30am	64	2.33	0.0050	60.6*
16-Jul	9:30am	88	2.17	0.0050	59.8*
19-Jul	9:00am	160	2.33	0.0050	65.4

Port E

Date	Time	Elasped Time (h)	Flowrate (mL/min)	Sample V (mL)	[TCE] (ug/mL)
13-Jul	9:00am	16	3.00	0.0050	N/A
14-Jul	9:30am	40	3.00	0.0050	543
15-Jul	9:30am	64	2.33	0.0050	690
16-Jul	9:30am	88	2.17	0.0050	660
19-Jul	9:00am	160	2.33	0.0050	716

Port F

Date	Time	Elasped Time (h)	Flowrate (mL/min)	Sample V (mL)	[TCE] (ug/mL)
13-Jul	9:00am	16	3.00	0.0050	N/A
14-Jul	9:30am	40	3.00	0.0050	398
15-Jul	9:30am	64	2.33	0.0050	461
16-Jul	9:30am	88	2.17	0.0050	579
19-Jul	9:00am	160	2.33	0.0050	578

Port G

Date	Time	Elasped Time (h)	Flowrate (mL/min)	Sample V (mL)	[TCE] (ug/mL)
13-Jul	9:00am	16	3.00	0.0050	N/A
14-Jul	9:30am	40	3.00	0.0050	873
15-Jul	9:30am	64	2.33	0.0050	610
16-Jul	9:30am	88	2.17	0.0050	589
19-Jul	9:00am	160	2.33	0.0050	662

Port H

Date	Time	Elasped Time (h)	Flowrate (mL/min)	Sample V (mL)	[TCE] (ug/mL)
13-Jul	9:00am	16	3.00	0.0050	N/A
14-Jul	9:30am	40	3.00	0.0050	956
15-Jul	9:30am	64	2.33	0.0050	741
16-Jul	9:30am	88	2.17	0.0050	894

EXPERIMENT #1   Start Date = 12-Jul 1999 @ 5:30pm
                           TCE Injected = 5.0 mL
                           $[KMnO_4]$ = 10.0 g/L

Pretreatment Water Flush

SAMPLING PORTS

Port H

Date	Time	Elasped Time (h)	Flowrate (mL/min)	Sample V (mL)	[TCE] (ug/mL)
19-Jul	9:00am	160	2.33	0.0050	940

Port I

Date	Time	Elasped Time (h)	Flowrate (mL/min)	Sample V (mL)	[TCE] (ug/mL)
13-Jul	9:00am	16	3.00	0.0050	N/A
14-Jul	9:30am	40	3.00	0.0050	1056
15-Jul	9:30am	64	2.33	0.0050	726
16-Jul	9:30am	88	2.17	0.0050	978
19-Jul	9:00am	160	2.33	0.0050	986

Port J

Date	Time	Elasped Time (h)	Flowrate (mL/min)	Sample V (mL)	[TCE] (ug/mL)
13-Jul	9:00am	16	3.00	0.0050	N/A
14-Jul	9:30am	40	3.00	0.0050	1045
15-Jul	9:30am	64	2.33	0.0050	1004
16-Jul	9:30am	88	2.17	0.0050	1036
19-Jul	9:00am	160	2.33	0.0050	989

Port K

Date	Time	Elasped Time (h)	Flowrate (mL/min)	Sample V (mL)	[TCE] (ug/mL)
13-Jul	9:00am	16	3.00	0.0050	N/A
14-Jul	9:30am	40	3.00	0.0050	346
15-Jul	9:30am	64	2.33	0.0050	373
16-Jul	9:30am	88	2.17	0.0050	368
19-Jul	9:00am	160	2.33	0.0050	402

N/A - sample not available
N/D - not detected
* estimated value - below LOD
LOD= Limit of Detection = 0.001385 ug/mL

EXPERIMENT #1   Start Date = 12-Jul 1999 @ 5:30pm
TCE Injected = 5.0 mL
[$KMnO_4$] = 10.0 g/L

KMnO₄ Flush

EFFLUENT

Date	Time	Elasped Time (h)	Flowrate (mL/min)	Sample V (mL)	[TCE] (ug/mL)
20-Jul	1:30pm	24	2.67	0.010	N/D
20-Jul	4:30pm	27	3.33	0.010	N/D
21-Jul	9:30am	44	1.70	0.010	N/D
21-Jul	4:30pm	51	3.20	0.010	N/D
22-Jul	9:30am	68	2.25	0.010	N/D
22-Jul	4:30pm	75	0.45	0.010	N/D

SAMPLING PORTS

Port B

21-Jul	9:30am	44	1.70	0.050	N/D
22-Jul	9:30am	68	2.25	0.050	N/D

Port C

21-Jul	9:30am	44	1.70	0.050	N/D
22-Jul	9:30am	68	2.25	0.050	N/D

Port D

21-Jul	9:30am	44	1.70	0.050	N/D
22-Jul	9:30am	68	2.25	0.050	N/D

Port E

21-Jul	9:30am	44	1.70	N/A	N/A
22-Jul	9:30am	68	2.25	0.050	N/D

Port F

21-Jul	9:30am	44	1.70	0.050	N/D
22-Jul	9:30am	68	2.25	N/A	N/A

Port G

21-Jul	9:30am	44	1.70	0.050	N/D
22-Jul	9:30am	68	2.25	N/A	N/A

EXPERIMENT #1   Start Date = 12-Jul 1999 @ 5:30pm
TCE Injected = 5.0 mL
[KMnO₄] = 10.0 g/L

KMnO₄ Flush

SAMPLING PORTS

Port H

Date	Time	Elasped Time (h)	Flowrate (mL/min)	Sample V (mL)	[TCE] (ug/mL)
21-Jul	9:30am	44	1.70	0.050	N/D
22-Jul	9:30am	68	2.25	0.050	N/D

Port I

Date	Time	Elasped Time (h)	Flowrate (mL/min)	Sample V (mL)	[TCE] (ug/mL)
21-Jul	9:30am	44	1.70	0.050	N/D
22-Jul	9:30am	68	2.25	0.050	N/D

Port J

Date	Time	Elasped Time (h)	Flowrate (mL/min)	Sample V (mL)	[TCE] (ug/mL)
21-Jul	9:30am	44	1.70	0.050	N/D
22-Jul	9:30am	68	2.25	0.050	N/D

Port K

Date	Time	Elasped Time (h)	Flowrate (mL/min)	Sample V (mL)	[TCE] (ug/mL)
21-Jul	9:30am	44	1.70	0.050	N/D
22-Jul	9:30am	68	2.25	0.050	N/D

N/A - sample not available
N/D - not detected
* estimated value - below LOD
LOD= Limit of Detection = 0.001385 ug/mL

EXPERIMENT #2   Start Date = 9-Aug 1999 @ 2:30pm
                 PCE Injected = 5.0 mL
                 [KMnO₄] = 5.0 g/L

Pretreatment Water Flush

EFFLUENT

Date	Time	Elasped Time (h)	Flowrate (mL/min)	Sample V (mL)	[PCE] (ug/mL)
10-Aug	9:15am	19	2.33	0.010	N/D
10-Aug	4:00pm	26	2.17	0.010	N/D
11-Aug	9:15am	43	2.33	0.010	10.9*

KMnO₄ Flush

EFFLUENT

Date	Time	Elasped Time (h)	Flowrate (mL/min)	Sample V (mL)	[PCE] (ug/mL)
12-Aug	10:00am	24	2.33	0.010	N/D
12-Aug	4:00pm	30	2.33	0.010	N/D
13-Aug	9:30am	48	2.50	0.010	N/D
13-Aug	4:00pm	54	2.33	0.010	N/D
14-Aug	4:00pm	78	2.33	0.010	N/D
15-Aug	4:00pm	102	2.33	0.010	N/D

SAMPLING PORTS

Port B

13-Aug	9:30pm	48	2.50	0.050	N/D

Port C

13-Aug	9:30pm	48	2.50	0.050	N/D

Port D

13-Aug	9:30pm	48	2.50	N/A	N/A

Port E

13-Aug	9:30pm	48	2.50	N/A	N/A

EXPERIMENT #2   Start Date = 9-Aug 1999 @ 2:30pm
                     PCE Injected = 5.0 mL
                     [KMnO₄] = 5.0 g/L

KMnO₄ Flush

SAMPLING PORTS

Port F

Date	Time	Elasped Time (h)	Flowrate (mL/min)	Sample V (mL)	[PCE] (ug/mL)
13-Aug	9:30pm	48	2.50	N/A	N/A

Port G

13-Aug	9:30pm	48	2.50	0.050	N/D

Port H

13-Aug	9:30pm	48	2.50	0.050	N/D

Port I

13-Aug	9:30pm	48	2.50	0.050	N/D

Port J

13-Aug	9:30pm	48	2.50	0.050	N/D

Port K

13-Aug	9:30pm	48	2.50	0.050	N/D

N/A - sample not available
N/D - not detected
* estimated value - below LOD
LOD= Limit of Detection = 0.01875 ug/mL

EXPERIMENT #3   Start Date = 13-Sep 1999 @ 12:00pm
PCE Injected = 2.0 mL
[KMnO₄] = 1.0 g/L

Pretreatment Water Flush

EFFLUENT

Date	Time	Elasped Time (h)	Flowrate (mL/min)	Sample V (mL)	[PCE] (ug/mL)
14-Sep	9:15am	21	2.17	0.010	N/D
14-Sep	9:15am	21	2.17	0.050	N/D
14-Sep	4:00pm	28	2.00	0.010	N/D
14-Sep	4:00pm	28	2.00	0.050	N/D
15-Sep	9:45am	46	2.17	0.010	N/D
15-Sep	9:45am	46	2.17	0.050	N/D

SAMPLING PORTS

Port C

14-Sep	9:15am	21	2.17	0.25	N/D
14-Sep	4:00pm	28	2.00	0.25	0.75*
15-Sep	9:45am	46	2.17	0.25	0.90*

Port D

14-Sep	9:15am	21	2.17	0.25	87.2
14-Sep	4:00pm	28	2.00	0.25	95.5
15-Sep	9:45am	46	2.17	0.25	111

Port E

14-Sep	9:15am	21	2.17	0.25	62.4
14-Sep	4:00pm	28	2.00	0.25	97.2
15-Sep	9:45am	46	2.17	0.25	104

Port F

14-Sep	9:15am	21	2.17	0.25	4.18
14-Sep	4:00pm	28	2.00	0.25	5.69
15-Sep	9:45am	46	2.17	0.25	6.89

Port G

14-Sep	9:15am	21	2.17	0.25	8.35
14-Sep	4:00pm	28	2.00	0.25	1.34*
15-Sep	9:45am	46	2.17	0.25	1.31*

EXPERIMENT #3   Start Date = 13-Sep 1999 @ 12:00pm
PCE Injected = 2.0 mL
[KMnO₄] = 1.0 g/L

KMnO₄ Flush

EFFLUENT

Date	Time	Elasped Time (h)	Flowrate (mL/min)	Sample V (mL)	[PCE] (ug/mL)
16-Sep	5:00pm	18	2.33	0.010	N/D
17-Sep	9:10am	34	2.33	0.010	N/D
17-Sep	4:00pm	41	2.50	0.010	N/D
18-Sep	5:00pm	66	2.50	0.010	N/D
19-Sep	3:00pm	88	2.33	0.010	N/D
20-Sep	9:30am	107	2.50	0.010	N/D
21-Sep	10:00am	131	2.33	0.010	N/D
22-Sep	9:30am	155	2.50	0.010	N/D
23-Sep	10:00am	179	⁻2.17	0.010	N/D
24-Sep	10:00am	203	2.17	0.010	N/D
25-Sep	5:30pm	235	2.17	0.010	N/D
27-Sep	9:30am	275	2.33	0.010	N/D
28-Sep	10:00am	299	2.17	0.010	N/D
29-Sep	10:30am	324	2.33	0.050	N/D
30-Sep	9:30am	347	2.33	0.050	N/D
1-Oct	9:30am	371	2.33	0.050	N/D
2-Oct	4:30pm	402	2.33	0.050	N/D
3-Oct	12:00pm	421	2.50	0.050	N/D
4-Oct	9:30am	443	2.33	0.010	N/D
4-Oct	6:00pm	451	2.33	0.010	N/D
5-Oct	10:00am	467	2.17	0.010	N/D

N/A - sample not available
N/D - not detected
* estimated value - below LOD
LOD= Limit of Detection = 0.01875 ug/mL

EXPERIMENT #3   Start Date = 13-Sep 1999 @ 12:00pm
                       PCE Injected = 2.0 mL
                       [KMnO₄] = 1.0 g/L

Post-treatment Water Flush

EFFLUENT

Date	Time	Elasped Time (h)	Flowrate (mL/min)	Sample V (mL)	[PCE] (ug/mL)
5-Oct	4:00pm	473	2.33	0.010	N/D
6-Oct	10:00am	491	2.33	0.010	N/D
6-Oct	3:30pm	497	2.33	0.010	N/D
7-Oct	9:30am	515	2.33	0.010	N/D
7-Oct	4:30pm	522	2.33	0.010	N/D
8-Oct	10:00am	539	2.33	0.010	N/D
8-Oct	4:00pm	545	2.33	0.010	N/D
11-Oct	2:30pm	616	2.33	0.010	9.76*
12-Oct	10:00am	635	2.50	0.010	N/D
13-Oct	9:30am	659	2.50	0.010	9.99*
14-Oct	10:00am	683	2.17	0.010	10.5*
15-Oct	10:00am	707	2.00	0.010	9.55*
16-Oct	5:00pm	738	2.17	0.010	8.38*
18-Oct	10:30am	780	2.17	0.010	8.34*
19-Oct	10:00am	803	2.17	0.010	9.05*
20-Oct	10:00am	827	2.17	0.010	7.92*
21-Oct	10:00am	851	2.17	0.010	7.09*

Injection Port

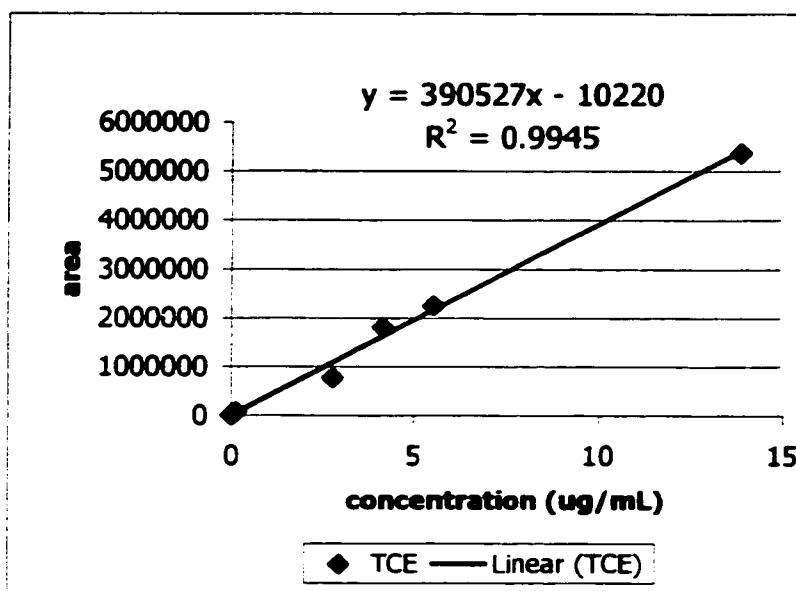| Date	Time	Elasped Time (h)	Flowrate (mL/min)	Sample V (mL)	[PCE] (ug/mL)
14-Oct	10:30am	684	2.17	0.10	145

N/A - sample not available
N/D - not detected
* estimated value - below LOD
LOD= Limit of Detection = 0.01875 ug/mL

APPENDIX E

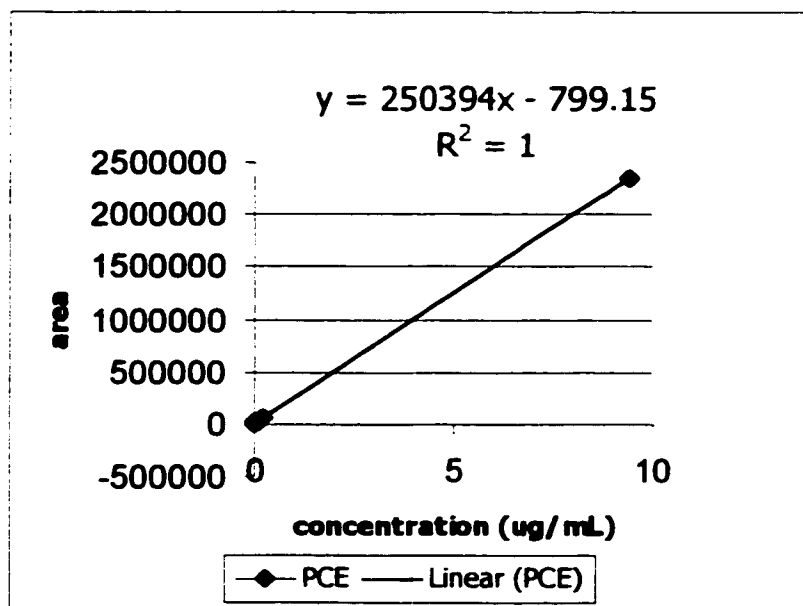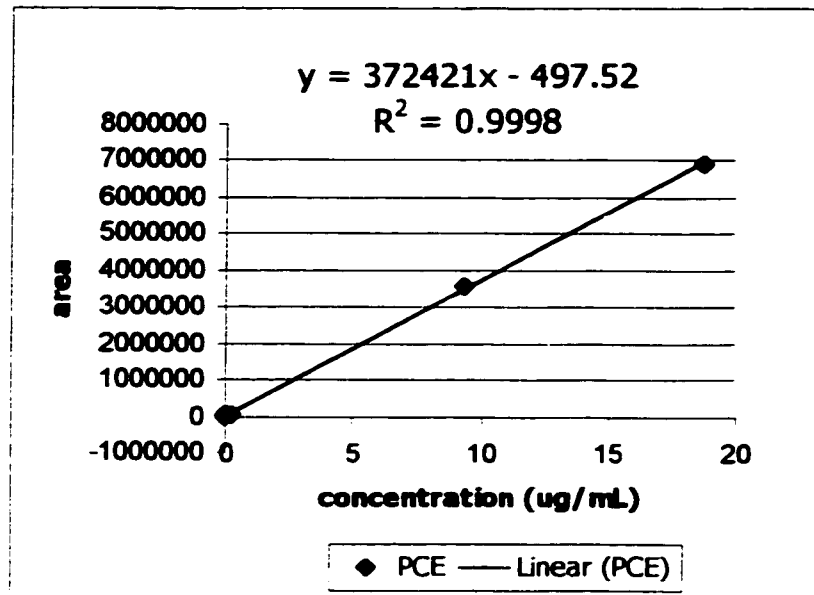Standard Curves for PCE and TCE

TCE Standard Curve:

$$y = 390527x - 10220$$
$$R^2 = 0.9945$$

Chart: area (y-axis, 0 to 6000000) vs concentration (ug/mL) (x-axis, 0 to 15)

Legend: ◆ TCE —— Linear (TCE)

PCE Standard Curve:

$$y = 250394x - 799.15$$
$$R^2 = 1$$

Chart: area (y-axis, -500000 to 2500000) vs concentration (ug/mL) (x-axis, 0 to 10)

Legend: ◆ PCE —— Linear (PCE)

129

PCE Standard Curve:

$$y = 372421x - 497.52$$
$$R^2 = 0.9998$$

Chart showing area vs. concentration (ug/mL) for PCE with a linear fit. Legend: ◆ PCE —— Linear (PCE)

VITA AUCTORIS

Name: Melanie Rae Marshall

Place of birth: Windsor, Ontario, Canada

Date of birth: November 10, 1974

Education:

Master's of Applied Science
Environmental Engineering
University of Windsor
Windsor, Ontario, Canada
1998-2000

Bachelor's of Applied Science
Environmental Engineering
University of Windsor
Windsor, Ontario, Canada
1993-1997

Work/Experience:

Research Assistant
Civil and Environmental Engineering
University of Windsor
Windsor, Ontario, Canada
1998-2000

Awards and Scholarships:

Summer Research Scholarship, 1999
President's Roll, 1999
Dean's Honour List, 1997
Entrance Scholarship, 1993